THE ROLE OF CLOCK IN THE REGULATION OF DOPAMINE

NEUROTRANSMISSION IN THE *CLOCK*Δ19 MUTANT MOUSE MODEL

APPROVED BY SUPERVISORY COMMITTEE

Colleen McClung, Ph.D.

Matthew Goldberg, Ph.D.

Michael Lutter, MD., Ph.D.

Carla Green, Ph.D.

DEDICATION

I dedicate this work to my husband, Lionell Bunton, for helping me preserve my sanity through this long, arduous process.

To my parents, Dwight and Marilyn Spencer, for their unconditional love and encouragement even when I didn't feel worthy of it.

To my sister and friend, Crystal Mills, for teaching me that when you try to spite someone else, you only end up spiting yourself.

To my brother, Dwight Spencer, for setting the bar so high for all of us.

ACKNOWLEDGEMENTS

For their direction and advice, I would like to thank my committee members Drs. Matthew Goldberg, Michael Lutter, and Carla Green. I would like to thank my mentor, Colleen McClung, for her patience and guidance and the opportunity to work in such a wonderful lab with such a talented group of people. Among those, I would like to thank all of my post-docs, Drs. Angela Ozburn, Andrea Gillman, Michelle Sidor, and Laurent Coque, for their advice and expertise on matters both scientific and not. I am grateful to Dr. Shibani Mukherjee for her seemingly endless knowledge base and invaluable assistance especially upon the relocation of the rest of lab. I thank my fellow left-behind lab mates, Rachel Arey and Edgardo Falcon, for always being willing to offer an extra set of hands, eyes, or ears depending on the particular situation. To my neuroscience program classmates, our discussions and your feedback have been pivotal to my scientific development. I thank the psychiatry department faculty and staff for fostering such a collaborative environment in which to work especially particular individuals within the Bibb lab (Dr. Melissa Torres-Altoro), the Cowan lab (Dr. Makoto Taniguchi and Maria Carreira), and the Self lab (Nicole Buzin). I am indebted to Drs. Nancy Street and Nancy Monson for taking a chance on me at the admissions stage. Thank you to Dr. Street for continuing to check up on my progress and act as one of my biggest cheerleaders. Thank you to Dr. Monson for investing so much in me during in my first rotation. I am appreciative of the NIH/NIMH for research support during my training. And to all my family and friends, thank you for your unending encouragement and support!

THE ROLE OF CLOCK IN REGULATION OF DOPAMINE NEUROTRANSMISSION IN THE *CLOCK*Δ19 MUTANT MOUSE MODEL

by

SADE MONIQUE SPENCER

DISSERTATION

Presented to the Faculty of the Graduate School of Biomedical Sciences

The University of Texas Southwestern Medical Center at Dallas

In Partial Fulfillment of the Requirements

For the Degree of

DOCTOR OF PHILOSOPHY

The University of Texas Southwestern Medical Center at Dallas

Dallas, Texas

May, 2012

THE ROLE OF CLOCK IN REGULATION OF DOPAMINE NEUROTRANSMISSION IN THE *CLOCK*Δ19 MUTANT MOUSE MODEL

Sade Monique Spencer

The University of Texas Southwestern Medical Center at Dallas, 2012

Colleen A. McClung, Ph.D.

Mice with a mutation in the circadian gene *Clock* (*Clock*Δ19) display a behavioral profile which parallels a euphoric manic-like state including hyperactivity, disrupted activity rhythms, increased substance abuse vulnerability, and decreases in anxiety and depression-related behavior. The molecular clock has significant cross-talk with many of the brain's neurotransmitter systems. The purpose of this dissertation is to characterize the role of CLOCK in regulating dopamine transmission in mood and reward-related circuits. We present a mechanism by which CLOCK regulates dopaminergic activity in the mesoaccumbens circuit and contributes to anxiety-related behavior. *In vivo*

recording of ventral tegmental area (VTA) dopamine cells throughout the 24 hour cycle revealed that firing and bursting was elevated in *Clock*Δ19 mutants with the most significant deviations early in the light cycle. Mimicking this increase in dopaminergic activity using optogenetic targeting resulted in decreased anxiety-related behavior similar to the *Clock*Δ19 phenotype. Consistent with the electrophysiological findings, *tyrosine hydroxylase (TH)* mRNA and protein was elevated in the VTA in a daytime-specific manner leading to increased dopamine synthesis in the nucleus accumbens. CLOCK binding was detected at E-box elements within the *TH* promoter with greater enrichment observed during the light phase when *TH* expression is low. These results suggest a negative regulation of *TH* by CLOCK. To examine alterations in the nigrostriatal dopamine circuit, HPLC measurements of dopamine and metabolites were performed in the dorsal striatum revealing significant increases in DOPAC and HVA. Dopamine receptor agonists and antagonists were used to pharmacologically probe dopamine receptor function. An enhancement of the locomotor suppressing response to dopamine antagonists in *Clock*Δ19 mice suggested increased dopaminergic tone. *Clock*Δ19 mice were insensitive to the locomotor stimulating effects of a D1 agonist, but displayed increased levels of D1DR protein. Conversely, the *Clock*Δ19 mutants displayed enhanced locomotor suppression to a D2 agonist and a coincident increase in D2DR protein. Forskolin stimulation of cAMP resulted in blunted molecular responses in the *Clock*Δ19 mutants consistent with impairments in D1 signaling and/or enhancements in D2

signaling. In summary, normal CLOCK function appears to be involved in the regulation of dopamine transmission in the striatum.

TABLE OF CONTENTS

PRIOR PUBLICATIONS

L Coque, S Mukherjee, JL Cao, S Spencer, M Marvin, E Falcon, MM Sidor, SG Birnbaum, A Graham, RL Neve, E Gordon, AR Ozburn, MS Goldberg, MH Han, DC Cooper, and CA McClung. Specific role of VTA dopamine neuronal firing rates and morphology in the reversal of anxiety-related but not depression-related behavior in the *Clock*Δ*19* mouse model of mania. Neuropsychopharmacology (2011) 36(7):1478-88.

JF Enwright III, M Wald, M Paddock, E Hoffman, RN Arey, S Edwards, S Spencer, EJ Nestler, CA McClung. ΔFosB indirectly regulates *Cck* promoter activity. Brain Research. (2010) 1329: 10-20.

EM Cameron, S Spencer, J Lazarini, CT Harp, ES Ward, M Burgoon, GP Owens, MK Racke, JL Bennett, EM Frohman, NL Monson. Potential of a unique antibody gene signature to predict conversion to clinically definite multiple sclerosis. Journal of Neuroimmunology. (2009) 213 (1-2):123-130.

AR Ozburn, E Falcon, S Mukherjee, RN Arey, S Spencer, and CA McClung. Role of CLOCK in Ethanol-Related Behaviors. (In press, Psychopharmacology)

S Spencer*, M Sidor*, RN Arey, K Dzirasa, KM Tye, M Warden, JF Enwright III, JPR Jacobson, EN Remillard, R Hale, M Caron, K Deisseroth and CA McClung. Direct regulation of dopaminergic activity by CLOCK and its importance in anxiety-related behaviors. (Submitted to Nature Neuroscience)(*These authors contributed equally to this work)

RN Arey, JF Enwright III, S Spencer, AR Ozburn, E Falcon, and CA McClung. An important role for *Cholecystokinin,* a CLOCK target gene, in the development and treatment of manic-like behaviors. (Submitted to Nature Neuroscience)

E Falcon*, S Spencer*, J Kumar, S Birnbaum, and CA McClung. Circadian genes *Period 1* and *Period 2* in the nucleus accumbens regulate anxiety-related behavior. (In preparation for submission) (*These authors contributed equally to this work)

S Spencer, E Falcon, RN Arey, and CA McClung. A mutation in CLOCK leads to altered dopamine receptor function. (In preparation for submission)

RN Arey, S Spencer, and CA McClung. Cholecystokinin as a common target of the anti-manic actions of mood stabilizers. (In preparation for submission)

E Falcon, AR Ozburn, S Mukherjee, RN Arey, S Spencer, CA McClung. NPAS2 regulates cocaine reward and dopamine receptors in the ventral striatum. (In preparation for submission)

ABSTRACTS

Spencer S, Arey R, Falcon E, McClung CA. (2011) Altered dopamine receptor activity in the *Clock* mutant mice. 41st Annual Meeting of the Society for Neuroscience.

Spencer S, Falcon E, Arey RN, McClung CA. (2011) Dopamine receptor dysfunction in *Clock* mutant mice. Gordon Research Conference on Catecholamines.

Spencer S, Arey RN, McClung CA. (2010) Dysregulation of genes that control dopaminergic activity in the *Clock* mutant mice, a model of mania. 43rd Annual Winter Conference on Brain Research.

Ozburn A, Falcon E, Mukherjee S, Kumar J, Gillman A, Spencer S, McClung CA (2010). The role of *Clock* in ethanol-related behaviors. 50th Annual Meeting of the American College of Neuropsychopharmacology.

Arey RN, Spencer S, Falcon E, Enwright J, McClung CA. (2009) Regulation of the cholecystokinin gene by lithium in a mouse model of mania. 39th Annual Meeting of the Society for Neuroscience.

Falcon E, Arey RN, Spencer S, McClung CA. (2008) Chronic cocaine alters circadian and dopaminergic gene expression rhythms in reward-related areas. 37th Annual Meeting of the Society for Neuroscience.

Coque LF, Dancy EA, Mukherjee S, Gordon EA, Salari SK, Spencer S, McClung CA. (2008) Cellular and morphological markers of bipolar disorder in the *Clock* mouse. 37th Annual Meeting of the Society for Neuroscience.

LIST OF FIGURES

LIST OF TABLES

LIST OF APPENDICES

LIST OF ABBREVIATIONS

3-MT- 3-methoxytryamine

5-HT- serotonin

AADC- aromatic amino acid decarboxylase

AAV- adeno-associated virus

AC- adenylate cyclase

ADHD- attention deficit hyperactivity disorder

AKT- protein kinase B

AMP- adenosine monophosphate

AMPA- 2-amino-3-(5-methyl-3-oxo-1,2- oxazol-4-yl) propanoic acid

ANOVA- analysis of variance

AP- anterior – posterior

ATF-5- activating transcription factor 5

ATP- adenosine triphosphate

βArr2- Beta-arrestin 2

BD- Bipolar disorder

BDNF- brain derived neurotrophic factor

bHLH- basic helix-loop-helix

bHR- bred high responder

bLR- bred low responder

BMAL- brain and muscle Arnt-like protein

Ca^{2+} - calcium

CAMKII- Ca^{2+}/calmodulin-dependent protein kinase

cAMP- cyclic AMP

CCG- clock controlled gene

ChIP- chromatin immunoprecipitation

ChR2- channelrhodopsin 2

CK- casein kinase

CLOCK- circadian locomotor output cycles kaput

COMT- catechol-O-methyltransferase

CP- caudate putamen

CPP- conditioned place preference

CREB- cyclic AMP response element binding protein

Cry- cryptochrome

cT- cycle threshold

D1DR- D1 dopamine receptor

D2DR- D2 dopamine receptor

D3DR- D3 dopamine receptor

DA- dopamine

DAG- diacyl glycerol

DAPI- 4',6-diamidino-2-phenylindole

DARPP-32- dopamine- and cAMP- regulated protein, Mr 32 kDa

DAT- dopamine transporter

DBH- dopamine beta-hydroxylase

DD- dark-dark/ constant darkness

DNA- deoxyribonucleic acid

DOPAC- 3,4-dihydroxyphenylactic acid

DV- dorsal – ventral

EMSA- electrophoretic mobility shift assay

ENU- N-ethyl-N-nitrosurea

EPM- elevated plus maze

ERK- extracellular signal related kinase

eYFP- enhanced yellow fluorescent protein

FASPS- familial advanced phase sleep syndrome

DSM-IV- Diagnostic and Statistical Manual for Mental Disorders, Fourth Edition

GAPDH- glyceraldehyde-3-phosphate dehydrogenase

GIRK- G-protein coupled inwardly rectifying potassium channels

GluR1- glutamate receptor subunit 1

GMP- guanosine monophosphate

GPCR- G-protein coupled receptor

GSK3- glycogen synthase kinase 3

HCN- hyperpolarization-activated cyclic nucleotide gated channels

HPLC-EC- high pressure liquid chromatography electrochemical detection

HVA- homovanillic acid

ICSS- intracranial self-stimulation

Ip- intraperitoneal

IP_3- inositol 1,4,5-triphosphate

IRES- internal ribosome entry site

K^+- potassium

LC- locus coeruleus

LCM- laser capture microdissection

L-DOPA- L-dihidroxy-phenylalanine

LDTg- lateral dorsal tegmental area

LFP- local field potentials

MAO- monoamine oxidase

MAPK- Mitogen-Activated Protein Kinase

MEK- MAP/ERK kinase

MFB- medial forebrain bundle

ML- medial - lateral

mRNA- messenger RNA

NAc- nucleus accumbens

NMDA- N-methyl-D-aspartate

NOS- not otherwise specified

NPAS- neuronal PAS-domain containing protein

NREM- non rapid eye movement sleep

NSD 1015- 3-hydroxy-benzylhydrazine

PC-12- pheochromocytoma-12

PCR- polymerase chain reaction

PDK1- phosphoinositide-dependent kinase 1

Per- Period

PET- positron emission tomography

Pi3K- phosphatidyl inositol 3-kinase

PIP2- phosphatidylinositol 4,5-bisphosphate

PKA- Protein kinase A

PKC- Protein kinase C

PLC- phospholipase C

PP2A- protein phosphatase 2A

PP2B- protein phosphatase 2B

PPTg- pedunculopontine tegmental are

PTSD- post-traumatic stress disorder

REM- rapid eye movement sleep

RNA- ribonucleic acid

RRE- Rev response element

RTK- receptor tyrosine kinase

SAD- seasonal affective disorder

SCN- suprachiasmatic nucleus

shRNA- short hairpin RNA

SN- substantia nigra

SNc- substantia nigra pars compacta

SNP- single nucleotide polymorphism

SSRI - selective serotonin reuptake inhibitor

STEP- striatal enriched phosphatase

SWS- slow wave sleep

TH- tyrosine hydroxylase

TTF-1- terminating transcription factor 1

VIP- vasoactive intestinal peptide

VLPO- ventrolateral preoptic nucleus

VMAT2- vesicular monoamine transporter 2

VTA- ventral tegmental area

WT- wild type

ZT- zeitgeber

CHAPTER ONE
Introduction

DOPAMINE NEUROTRANSMISSION, BIPOLAR DISORDER, AND THE CIRCADIAN CLOCK

The dopamine system

Dopamine (DA) is a monoamine neurotransmitter derived from the two-step conversion of the amino acid tyrosine shown in Figure 1.1A. Tyrosine is converted to L-dihydroxy-phenylalanine (L-DOPA) by the enzyme tyrosine hydroxylase (TH) which is the rate limiting step in dopamine and norepinephrine synthesis (Holtz 1959; Nagatsu, Levitt et al. 1964). As such, TH is commonly used as a molecular marker to identify catecholamine cells. There are several major dopaminergic projections within the brain as depicted in Figure 1.1B. The midbrain cell groups, designated as A8, A9, and A10 per the early conventions of Dahlstrom and Fuxe, correspond to the retrorubral area, the substantia nigra (SN), and the ventral tegmental area (VTA) (Dahlstrom 1964; Albanese 1986). These three nuclei encompass approximately 90% of all brain dopamine cells (Binder, Kinkead et al. 2001). The A11-A14 cell groups originate in the thalamus and hypothalamus sending descending projections to the spinal cord and brain stem and regulating neuroendocrine functions (Albanese 1986). The A16-A17 populations are located in the olfactory bulb and retina, respectively, where they contribute to sensory information processing (Albanese 1986; Masson, Mestre et al. 1993; Pignatelli, Kobayashi et al. 2005).

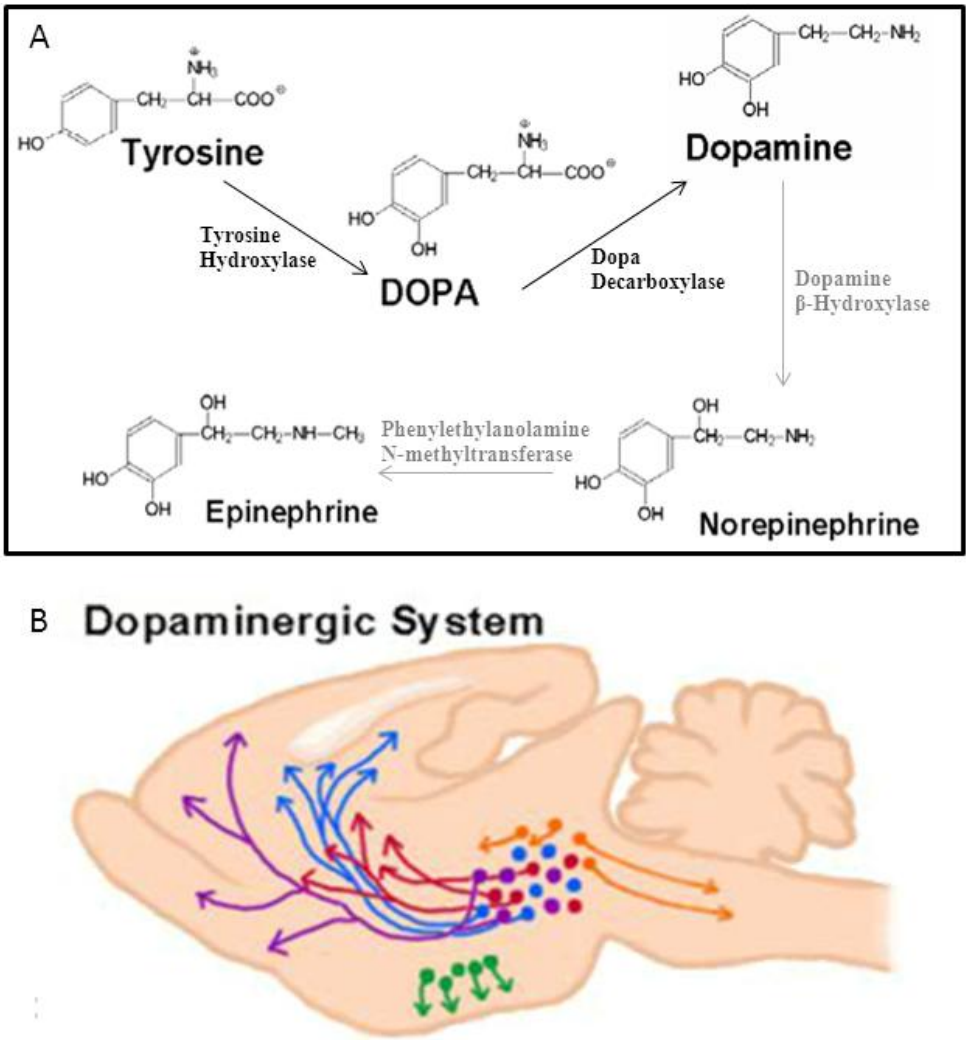

Figure 1.1 The dopamine system. A. Dopamine synthesis pathway. Tyrosine is converted to dihydroxyphenylalanine (L-DOPA) by the tyrosine hydroxylase (TH) enzyme. DOPA is converted to dopamine by the aromatic amino acid decarboxylase (AADC) enzyme in a subsequent reaction that is almost instantaneous, thus the conversion of tyrosine to L-DOPA represents the rate-limiting step in DA synthesis. In noradrenergic brain regions DA is further processed into norepinephrine by dopamine beta-hydroxylase (DBH). **B.** Major dopaminergic nuclei and their projection systems. Dorsal (blue) and ventral (red) mesostriatal neurons originate in the substantia nigra and project to various striatal structures. The mesocorticolimbic pathway neurons (purple) originate in the ventral tegmental area and synapse onto limbic structures. The periventricular (orange) and tuberohypophyseal (green) dopamine systems originate in the hypothalamus and modulate basic functions such as appetite, sex, and lactation. Adapted from UTH Neuroscience Online Textbook.

This thesis will focus on the SN and VTA dopaminergic nuclei and their projections onto striatal brain structures. Dopamine neurons of the SN project to a number of brain regions the principal of these being the dorsal striatum. The nigrostriatal dopamine pathway has been studied extensively for its involvement in controlling voluntary motor movement. The neurodegenerative motor disorder Parkinson's disease occurs as a result of loss of substantia nigra pars compacta dopamine cells (Barzilai and Melamed 2003). The VTA sends major projections to limbic structures including the nucleus accumbens, hippocampus, and amygdala constituting the mesolimbic dopamine pathway while other afferents extend to areas of the cerebral cortex forming the mesocortical pathway. The mesocorticolimbic dopamine system has been acknowledged for its role in mediating reward, motivated behavior, and learning and memory processes (Mogenson, Jones et al. 1980; Cools 2008). The striatum, a major component of the basal ganglia, is the one of the main outputs for midbrain dopamine nuclei. It is primarily composed of medium spiny neurons (MSNs) which account for >90% of the cell population (Gerfen, Engber et al. 1990). Striatal MSNs are GABA (gamma-aminobutyric acid) containing projection neurons that receive and integrate glutamatergic inputs from the cortex and thalamus, dopaminergic inputs from the midbrain, and intrastriatal gabaergic and cholinergic inputs. The striatum is classically divided into the anatomically distinct dorsal and ventral regions based on their afferent connections. The dorsal striatum (also caudate putamen, CP) receives inputs from the SN and cortex while the ventral striatum (also

nucleus accumbens, NAc) receives inputs from the VTA, prefrontal cortex, and amygdala. The dorsal and ventral striatum are also delineated based on their functional contribution to behavioral processes as defined above.

Dopamine receptors and signaling

Dopamine interacts with five subtypes of dopamine receptors which are functionally divided into two classes (D1 and D2) based on their contrasting effects on adenylyl cyclase (AC) activity (Stoof and Kebabian 1981). Dopamine receptors are seven transmembrane domain containing metabotropic G-protein coupled receptors (GPCRs) whose signaling is summarized in Figure 1.2 (reviewed in (Beaulieu and Gainetdinov 2011)). The D1 class of receptors (D1 and D5) are coupled to Gαs/olf or Gαq subunits. Gαs/olf coupled receptors activate AC which converts ATP to cAMP and activates cAMP dependent protein kinase (PKA). PKA, in turn, phosphorylates a number of targets leading to a variety of downstream signaling events. Gαq coupled receptors activate Phospholipase C (PLC) which cleaves phosphatidylinositol 4,5-bisphosphate (PIP2) into diacyl glycerol (DAG) and inositol 1,4,5-triphosphate (IP_3) initiating an IP_3 signaling cascade. The D2 class of receptors (D2, D3, and D4) is coupled to Gαi/o subunits and serves to inhibit AC activity and decrease PKA activity. D2 receptors can also elevate intracellular calcium levels and activate a PLC and protein phosphatase 2B (PP2B) cascade (Nishi, Snyder et al. 1997).

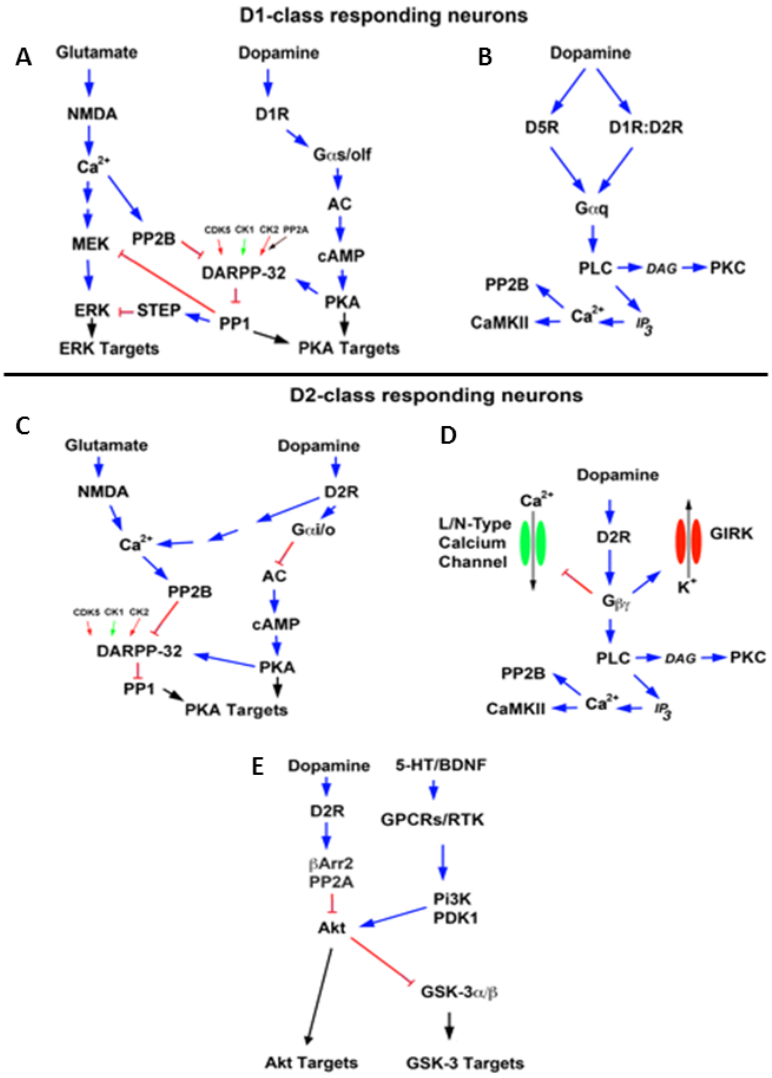

Figure 1.2 Dopamine receptor signaling. Top. Signaling networks regulated by D1-class DA receptors. **A.** Regulation of Gαs/cAMP/PKA signaling by D1-class DA receptors. **B.** Regulation of Gαq/PLC signaling by D1-class DA receptors or D1:D2 dopamine receptor heterodimers. **Bottom.** Signaling networks regulated by D2-class DA receptors. **C.** Regulation of Gαi/o/cAMP/PKA signaling by D2-class receptors. **D.** Regulation of Gβγ signaling by D2-class receptors. **E.** Regulation of β-arrestin 2/Akt/GSK-3 signaling by D2 and D3 dopamine receptors. The action of other neurotransmitters, growth factors, and neurotrophin has been included to illustrate the role of many of these intermediates as signal integrators. Blue arrows = activation, red T-arrows = inhibition, and green arrows = amplification of an already activated function. Black arrows = actions that can either be activating or inhibitory on the function of specific substrates. All abbreviations defined in List of Abbreviations. Adapted from Beaulieu and Gainetdinov 2011.

Recently, a Protein Kinase B (AKT)/ β-arrestin 2/protein phosphatase 2A (PP2A) pathway has been described downstream of D2 and D3 receptors (Beaulieu, Sotnikova et al. 2005). G proteins can additionally signal through their Gβγ subunits as well as initiate G-protein independent signaling.

The D1 and D2 dopamine receptors are the most broadly expressed within the brain, and both are highly expressed on MSNs in the nucleus accumbens and dorsal striatum. D2-type receptors have both pre and post-synaptic expression profiles. Presynaptically they serve as autoreceptors mediating autoregulatory feedback inhibition of further dopamine cell firing, synthesis, and release (Beaulieu and Gainetdinov 2011). Postsynaptically, dopamine D1 and D2 receptors in the striatum largely segregate into distinct populations with unique molecular profiles and projection targets. Until recently there was believed to be little functional overlap, but it is now increasingly clear that dopamine receptor heteromers represent a biologically relevant subpopulation within the brain with unique pharmacological and signal transduction profiles (Hasbi, O'Dowd et al. 2011). The co-occurrence of D1 and D2 receptors has been estimated at 6-7% in dorsal striatum and as much as 20-30% in the nucleus accumbens (Hasbi, O'Dowd et al. 2011).

Dopamine and psychiatric disease

Aberrant dopamine function is postulated to contribute to the pathology of several neuropsychiatric disorders. The dopamine hypothesis of schizophrenia

postulates that the positive symptoms of the disease are initiated due to over-activity of striatal D2 receptor pathways and the negative symptoms are due to hypoactivity in prefrontal cortical dopamine (Toda and Abi-Dargham 2007). Similarly, a dopamine hypothesis of bipolar disorder (BD) gained popularity with the manic phase of BD associated with amplified dopaminergic tone while depressive states were associated with deficits in the neurotransmitter. This role was supported by the fact that mania can be triggered by dopamine agonists or administration of the catecholamine precursor L-DOPA (Murphy, Brodie et al. 1971; Cousins, Butts et al. 2009). Likewise, dopamine depletion or dopamine receptor antagonism can lead to depression-like symptoms (Kummer and Teixeira 2008). Additional evidence comes from an analysis of post-mortem brain samples of the pre-frontal cortex from diseased brains and healthy controls that found *DRD2* expression increased in bipolar patients and decreased in schizophrenics relative to controls (Zhan, Kerr et al. 2011). Furthermore, the important signaling molecule downstream of dopamine receptor activation, DARPP-32, was increased in both patient populations in this same study. However, post-mortem studies are difficult to interpret because anti-psychotics modify the dopamine system. Data collected from *in vivo* imaging studies of D2 receptor occupancy within the basal ganglia have reported an increase in binding in bipolar psychotic patients (Wong, Pearlson et al. 1997; Nikolaus, Antke et al. 2009). PET imaging studies show an increase in vesicular monoamine transporter (VMAT2) binding, a marker of monoamine cells, in the thalamus and ventral brainstem of BD patients demonstrating psychosis compared to healthy

controls (Zubieta, Huguelet et al. 2000). The commonly prescribed mood stabilizer lithium also has an effect on dopamine transmission. Rats chronically treated with lithium display lower levels of dopamine release compared to non-treated controls which returns to normal levels after several days of withdrawal from treatment (Ferrie, Young et al. 2005). Taken together, these studies support a role for the involvement of dopaminergic mechanisms in the pathology and treatment of neuropsychiatric diseases.

Bipolar Disorder diagnosis and classification

Bipolar disorder, historically termed manic-depressive illness, is a chronic psychiatric disease marked by dramatic fluctuations in mood and behavior. While every individual experiences normal highs and lows in emotion, these mood states are heightened beyond the normal range and last for extended periods of time in individuals with BD as illustrated in Figure 1.3. Symptoms may emerge at any age including pediatric diagnoses, but at least 50% of all cases are identified before the age of 25 (Kessler, Berglund et al. 2005). BD is not one single disease, but rather a spectrum of disorders that fall within a continuum. The *Diagnostic and Statistical Manual for Mental Disorders,* Fourth Edition (DSM-IV) recognizes Bipolar I, Bipolar II, Bipolar Disorder not otherwise specified (BD-NOS) and cyclothymic disorder as distinct classifications (APA 2000), and Table 1.1 identifies the criteria for identification of these discrete subtypes based on the manifestation of manic or depressive mood states.

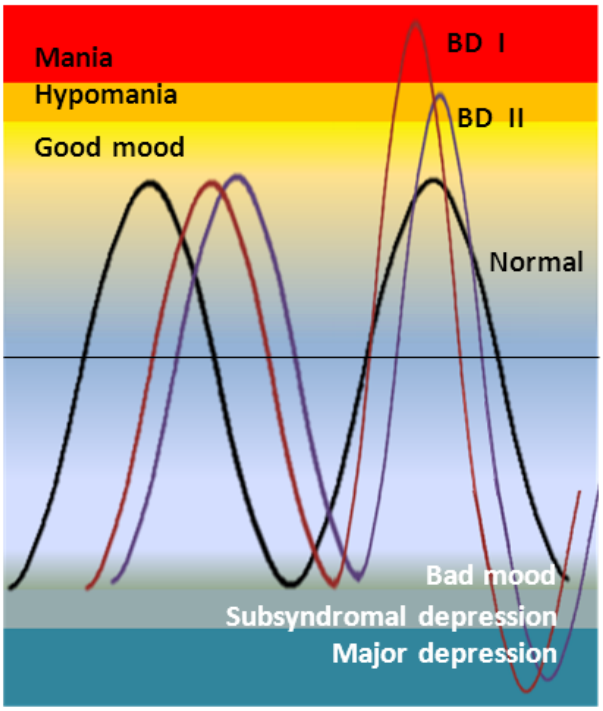

Mania

- Excessively "high" mood
- Irritable and agitated
- Racing thoughts
- Distractibility
- Restless/decreased sleep
- Delusions of grandeur
- Impulsivity and risk-taking
- Increased goal-directed activities

Depression

- Excessive worry or sadness
- Lose interest in pleasurable activities
- Exhaustion, feeling rundown
- Problems with concentration, memory and decision-making
- Restless or irritable
- Changes in eating
- Deviations in sleeping patterns
- Thoughts of suicide

Figure 1.3 Normal and abnormal mood cycles. The image graphically depicts the common course of mood episodes in a normal individual (black line) who experiences both good and bad mood states within a socially acceptable range compared to individuals with different types of bipolar disorder (Bipolar I-maroon; Bipolar II- purple) who cycle between manic and depressive episodes of varying intensity. Boxed to the right are summaries of DSM- IV criteria for manic and major depressive episodes. Adapted from the Cleveland Clinic Foundation Disease Management Project.

	Mania	Hypomania	Depression (MDE)
Bipolar I	Yes	Yes	Often; Not required
Bipolar II	No	Yes	Yes
Cyclothymia	No	Yes	1-2yr without full MDE but frequent high and unstable mood
Bipolar NOS	No	Yes	No MDE, but some symptoms of depression
or			
Bipolar NOS	No	Some symptoms	Yes

Table 1.1 Criteria for inclusion into Bipolar Spectrum Disorder subtypes. Bipolar disorder refers to a spectrum of diseases as indicated in the above table. Diagnosis of a particular subtype depends on the presence and severity of manic and/or depressive symptoms. Adapted from Sachs, 2007.

Mania, the hallmark of a Bipolar I diagnosis, is a distinctive period of abnormally elevated mood with associated features such as racing thoughts and delusions of grandeur. Conversely, a major depressive episode is marked by periods of dysphoria, fatigue, and commonly suicidal ideations (see Figure 1 for full list of associated features) (APA 2000). In addition to purely manic or depressive episodes, mixed states of both mania and depression are common in bipolar disorder. The occurrence of these mixed states is problematic on a number of levels. There is a lack of consensus in terms of the diagnostic criteria used to identify a mixed type episode, and these subjects are more difficult to treat (Vieta and Moralla, 2010). Additionally, evidence suggests that for BD patients with a first major episode of a mixed-state versus mania there is a poorer prognosis with higher rates of morbidity at follow-up (Baldessarini et al, 2010). The presence of these mixed states of mania and depression adds yet more complexity to the bipolar spectrum.

Bipolar disorder outcomes and comorbidity

Bipolar spectrum disorders affect some 3-5% of the population with varying degrees of severity (Kessler, Berglund et al. 2005). While it is a treatable illness, there is no cure. Furthermore, most treatments are aimed at ameliorating the clinical symptoms while sub-syndromal symptoms and cognitive deficits may persist leading to an overall decrease in quality of life in terms of social and occupational outcomes (Sanchez-Moreno, Martinez-Aran et al. 2009). The World Health Organization reports that BD is the sixth leading cause of disability

worldwide with a contributing factor being that only 1/3 of patients will recover full social and occupational function after receiving treatment (Huxley and Baldessarini 2007). Worse yet, 25-50% of BD patients will make at least one suicide attempt, and their rate of completed suicides per attempt is much higher than the general population (Leahy 2007).

Bipolar disorder is often comorbid with other medical and mental disorders which may complicate its diagnosis and treatment. As early as the 1920s it was recognized that individuals with manic depressive illness abused alcohol at higher rates than the general population (Sherwood Brown, Suppes et al. 2001). The same appears to be true for many other drugs of abuse with overall rates of comorbidity nearing 60% (Krishnan 2005). Other mental diagnoses also have particularly high rates of comorbidity with BD including anxiety disorders (71%), social phobia (47%), and personality disorders (36%) (Krishnan 2005). In a cross-sectional and longitudinal retrospective analysis of veterans diagnosed with bipolar disorder a full 81% of this population was found to have medical comorbidities (Fenn, Bauer et al. 2005). A number of metabolic disturbances including cardiovascular disease, thyroid disease, diabetes and obesity are over-represented in the BD population compared to controls (Leahy 2007; McIntyre 2008). In many cases, it is unclear whether these syndromes are truly comorbid or whether they are merely consequences of the treatments.

Genetics of Bipolar Disorder

Like most psychiatric diseases, bipolar disorder is a multifactorial illness with a strong genetic component and clear-cut environmental triggers. Heritability estimates of BD from twin studies indicate concordance rates upwards of 80-90% (McGuffin, Rijsdijk et al. 2003). A large number of linkage, association, and polymorphism analyses have revealed a number of genetic loci with nominal association with the disease. These studies have notoriously suffered from a lack of reproducibility between laboratories, but a systematic review of the literature denotes a handful of genes that have been repeatedly linked with bipolar illness. Among these are genes involved in dopaminergic (*DRD4, dopamine D4 receptor; SLC6A3, dopamine transporter*) glutamatergic (*DAOA, D-amino acid oxidase activator; DTNBP1, dystrobrevin binding protein 1*) and serotonergic transmission (*SLC6A4, serotonin transporter; TPH2, tryptophan hydroxylase 2*) as well as others involved in the regulation of cell growth and maintenance (*NRG1, neuregulin 1; DISC1, disrupted in schizophrenia 1; BDNF, brain-derived neurotrophic factor*) (Serretti and Mandelli 2008). These results point to disturbances in neurotransmission as a common mechanism underlying the pathogenesis of bipolar disorder. More recently, candidate gene studies have been initiated to identify circadian genes associated with affective disorders like BD due to the behavioral cycling characteristic of these diseases. These studies have identified polymorphisms in a handful of circadian genes with suggested association with BD, and the results will be discussed in more detail in the subsequent sections.

The mammalian circadian clock

Circadian, literally meaning “about a day”, refers to the approximately 24 hour rhythms in physiology and behavior observed from humans down to unicellular organisms. The master pacemaker, so called because it is required for synchronous rhythms of gene expression throughout the brain and peripheral tissues, resides in the suprachiasmatic nucleus (SCN) of the hypothalamus, but the molecular machinery is present throughout the brain and body in peripheral oscillators. Over 10% of all mammalian transcripts are rhythmic, and surprisingly there is limited overlap in rhythmic expression profiles between different tissues (Lowrey and Takahashi 2004). The core molecular clockwork is composed of transcriptional and translational feedback loops which govern this cycle. The transcription factors Circadian Locomotor Output Cycles Kaput (CLOCK) and Brain and Muscle Arnt-Like protein 1 (BMAL1 or ARNTL1), illustrated in Figure 1.4, heterodimerize and bind to E-box containing sequences (CACGTG) in their responsive genes termed clock-controlled genes (CCGs) (reviewed in (Ko and Takahashi 2006)). The CLOCK:BMAL1 dimer positively regulates the transcription of the three *Period* genes *(Per1, Per2, and Per3)* and two *Cryptochrome* genes *(Cry1, Cry2)* among others. The protein products of *Per1* and 2 and *Cry1* and 2 themselves function as core clock components. PER and CRY dimerize and return to the nucleus where they inhibit CLOCK:BMAL1 function forming a negative feedback loop. In an adjacent loop, CLOCK:BMAL1 activates the transcription of the retinoic-acid related orphan nuclear receptors

Rev-erbα and *Ror-α*. On the negative limb of this loop, transcription factors REV-ERBα and RORα inhibit or induce *Bmal1* transcription, respectively.

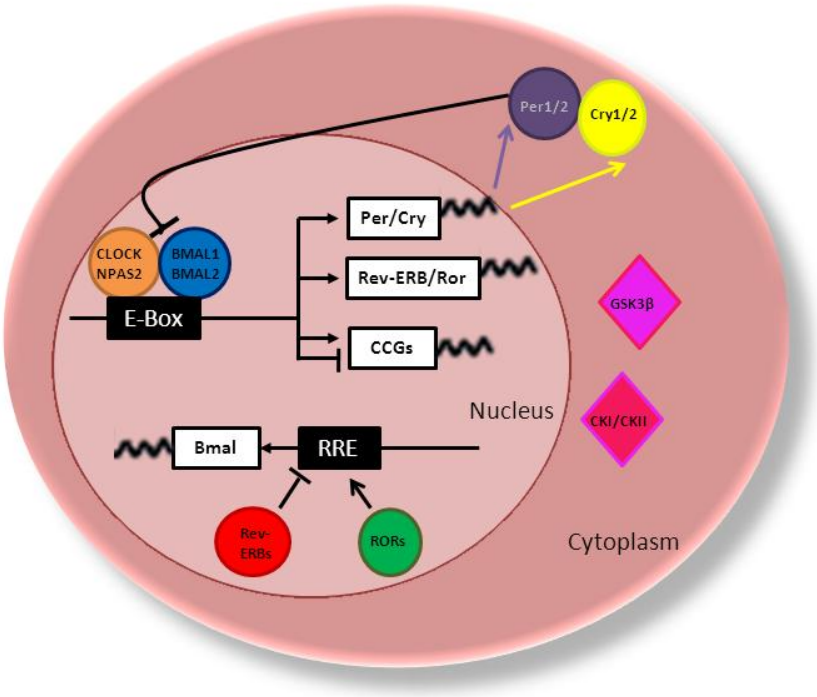

Figure 1.4 The mammalian circadian clock. CLOCK and BMAL1 (or NPAS2 and BMAL1) regulate the expression of many clock controlled genes (CCGs) including the *Period* and *Cryptochrome* genes. These are translated in cytoplasm and re-enter the nucleus to inhibit the activity of CLOCK:BMAL1. A separate loop depicted at the bottom of the nucleus shows the regulation of *Bmal1* by ROR and REV-ERB. Additionally, kinases like GSK3β and CK1 act on core clock components to regulate protein stability, localization, and activity.

Redundancy of the clock

Due to the critical importance of the circadian mechanism, it is not surprising that a certain level of functional redundancy has been built into the

system. Many of the proteins have homologs which fully or partially substitute for their absence or dysfunction. Neuronal Period Arnt Single-minded (PAS) Domain protein 2 (NPAS2) is a forebrain-specific CLOCK homolog which can dimerize with BMAL1 and control CCG expression. In the absence of CLOCK, NPAS2 compensates to maintain circadian function in the SCN (DeBruyne, Weaver et al. 2007). Until recently, BMAL1 was considered the only exception to the redundancy rule because the knockout of the single gene results in arrhythmic behavior and significant detrimental effects on health and longevity measures suggesting that homolog BMAL2 (ARNTL2) cannot functionally substitute for BMAL1. When BMAL1 knockout mice were combined with constitutively expressing BMAL2 transgenic animals these phenotypes were rescued (Shi, Hida et al. 2010). Researchers discovered that the BMAL1 knockout is functionally a BMAL1 knockout /BMAL2 knockdown because BMAL2 is downstream of CLOCK:BMAL1 transactivation (Shi, Hida et al. 2010). *Per1* and *Per2*, though not fully functionally redundant, can compensate for each other to some extent. The single knockout of either of these genes results in severe disruption of locomotor activity rhythms in constant darkness (DD), but they display shortened free-running rhythms for several days before becoming arrhythmic (Bae, Jin et al. 2001). In contrast, the *Per1/Per2* double mutants immediately lose behavioral rhythmicity when switched to DD conditions (Bae, Jin et al. 2001). Mice with disruptions in *Per3* function do not display a loss of behavioral rhythms, but their circadian period is significantly shorter in DD (Shearman, Jin et al. 2000). Furthermore, the combined loss of *Per3* with *Per1* or

Per2 does not enhance the severity of the phenotype (Bae, Jin et al. 2001). These results seemed to indicate that *Per3* is not an essential component of the circadian clock; however, recent studies suggest a more tissue-specific role for *Per3* in circadian timekeeping of peripheral oscillators throughout the body, like the liver, lung, and esophagus (Pendergast, Niswender et al. 2012). Similar to *Per1* and *Per2,* the *Cry1* and *Cry2* single mutants have functional overlap. The single knockout of either gene does not result in a loss of rhythms although there is a significant deviation from the 24 hour period in both *Cry1-/-* (τ = 22.51) and *Cry2 -/-* (τ =24.63) mice but, the *Cry1/Cry2* double mutants immediately become arrhythmic in DD conditions (Horst, Muijtjens et al. 1999). The level of redundancy built into this single system attests to its importance in maintaining proper control over diverse biological processes.

Post-translational regulation of the clock

There are a number of key proteins outside of the core transcriptional feedback loop that regulate circadian timing through post-translational mechanisms. Phosphorylation is central among these modifications with roles including regulation of protein stability and nuclear translocation. Casein Kinase one delta and epsilon proteins (CKIδ and CKIε) are important regulators of the mammalian clock acting on the circadian substrates PER1, PER2, CRY1, CRY2 and BMAL1 (Virshup, Eide et al. 2007). In fact, the first identified mammalian circadian rhythms mutant was the *tau* hamster which was eventually identified as a gain-of-function mutation in CKIε resulting in a shortened period (Virshup, Eide

et al. 2007). A mutation in the human CK1δ (T44A) is associated with familial advanced phase sleep syndrome (FASPS), and transgenic mice carrying this mutation likewise have a shortened circadian period (Xu, Padiath et al. 2005). CKIδ and CKIε control the abundance of PER1 and PER2 through phosphorylation which leads to the recruitment of the ubiquitin ligase βTrCP (Beta-transducin repeat containing protein) targeting the proteins for proteolysis (Virshup, Eide et al. 2007). Protein degradation is a critical modulator of the circadian clock as research demonstrates that the stoichiometric relationship between the levels of the circadian proteins actually regulates the amplitude of the circadian oscillation (Lee, Chen et al. 2011). In addition to its role in protein stability, CKI also phosphorylates BMAL1 and enhances its transcriptional activity (Eide, Vielhaber et al. 2002).

Glycogen synthase kinase 3-β (GSK3β) is a serine/threonine protein kinase that regulates the circadian clock (Iitaka, Miyazaki et al. 2005). GSK3β acts as a key signaling molecule that regulates a wide range of fundamental cellular processes including neuronal development, metabolism, gene expression, and synaptic plasticity. Aberrant activity of the enzyme has been implicated in a number of diseases including metabolic disorders, cancer, neurodegenerative diseases, and neuropsychiatric disorders. Molecules targeting GSK3 have been tested in clinical and pre-clinical trials for Alzheimer's disease, depression, Amyotrophic lateral sclerosis (ALS), and bipolar disorder (Chico, Van Eldik et al. 2009). In the mammalian molecular clock, phosphorylation of core clock components by GSK3β has a variety of outcomes. GSK3β phosphorylates

PER2 promoting its nuclear entry (Iitaka, Miyazaki et al. 2005). Phosphorylation by GSK3β increases the protein stability of Rev-erbα but targets CRY2 and CLOCK for proteasomal degradation (Iitaka, Miyazaki et al. 2005; Spengler, Kuropatwinski et al. 2009; Kurabayashi, Hirota et al. 2010). Interestingly, GSK3β is directly inhibited by the common mood-stabilizer lithium. It has been widely hypothesized that its therapeutic benefits are derived by this mechanism, but the evidence has been equivocal. Lithium is known to lengthen the circadian period both *in vitro* and in a variety of organisms (Welsh and Moore-Ede 1990; Abe, Herzog et al. 2000).Yet, in a high-throughput circadian function screen of small molecules, inhibitors of GSK-3β consistently led to a shortened period indicating that the long-period phenotype observed with lithium treatment is likely due to its actions on targets other than GSK3β (Hirota, Lewis et al. 2008). In further support of this data, the short period effect was replicated by a siRNA-mediated knockdown of GSK-3β (Hirota, Lewis et al. 2008). Understanding these discrepancies is of great interest because GSK-3β inhibitors are being pursued as targets for a variety of diseases which may be affected by the clock. Less is known about other kinases and phosphatases that regulate the mammalian clock, but it is recognized that post-translational modifications are essential for the generation of circadian rhythms.

Mood disorders and circadian disruption

Based upon the clinical observation of behavioral rhythm disturbances in patients with affective disorders, it has been hypothesized that disruptions of the

circadian clock may play an important role in the development of these disorders. Analysis of activity patterns in human patients with bipolar disorder reveals major deviations from a normal diurnal or circadian rhythm. Curt Paul Richter wrote a seminal review of biological clocks in medicine and psychiatry in which he assimilated decades of case studies detailing cycles in physiology and behavior present in various pathologies (Richter 1960). Based on his own observations and a thorough review of the literature he came up with a theory termed the "shock phase hypothesis" which posited that clocks manifested themselves in physical and mental symptoms of humans under abnormal conditions. According to this theory, all of the body's organs and systems contain clocks that cycle independently and out of phase, but in the presence of some trauma or shock they become synchronized leading to a disease state in which the underlying rhythm is revealed. Over the last 50 years of chronobiological research, several researchers have disproved this theory and discovered the opposite to be true, but Richter's notions inspired much of the subsequent investigation.

Richter's hypothesis was based on the observation that while animals from fruit flies to lab rats had clear endogenous rhythms, humans seemed to operate on an exogenous clock with minimal cycling under normal conditions. Unlike in the laboratory setting, observation of human behavior was hampered by a lack of control over external stimuli. In 1965, Jürgen Aschoff decided to address this issue by performing studies on humans in isolation bunkers to determine whether true circadian rhythms were present in biological and activity measures. He reported rhythms in urine excretion, body temperature, and activity

in this artificial environment in the absence of external light and time cues although the free-running period varied dramatically for each subject (Aschoff 1965). Disruptions in these physiological rhythms either through genetic or behavioral desynchronization can lead to a multitude of maladaptive conditions including sleep disorders, cancer, metabolic syndrome, addiction, and mood disorders (Bechtold, Gibbs et al. 2010). As mentioned previously, sleep disturbances are a prominent feature of many affective disorders including mania and depression. The DSM-IV lists both insomnia and hypersomnia as symptoms of major depression and a decrease in the subjective need for sleep as a symptom of a manic episode (APA 2000). Research indicates that sleep disturbances are not simply a consequence of the disease state but may be a contributing factor to the onset of a depressive or manic episode (Harvey 2011). Sleep dysregulation is not the only means by which the internal and external clocks may be uncoupled. Shift work disorder, brought on by a work period that coincides with the usual sleep phase, has garnered much attention of late as it can lead to major health complications including heart disease, metabolic syndrome, and mood disorders (Basner 2005). Even acute disruptions of the biological clock as occurs with transcontinental flight can lead to feelings of disorientation and fatigue which can last for several days, a phenomenon commonly called “jet-lag.”

If desynchronization can have pathologic effects, it is not surprising that resynchronization or resetting of the clock can have therapeutic benefits. Bright light therapy has been in use for over two decades as a treatment

for seasonal affective disorder (SAD) or winter depression, but more recently its circadian phase-shifting effects have been investigated for efficacy in treating major depression, bipolar depression, and even depression associated with Parkinson's disease (Michael 2007). Other non-pharmacological chronotherapeutic interventions include total or partial sleep deprivation for rapid but transient alleviation of depressive symptoms and interpersonal and social rhythm therapy for long-term maintenance of mood in BD patients (Monteleone et al. 2010). Several traditional pharmacologic agents effective in treating mood disorders also have effects on circadian rhythms. The antidepressants desipramine (tricyclic) and fluoxetine (selective serotonin reuptake inhibitor, SSRI) shorten the circadian period while imipramine (tricyclic) and the mood stabilizer lithium lengthen the period (Abe, Herzog et al. 2000; Rosenwasser 2001). It is hypothesized that these mood stabilizers and antidepressants ultimately converge on the clock by affecting ascending serotonergic projections from the raphe nuclei which modulate SCN neuronal firing rate or response to light (Monteleone et al. 2010). Research and development of novel therapies for affective disorders like depression and bipolar disorder have been motivated in part by efforts to cultivate new treatments that directly target the circadian system rather than neurotransmitter systems.

Identification of possible targets has benefited from advancements in molecular biology over the past 20 years, and the identification of key players involved in regulating the molecular clock. Recent genetic studies have begun to identify circadian genes with significant association with affective disorders. A

single nucleotide polymorphism (SNP) in the core clock gene *Cry2* was associated with rapid cycling bipolar disorder (Sjöholm, Backlund et al. 2010) and vulnerability for depression in a Swedish population (Lavebratt, Sjöholm et al. 2010). In a Spanish population, several SNPs in *CLOCK* and *VIP* (*vasoactive intestinal peptide*) showed a nominal association with BD while variations in *Cry1* and *Npas2* were associated with depression (Soria, Martinez-Amoros et al. 2010). Noticeably, these candidate gene studies did not yield consistent results, and the incongruent findings in these reports limit the interpretation of these and similar studies that have been carried out on small populations. Recent large-scale genome wide association studies failed to identify clock genes associated with BD, perhaps owing to the fact that bipolar disorder is caused by a large number of genetic variants rather than one or two loci (Ferreira et al. 2008; Scott et al. 2009); However an extensive network analysis revealed that associations with BD spectrum disorders and lithium responsiveness were enriched among core clock genes (McCarthy, 2012). Thus despite inconsistent findings at the single gene level, taken together these studies suggest that disruptions in the circadian clockwork are linked to mood dysregulation.

Dopamine and the clock

Early on it was discovered that dopamine-containing retinal amacrine cells displayed persistent circadian rhythms in dopamine levels and synthesis (Wirz-Justice, Da Prada et al. 1984). This finding was intriguing because it belied a major role for retinal dopamine in transmitting phase-setting information to the

SCN. As a result, numerous studies have concentrated their efforts on understanding the relationship between dopamine neurotransmission and the circadian clock in the retinal system. We now know that dopamine through interactions with the D4 dopamine receptor and negative coupling to adenylyl cyclase 1 (AC1) regulates a number of molecular circadian rhythms within the retina (Jackson, Chaurasia et al. 2011). Outside of the retina, mounting evidence indicates that there is significant cross-talk between the dopamine system and the circadian clock in other nuclei including the midbrain dopamine system. Diurnal or circadian rhythms have been reported for dopamine release, receptor expression and binding, and levels of related enzymes (Wirz-Justice 1987; Ozaki, Duncan et al. 1993; Castañeda, de Prado et al. 2004; Akhisaroglu, Kurtuncu et al. 2005). Recently, it has been reported that the transcription of the catabolic enzyme Monoamine Oxidase A (Maoa) is directly regulated by circadian components BMAL1, NPAS2, and PER2 (Hampp, Ripperger et al. 2008). Conversely, endogenous dopamine has been reported to regulate levels of the circadian protein PER2 in the striatum (Hood, Cassidy et al. 2010). Interestingly, many psychoactive drugs or compounds that specifically target the dopamine system modify the expression of core circadian genes both *in vivo* and in culture systems. For example, administration of D1 or D2 receptor specific agonists to primary striatal cultures (SKF 38393 or quinpirole) resulted in opposite modulation of circadian gene expression with SKF causing across the board increases in the expression of *mClock, m NPAS2, mBmal1* and *mPer1*

while quinpirole selectively decreased *mClock* and *mPer1* (Imbesi, Yildiz et al. 2009).

The Clock mutant mouse model of mania

In 1994, Joseph Takahashi and colleagues reported the identification of the second mammalian circadian mutant, the *Clock* mutant mouse. Researchers used an N-ethyl-N-nitrosurea (ENU) mutagenesis forward genetics screen to identify animals that deviated from the normal circadian period length of the founder C57BL/6J strain of 23.3-23.7 hours (Vitaterna, King et al. 1994). Out of 304 heterozygous G_1 offspring tested, 1 animal displayed an abnormal circadian period that lengthened to 24.6 hours in constant darkness conditions (Vitaterna, King et al. 1994). This animal was backcrossed and progeny were intercrossed with BALB/cJ mice to generate homozygous C56xBALB *Clock/Clock* mice with a longer (~27.3 hr-cite) period in DD that eventually dampened out leaving an ultradian pattern (Vitaterna, King et al. 1994). This mutation was mapped to chromosome 5 and positional cloning identified the exact locus and nature of the *Clock* mutation. Sequence analysis predicted that CLOCK was a novel bHLH-PAS domain transcription factor. ENU mutagenesis usually produces point mutations, and researchers discovered an A→T change at the 5' donor splice site of exon 19 resulting in exon skipping and a 51 amino acid deletion within the glutamine-rich region of the C-terminus of the CLOCK, thus it was renamed the *Clock*Δ19 mutation. This mutation was anticipated to affect the transactivation activity of the predicted transcription factor while leaving the protein dimerization

and DNA binding functions intact (King, Vitaterna et al. 1997). This explanation would account for the apparent dominant-negative phenotype observed with the mutation. In a subsequent study, this hypothesis was confirmed and BMAL1, a protein of then unknown function, was identified as a heterodimerization partner of CLOCK in a yeast two-hybrid screen (Gekakis, Staknis et al. 1998). The CLOCK:BMAL1 heterodimer induced transcription of the circadian *mPer1* gene by binding to E-box elements in the promoter. As predicted, the CLOCKΔ19 protein still dimerized with BMAL1 and bound to DNA, but it was no longer able to drive transcription of *mPer1* (Gekakis, Staknis et al. 1998).

We now know that CLOCK is core element of the circadian lock mechanism involved in a number of essential processes, thus it is not surprising that the *Clock*Δ19 mutant phenotype extends beyond circadian rhythms. The *Clock*Δ19 mutants also sleep significantly less than their wild type counterparts by approximately 2 hours due to a loss of non-rapid eye movement sleep (NREM) under normal 12:12 LD conditions (Naylor, Bergmann et al. 2000). This difference is maintained under free-running constant darkness conditions. The mutants additionally have widespread energy and metabolism related phenotypes. The mutants display disrupted feeding patterns and increased caloric intake coupled with a cumulative 10% decrease in energy expenditure which eventually results in an overweight phenotype beginning at six weeks of age (Turek, Joshu et al. 2005). The mutant mice show a variety of biochemical abnormalities with increases in serum triglycerides, cholesterol, glucose, and

leptin concentrations indicative of a metabolic syndrome (Turek, Joshu et al. 2005).

More recently, our laboratory has undertaken studies in the *Clock*Δ19 mutant related to affect because circadian rhythms have such a strong association with mood disorders. A comprehensive study was conducted by Roybal et al to determine if the *Clock*Δ19 mice had any mood, reward or anxiety-related phenotypes (Roybal, Theobold et al. 2007). They found that in mutants the current required to elicit intracranial self-stimulation (ICSS) of the medial forebrain bundle (MFB) was significantly lower than that of wild types indicating a lower reward threshold. Furthermore, *Clock*Δ19 mutants have an increased preference for cocaine at a relatively low 5 mg/kg dose (McClung, Sidiropoulou et al. 2005), and a significantly lower dose of cocaine is required to lower the ICSS threshold of the mutants (Roybal, Theobold et al. 2007). Likewise, for a natural sucrose reward, the mutants developed a larger preference. This reward-related phenotype is consistent with the symptoms of extreme euphoria and the propensity toward drug use observed in the manic state. In the Porsolt swim test and learned helplessness paradigms, measures of behavioral despair, the *Clock*Δ19 mutants had less depression-related behavior (Roybal, Theobold et al. 2007). Moreover, anxiety-related behavior as measured by time spent in the center of an open field and entries onto the open of arms of an elevated plus maze was significantly lower in the *Clock* mutants (Roybal, Theobold et al. 2007). The increase in exploratory activity in these tasks can arguably be equated to an increase in risk-taking behavior that is often associated with mania. Interestingly,

chronic treatment with the mood-stabilizer lithium normalized their behavioral phenotypes (Roybal, Theobold et al. 2007). Taken together, the data suggested that the *Clock*Δ19 mutant mice might represent a valid model of mania. It should be acknowledged that the interpretation of the anxiety-related phenotype is controversial to some because anxiety disorders are highly comorbid with BD; but both mania and mixed states can be further divided into several subtypes including purely euphoric mania and depressed or anxious mania that differ in their presentation of symptoms (Young et al. 2011). As with all animal models of complex human diseases, it is impossible to recreate every facet of the human condition, but the *Clock*Δ19 mutants may come close to approximating the state of euphoric mania.

As a consequence of these findings, much of the work in our lab has been dedicated to identifying the mechanisms underlying these phenotypes. Much attention has focused on the ventral tegmental area (VTA) because dopaminergic dysfunction could account for a number of the behavioral changes. In validation of this hypothesis, rescue of CLOCK function with viral over-expression in the VTA ameliorates the locomotor hyperactivity to novelty and anxiety-related phenotypes (Roybal, Theobold et al. 2007) while knock-down of CLOCK via short-hairpin RNA (shRNA) in the VTA reproduces the hyperactivity and anti-anxiety phenotype of the *Clock*Δ19 mutants (Mukherjee, Coque et al. 2010). Additionally, *Clock*Δ19 mice display increased bursting and firing of VTA dopamine cells, while a specific reduction of firing rates in the VTA of *Clock*Δ19 mice reverses many of their abnormal behavioral phenotypes (McClung,

Sidiropoulou et al. 2005; Coque, Mukherjee et al. 2011). Microarray analysis of the VTA of *Clock*Δ19 mice has revealed dysregulation in the levels of several key genes involved in dopamine transmission, including *TH,* the rate-limiting enzyme in dopamine synthesis (McClung, Sidiropoulou et al. 2005). The research compiled in this thesis expands upon these previous results and further identifies a role for alterations in dopaminergic transmission as a key contributor to certain facets of the manic-like phenotype in this mouse model.

Goals of the dissertation research

The aim of the present study is to examine possible interactions between the circadian and dopamine systems in the context of a mouse mania model, the *Clock*Δ19 mutant. It is hypothesized that there are functionally significant perturbations in VTA dopamine function as a direct result of the loss of CLOCK. Furthermore, these changes in dopamine function are responsible for mediating the aberrant behavior. To that end, rhythmic expression tyrosine hydroxylase mRNA and protein will be assessed within the VTA. Furthermore, the presence of a direct regulation by CLOCK on *TH* transcription will be investigated as a mechanism underlying the molecular variation.

It is hypothesized that the *Clock*Δ mutant represents a model of hyperdopaminergia given that dopamine cell firing and TH levels are elevated in the VTA. Accordingly, assays will be performed to assess changes in dopamine and metabolites in striatal tissue. Given the premise of altered presynaptic dopamine function, it will be determined whether there are coincident changes in

dopamine receptor function by employing several different pharmacological and biochemical assays. Ultimately, this work may link two discrete hypotheses for the development of bipolar disorder. These results will give credence to the long-standing dopamine hypothesis of bipolar disorder and explain how a disruption of the circadian clock can impact neurotransmission.

CHAPTER 2
Results

DIRECT REGULATION OF DOPAMINERGIC ACTIVITY BY CLOCK AND ITS IMPORTANCE IN ANXIETY RELATED BEHAVIORS

(Submitted to Nature Neuroscience)

Sade Spencer*, Michelle M Sidor*, Rachel Arey, Kafui Dzirasa, John F Enwright III, Kay M Tye, Melissa Warden, Jacob PR Jacobsen, Sunil Kumar, Erin M Remillard, Marc Caron, Karl Deisseroth, and Colleen A McClung

Introduction

Anxiety is a complex mood state that arises from a dynamic interplay between physical, emotional, cognitive, and behavioral responses. In its natural state, anxiety can be considered a normal and adaptive expression of apprehension that manifests itself in response to events or situations perceived as threatening. Aberrant regulation of anxiety signaling, however, can alter these normal adaptive responses leading to inappropriate or disproportionate levels of anxiety. Anxiety disorders represent the most common mental health illnesses that occur across the lifespan (Zhan, Kerr et al. 2011) and are, themselves, highly co-morbid with a number of psychiatric disorders such as major depressive disorder and bipolar disorder (Keller 2006). Similarly, mice with a point mutation in the *Clock* gene (*Clock*Δ19) (King, Vitaterna et al. 1997; Gekakis, Staknis et al. 1998), a core regulatory component of the circadian transcriptional machinery, display notable deficits in anxiety-related behavior that occur within the context of an overall “manic-like” phenotype (Roybal, Theobold

et al. 2007; Dzirasa, McGarity et al. 2011) which includes hyperactivity, hyperhedonia, increased preference for cocaine and disrupted circadian rhythms (McClung, Sidiropoulou et al. 2005; Roybal, Theobold et al. 2007). Indeed, abnormalities in circadian rhythms appear to be a prominent and pervasive endophenotype of many psychiatric disorders. Moreover, therapeutic interventions aimed at manipulating the sleep-wake cycle or regulating daily social rhythms have proven efficacious in their treatment and management (Frank, Swartz et al. 2000; Plante and Winkelman 2008). Very few studies, however, have investigated the relationship between circadian genes and anxiety. Most recently, an association analysis of circadian-clock-related genes revealed single nucleotide polymorphisms (SNPs) in *Brain and muscle ARNT-like 2 (Bmal2)*, also known as *ARNTL2* and the *dopamine D2 receptor (DRD2*) that associated with human anxiety disorders (Sipila, Kananen et al. 2010). The co-occurrence of both circadian rhythm abnormalities and altered anxiety-related behavior within the *Clock*Δ19 mouse makes this a valid and intriguing animal model by which to further explore the role of circadian rhythms in mediating disease symptomology.

Converging lines of evidence have pointed to alterations in mesolimbic dopaminergic activity as a prominent mediator of the aberrant behavioral profile of the *Clock*Δ19 mouse. For instance, *Clock*Δ19 mice display increased bursting and firing of ventral tegmental area (VTA) dopamine cells, while specific reduction of firing rates in the VTA of *Clock*Δ19 mice reverses many of their abnormal behavioral phenotypes (McClung, Sidiropoulou et al. 2005; Coque,

Mukherjee et al. 2011). Microarray analysis of the VTA of *Clock*Δ19 mice has revealed dysregulation in the levels of several key genes involved in dopamine transmission, including *tyrosine hydroxylase* (*TH*), the rate-limiting enzyme in dopamine synthesis (McClung, Sidiropoulou et al. 2005). It is likely that the dopamine and circadian hypotheses are not mutually exclusive as there is mounting evidence indicating significant cross-talk between the circadian clock and various neurotransmitter systems. Indeed, a diurnal rhythm in dopamine levels, in levels of related enzymes, and even receptor expression has been reported in numerous studies (Wirz-Justice 1987; Ozaki, Duncan et al. 1993; Akhisaroglu, Kurtuncu et al. 2005). For instance the transcription of the catabolic enzyme Monoamine Oxidase A is directly regulated by the circadian components BMAL1, Neuronal PAS Domain Protein 2 (NPAS2), and PERIOD 2 (PER2) (Hampp, Ripperger et al. 2008). Conversely, administration of dopamine agonists alters circadian gene expression in primary striatal cultures (Imbesi, Yildiz et al. 2009), and more recently, endogenous dopamine has been reported to regulate PER2 protein levels in striatal regions (Hood, Cassidy et al. 2010). Interestingly, direct knock-down of *Clock* in the VTA of wild type mice recapitulated the anxiety-related behavioral profile of *Clock*Δ19 mice (Mukherjee, Coque et al. 2010), hinting at a potential role for CLOCK in regulating VTA dopaminergic activity and anxiety-related behavior. Given these results, the first aim was to establish a direct causal and functionally significant link between alterations in VTA dopaminergic activity and anxiety-related behaviors in wild type mice. To accomplish this, optogenetics was employed to introduce cell-type specific light-

sensitive microbial channelrhodopsins into the VTA to enable the direct control of dopamine neuronal firing. Whereas most studies to date have examined the acute effects of light-induced neuronal activity on behavior, this study employed a novel approach utilizing optogenetic activation of a neuronal population in a chronic manner in order to examine the impact of long-term manipulation of *in vivo* neuronal activity on behavior – a paradigm that more accurately recapitulates the chronic nature of psychiatric disease. Furthermore, optical stimulation was performed in a temporal-specific manner to parallel changes in VTA dopamine neural activity that were observed across the light-dark cycle in *Clock*Δ19 mutant mice. In addition to determining the consequences of a mutated CLOCK, as present in *Clock*Δ19 mice, on TH levels and rhythms in dopaminergic activity, a potential mechanism by which CLOCK may regulate the observed differences in TH activity and rhythms was sought. To this end, an examination was conducted to determine whether CLOCK, itself, may act as a direct transcriptional regulator of *TH*.

Results

Daytime-specific elevation in VTA cell firing and bursting in *Clock*Δ19 mice

An increase in VTA cell firing and bursting in *Clock*Δ19 mice as measured both *in vivo* and in slice preparations at a single time of day has been previously reported (McClung, Sidiropoulou et al. 2005; Coque, Mukherjee et al. 2011). It was investigated whether this elevation was temporally restricted or perceptible throughout the 24 hour cycle in individual animals. *In vivo* recordings of VTA

dopamine neurons were performed during REM sleep rather than during awake periods so that dopaminergic firing would not be influenced by locomotor activity. In addition, the firing of dopaminergic neurons during REM sleep was measured as opposed to anesthetized animals, since REM sleep is a normal physiological state characterized by increased dopamine release (Maloney, Mainville et al. 2002; Lena, Parrot et al. 2005). *Clock*Δ19 mice spent significantly less time in REM sleep during the light phase compared to wild type (WT) littermates and had a highly disrupted diurnal rhythm in overall REM sleep (Figure 2.1A). Firing rates were elevated in *Clock*Δ19 mutants throughout the light-dark cycle (Figure 2.1B). This difference in firing rate reached significance at ZT 0-6, signifying the beginning of the light phase. The bursting rate was also significantly elevated in *Clock*Δ19 mice with the largest effect at ZT 12-18 (Figure 2.1C). Since the data suggested that the difference in bursting rate between WT and *Clock*Δ19 mice was largely driven by a reduction in the bursting rate of dopaminergic neurons in WT mice during this time interval, additional firing pattern analysis on individual dopaminergic neurons that were recorded during both the light and dark cycle was performed. When the bursting rate of dopaminergic neurons in WT mice was compared during the ZT0-6 versus ZT12-18 epochs, it was found that these neurons displayed a significantly reduced bursting rate during the dark cycle (Bursting rate: 2.3±0.4 bursts/10 seconds and 1.4±0.3 bursts/10 seconds during ZT0-6 and ZT12-18, respectively; n=11 neurons).

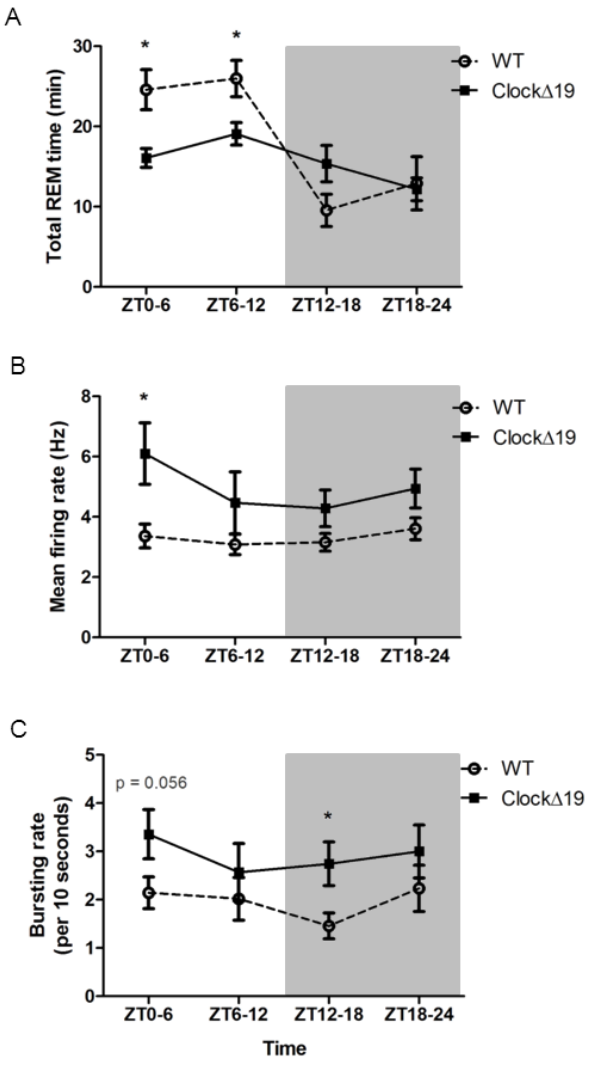

Figure 2.1. VTA firing rate during REM sleep. **A.** Two-way ANOVA of total REM time found a significant genotype by time segment interaction ($F_{3,67}$=6.37, p=0.008). Post-hoc tests revealed significant differences in total REM time during the light cycle (p<0.05 using student's t-test; wild type (WT) mice, n=8; *Clock*Δ19 mice, n=9). **B.** Two-way ANOVA of firing rate found a significant genotype effect ($F_{1,112}$=12.67, p=0.0006). Post-hoc tests revealed significant differences in the firing rate of dopaminergic neurons during the first 6 h of the light cycle and the last 6 h of the dark cycle (p<0.05 using student's t-test; n=14/14/16/12 and 14/14/17/12 for the number of dopaminergic neurons analyzed in WT and *Clock*Δ19 mice, respectively). **C.** Two-way ANOVA of bursting rate found a significant genotype effect [$F_{1,112}$=8.6, p=0.004] with post-hoc analyses revealing significant differences in the bursting rate of dopaminergic neurons during the first 6 h of the dark cycle (p<0.05, by student's t-test; n=14/14/16/12 and 14/14/17/12 for the number of dopaminergic neurons analyzed in WT and *Clock*Δ19 mice, respectively).

Conversely, no differences were observed in the bursting rate of dopaminergic neurons in *Clock*Δ19 mice during ZT0-6 versus ZT12-18 (Bursting rate: 3.4±0.6 bursts/10 seconds and 2.5±0.6 bursts/10 seconds during ZT0-6 and ZT12-18, respectively, n=12 neurons). When differences in firing rates were compared during these two time segments, it was observed that *Clock*Δ19 mice displayed

higher dopamine neuronal firing rates during ZT0-6 compared to ZT12-18 (Firing rate: 6.5±1.1 Hz and 4.8±0.4 Hz during ZT0-6 and ZT12-18, respectively, n=11 neurons). No firing rate differences were observed in WT mice between the two time segments (Firing rate: 3.4±0.5 Hz and 3.4±0.4 Hz during ZT0-6 and ZT12-18, respectively, n=12 neurons). Collectively, this data demonstrates a significant daytime elevation in dopaminergic activity and a loss in the diurnal rhythm of dopaminergic cell bursting in *Clock*Δ19 mice.

Chronic increases in VTA dopaminergic activity alter anxiety-related behavior

Given that *Clock*Δ19 mice exhibited increased firing and bursting rates of VTA dopamine neurons, with the greatest differences seen during the day, tests were carried out to determine if chronic elevation in daytime VTA dopaminergic activity was sufficient to alter anxiety-related behaviors. Optogenetic techniques were employed to selectively target dopamine neurons in the VTA and manipulate them in a temporal-specific manner. To restrict opsin expression to midbrain dopamine neurons, a Cre-dependent virus was injected into the VTA of TH::Cre mice. Due to the novel nature of the chronic stimulation paradigm employed, TH::Cre mice were injected with a mutated form of channelrhodopsin, the step-function opsin ChR2(C128S) (Berndt, Yizhar et al. 2009). The slower-off channel kinetics and enhanced sensitivity of the step-function opsin compared with the original channelrhodopsin offers the advantage of less frequent and intense stimulation being required over long time periods in order to maintain a

constant state of depolarization (Berndt, Yizhar et al. 2009; Diester, Kaufman et al. 2011). To control for the diurnal specificity of neural firing observed in ClockΔ19 mice, TH::Cre mice were optically stimulated selectively during the light phase. After seven days of one-hour bouts of optical stimulation of the VTA, mice were tested in a behavioral battery for exploratory and anxiety-like behaviors (Figure 2.3A). Accuracy of viral and optical fiber placement, and the specificity and efficiency of opsin expression in VTA dopamine neurons was confirmed *in vivo* (Figure 2.2).

Mice that received chronic daytime optical stimulation spent significantly more time in the open arms of the EPM (Figure 2.3B) and entered the open arms with greater frequency than non-stimulated controls (Figure 2.3C), suggesting an anti-anxiety phenotype. This was corroborated in the open field test as optically stimulated mice spent more time exploring the center of the open arena (Figure 2.3D) and had a profoundly decreased latency to enter the center at test commencement (Figure 2.3E). Importantly, no differences in locomotion, as measured by total distance travelled during the open field, were observed (data not shown). These results demonstrate that chronic daytime optical stimulation of VTA dopamine neurons leads to increased exploratory behavior consistent with a reduction in the levels of anxiety.

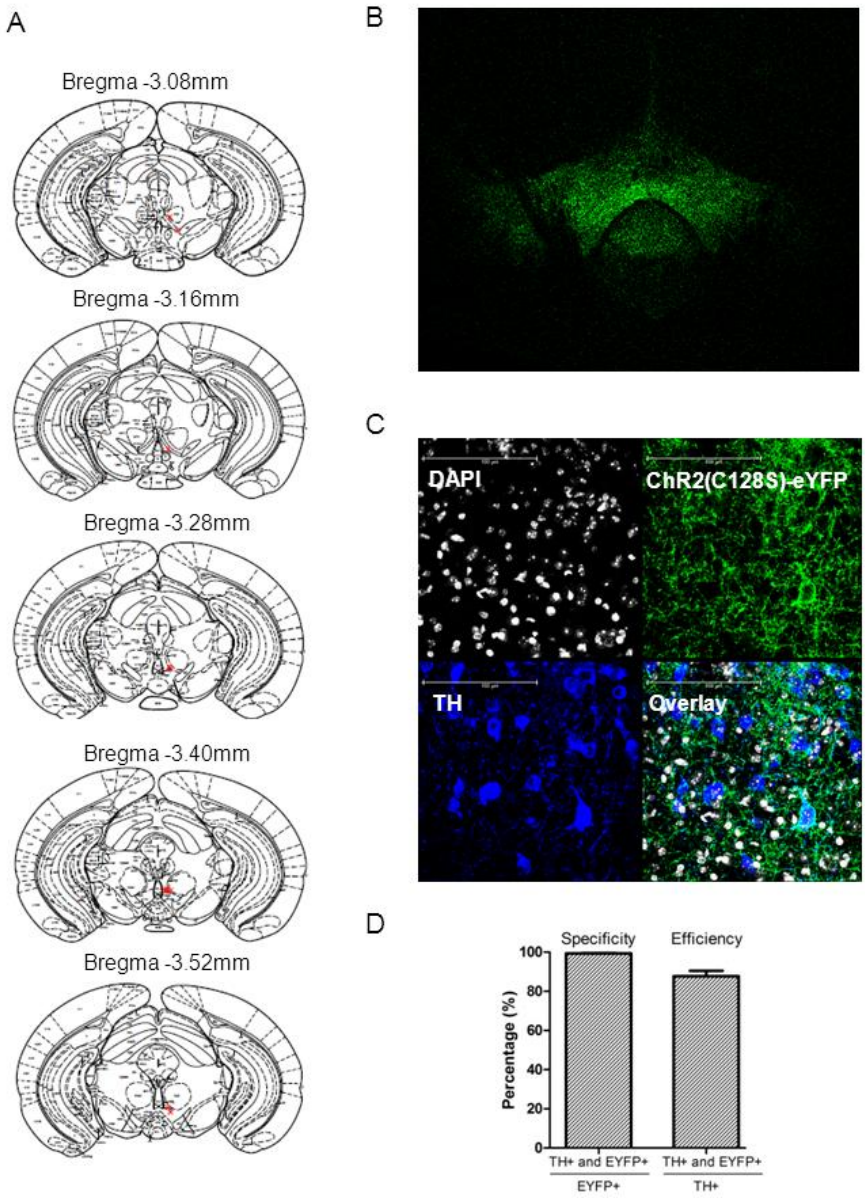

Figure 2.2. Histological verification of opsin and fiber optic placement. A. Coronal sections indicating unilateral virus injection sites into the VTA of TH::Cre mice (marked by red x). Accuracy of implantable optical fiber placement at DV-4.1mm (relative to Bregma) was confirmed visually in each mouse. **B.** Representative confocal image of a coronal section of the VTA from a TH::Cre mouse expressing ChR2(C128S) tagged with enhanced yellow florescent protein (eYFP). **C.-D.** Specificity and efficiency of viral transduction in dopamine neurons was confirmed by quantitating percentages of TH+ (n=200) and eYFP+ (n=177) neurons in a 200μmx200μm ROI.

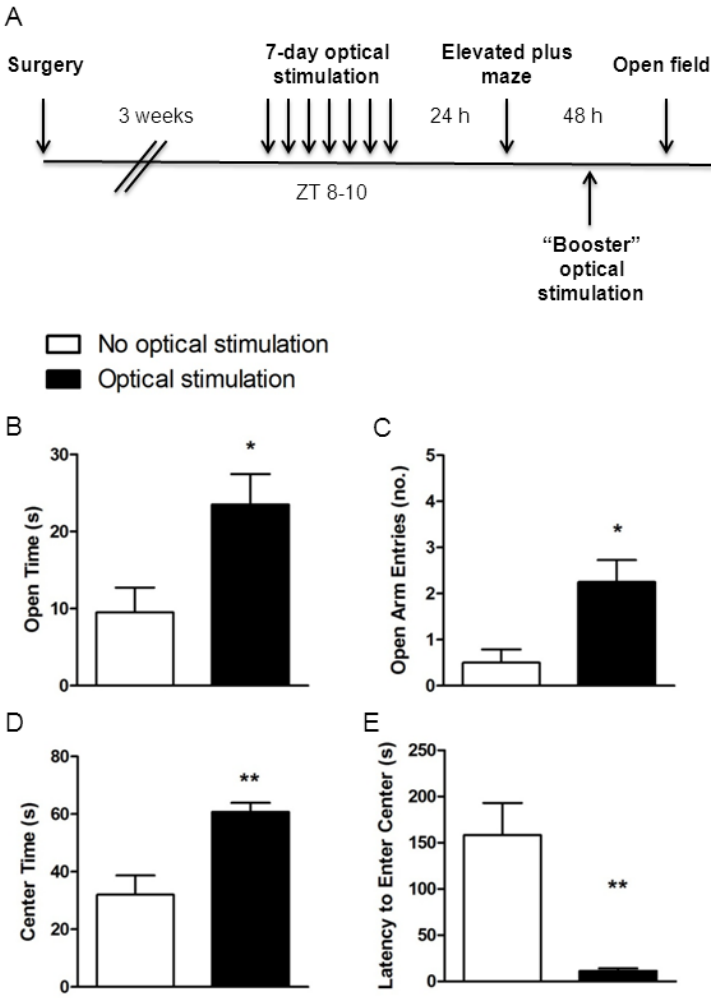

Figure 2.3. Effect of chronic optical stimulation of the VTA on anxiety-related behaviors. A. Chronic optical stimulation paradigm. Three weeks following viral-mediated delivery of the step-function opsin, ChR2(C128S) to the VTA, TH::Cre mice were optically stimulated with 473nm light for 1hr/day for 7 days between ZT8-10, followed by behavioral testing to assess anxiety-related behaviors. Control mice were treated identically but received no light during the stimulation paradigm. Note, that mice did not receive optical stimulation on the day of behavioral testing. **B.-E.** TH::Cre mice were assessed for anxiety-related behavior in both the elevated-plus maze (EPM; **B.-C.**) and the open field (**D.-E.**). TH::Cre mice that received chronic optical stimulation exhibited significantly decreased anxiety-related behavior in the EPM as evident by **B.** increased open arm time (t_6=2.74, p=0.03) and **C.** increased frequency of open arm entries (t_6=3.13, p=0.02), and in the open field test as evident by **D.** increased time spent in the center (t_7=3.56, p=0.009) and **E.** decreased latency to enter the center at test onset (t_7=3.71, p=0.008) relative to control mice that received no optical stimulation. n=4-5/treatment group.

Disruption of CLOCK alters VTA TH expression and protein levels

Given the current findings highlighting the importance of daytime VTA dopamine neural activity to anxiety-related behaviors, the potential differential *TH* expression in the VTA during the light and dark phases in *Clock*Δ19 mice and WT littermates was examined. *TH* mRNA levels were measured in the VTA at time points corresponding to the light cycle: ZT 0, ZT 4, ZT 8 and the dark cycle: ZT 12, ZT 16 and ZT 20. Q-PCR analysis revealed that WT mice exhibited a significant diurnal variation in *TH* mRNA expression with low levels during the light phase and higher expression during the dark phase (Figure 2.4A). *Clock*Δ19 mutant mice, however, exhibited an overall increase in levels of *TH,* with the greatest increase in expression mice observed during the day (Figure 2.4A). To begin to explore whether CLOCK, itself, may regulate the observed diurnal variation in *TH*, VTA *Clock* gene expression was measured across a 24 h period in WT mice and was found to be nearly opposite to that of *TH* expression, with a peak occurring during the light phase and a trough during the dark phase (Figure 2.4B), suggesting that CLOCK may act as a negative regulator of *TH*. Consistent with previous data, mutant *Clock* gene expression was elevated in *Clock*Δ19 mice (McClung, Sidiropoulou et al. 2005). To ensure that CLOCK can act as a transcriptional activator in brain regions outside of the suprachiasmatic nucleus (SCN), levels of *Per2* and *Cry2* expression were examined across the light-dark cycle given that they are well-established direct downstream targets of CLOCK transcriptional activation in the SCN. As expected, *Per2* and *Cry2* expression in

the VTA were decreased in *Clock*Δ19 mice, confirming that CLOCK can act as a transcriptional activator at gene targets in the VTA (Figure 2.5).

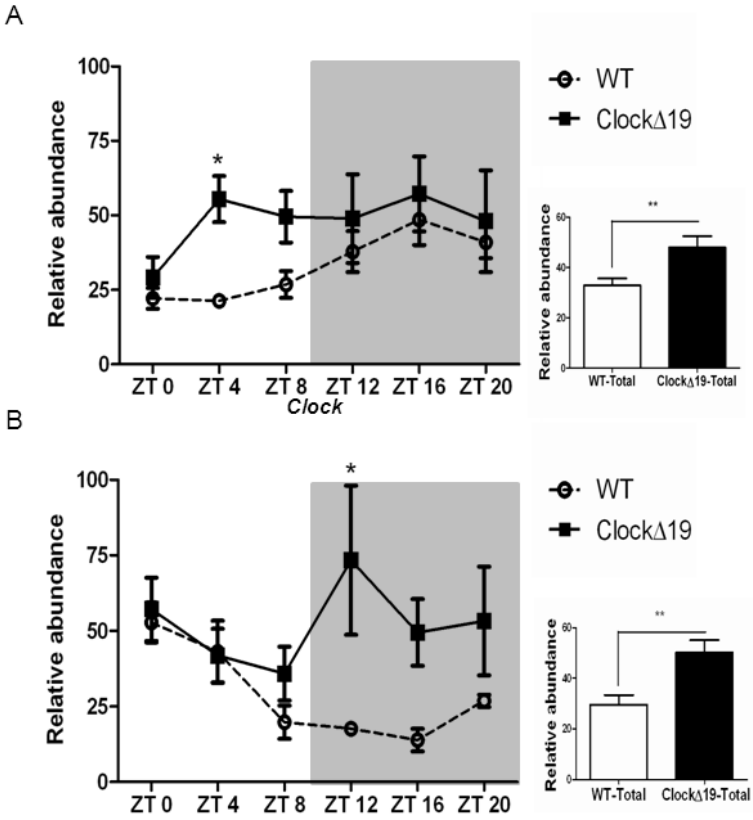

Figure 2.4. Time specific alterations in TH mRNA in *Clock*Δ19 mutant mice. **A.** Relative abundance of *TH* mRNA normalized to the expression of Gapdh. Two-way ANOVA revealed a significant genotype effect ($F_{(1,45)}$=9.42, p=0.004) with a specific increase in *TH* expression at ZT 4 in *Clock*Δ19 mice (p< 0.05). A significant diurnal variation was detected in WT mice (CircWave: $F_{(2,27)}$=10.63, p=0.0004), while *Clock*Δ19 mutants displayed none. Inset depicts a significant increase in total averaged *TH* expression in mutants compared to WT (t_{55}=2.918, p=0.005). **B.** Relative abundance of *Clock* mRNA normalized to the expression of an internal control, Gapdh. Analysis by two-way ANOVA revealed a significant main effect of genotype ($F_{(1,40)}$=14.61, p=0.0005) with an increase in *Clock* expression in mutants at ZT 12 (p<0.05; n = 3-5 animals/genotype/time point). Diurnal variation was statistically significant in WT (CircWave: $F_{(2,27)}$=16.45, p=0.00002), while *Clock*Δ19 mice displayed none. Inset depicts overall increase in total averaged *Clock* expression in mutants compared to WT (t_{50}=3.22, p=0.002).

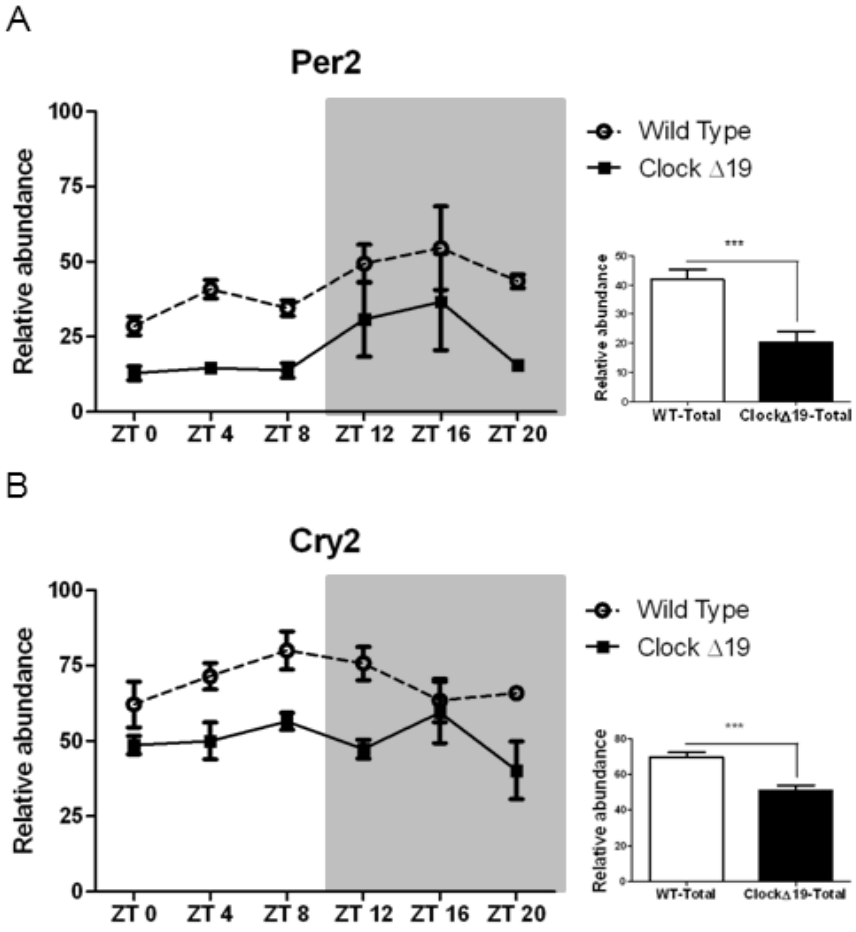

Figure 2.5. VTA circadian gene expression. A. Relative abundance of *Per2* mRNA normalized to the expression of an internal control, *Gapdh*. Analysis by two-way ANOVA revealed a significant main effect of genotype ($F_{(1,40)}$=18.48, p=0.0001) and time ($F_{(5,40)}$=3.00, p= 0.02; n=3-5 animals per genotype per time point). Diurnal variation was statistically significant in WT (CircWave: $F_{(2,27)}$=3.51, p=0.04) and *Clock*Δ19 mutant mice (CircWace: $F_{(2,27)}$ =3.42, p=0.05). Inset depicts overall decrease in total averaged *Per2* expression in *Clock*Δ19 mutant mice compared to WT mice (t_{50}=4.34, p<0.001). **B.** Relative abundance of *Cry2* mRNA normalized to the expression of an internal control, *Gapdh*. Analysis by two-way ANOVA revealed a significant effect of genotype ($F_{(1,37)}$=22.51, p<0.0001). Diurnal variation was statistically significant in WT mice (CircWave $F_{(2,27)}$=4.53, p=0.02) and blunted in *Clock*Δ19 mutant mice. Inset shows a significant decrease in total averaged *Cry2* expression in mutants compared to WT (t_{47}=4.67, p<0.0001).

To determine whether the observed increase in TH gene expression resulted in functional consequences at the protein level, TH protein levels were assayed at four time points (ZT 4, ZT 9, ZT 16 and ZT 21). Western blot analyses on VTA punches from *Clock*Δ19 mutants and WT littermates were performed to measure total TH protein as well as two of its phosphorylated forms known to increase enzymatic activity (p-TH at Ser 31 and p-TH at Ser 40) (Kumer and Vrana 1996). The overall pattern of diurnal TH-related protein expression in WT mice was consistent with previous findings in rodents, demonstrating peak levels of TH during the light phase that dropped off at night (Webb, Baltazar et al. 2009). *Clock*Δ19 mice exhibited a daytime-specific increase in total TH (Figure 2.5A) and in relative levels of p-THser40 to total TH (Figure 2.5B) at ZT 9, representing a time slightly following the observed increase in *TH* mRNA expression. No differences in p-THser31/TH protein levels were found (Figure 2.5C). Notably, diurnal changes in both TH gene and protein expression paralleled the diurnal pattern of VTA dopamine cell bursting rates observed in both WT and *Clock*Δ19 mice.

Daytime dopamine synthesis is increased in Clock∆19 mutants

Dopamine synthesis assays were performed at two time points to determine if the increased *TH* expression in *Clock*Δ19 mice resulted in increased dopamine synthesis in the nucleus accumbens (NAc).

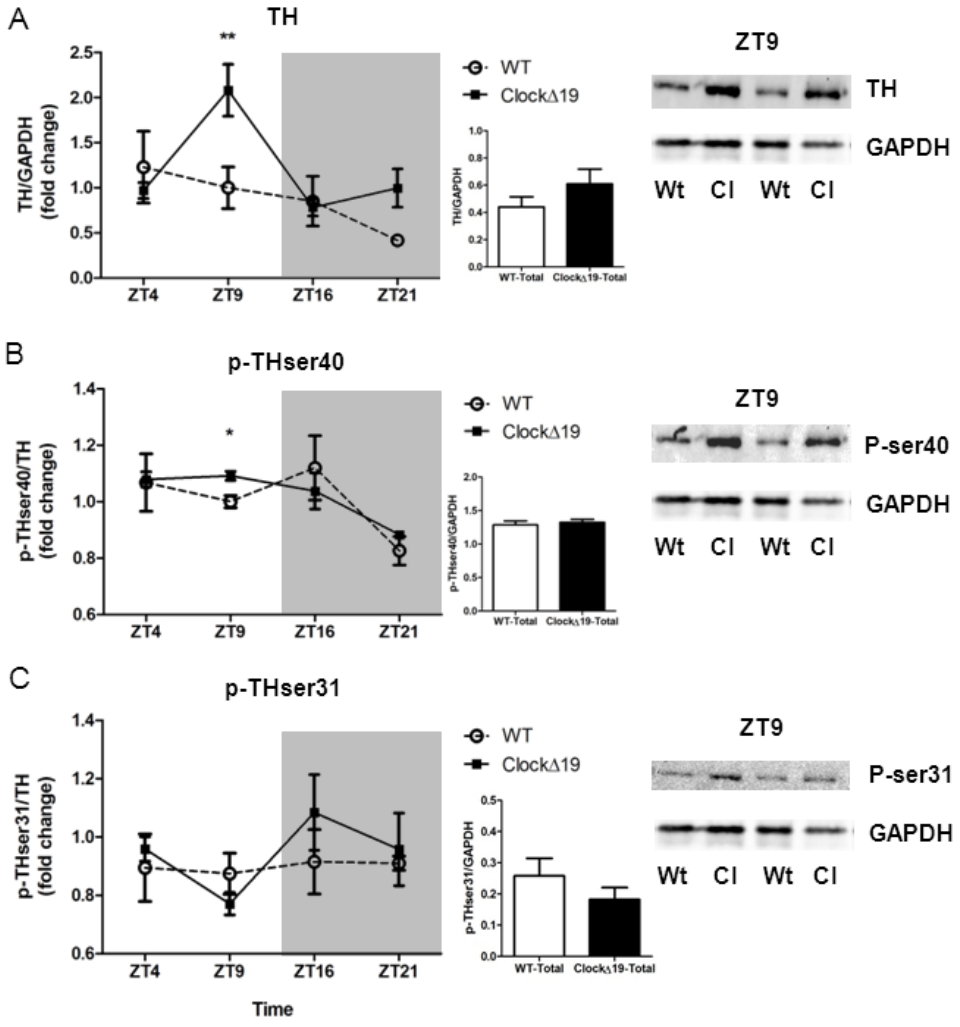

Figure 2.6. Time specific alterations in TH protein in *Clock*Δ19 mutant mice. **A-C.**Quantifications of immunoblots for total and phosphorylated TH across time with representative bands shown for ZT 9. **A.** A significant main effect of time was found for total TH ($F_{(3,28)}$=5.34, p=0.005), with an increase in *Clock*Δ19 mouse TH levels at ZT 9 (p < 0.01). Diurnal variation was statistically significant in mutants (CircWave: $F_{(2,17)}$=5.15, p=0.02). **B.** There was a significant effect of time on phosphorylated TH (ser 40) protein ($F_{(3,32)}$= 6.50, p=0.002), with *Clock*Δ19 mice exhibiting a specific increase in THser40 levels at ZT9 (p<0.05, student's t-test). Diurnal variation in THser40 was statistically significant in mutants (Circwave: $F_{(2,17)}$=7.18, p=0.005). **C.** No differences in phosphorylated TH (ser31) protein levels were found at any ZT time point measured. Inset depicts protein levels over 24 h.

The rate of dopamine synthesis was determined *in vivo* by measuring L-DOPA accumulation after administration of the DOPA-decarboxylase inhibitor 3-hydroxy-benzylhydrazine (NSD-1015, 100 mg/kg i.p.) 60 minutes before sacrifice. NAc and dorsal striatal tissue was harvested for high performance liquid chromatography (HPLC) analysis. A 20% increase in dopamine synthesis was observed in the NAc of *Clock*Δ19 mice during the light phase (ZT 4, Figure 2.6A). Predictably, no difference in L-DOPA accumulation was perceived during the dark phase between WT and *Clock*Δ19 mutants, but the WT mice displayed a significant diurnal increase in dopamine synthesis in the NAc (Figure 2.6A). Interestingly there were no significant alterations in dopamine synthesis in the dorsal striatum (Figure 2.6B), which is consistent with earlier work showing no differences in TH protein levels in the substantia nigra of *Clock*Δ19 mice (McClung, Sidiropoulou et al. 2005). This finding gives functional significance to the aforementioned observation of a time-restricted daytime increase in neural activity and TH mRNA and protein levels, and implies a direct relationship between TH levels and activity.

CLOCK binds to the tyrosine hydroxylase promoter in the VTA

To determine whether increased VTA dopamine levels and activity in *Clock*Δ19 mice may be due to CLOCK acting as a direct transcriptional regulator of *TH*, the ability of CLOCK to bind the *TH* promoter was first assessed.

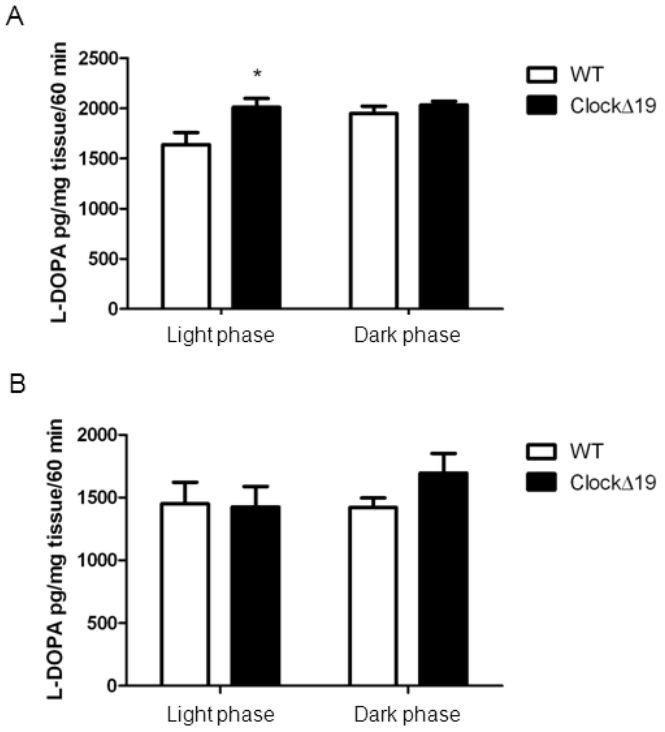

Figure 2.7. Dopamine synthesis assay. A. Dopamine synthesis was significantly increased in *Clock*Δ19 mutant mice and WT littermates as measured by L-DOPA in the nucleus accumbens after NSD-1015 administration during the light phase, at ZT 4 (t_9 = 2.546, p=0.03). There is a significant diurnal increase in dopamine synthesis in WT mice at ZT 16 (t_{10} = 2.3248, p=0.04). **B.** Dopamine synthesis was unaltered in the dorsal striatum of ClockΔ19 mutants (n=5-8 per group; dark phase = ZT16).

Chromatin immunoprecipitation (ChIP) assays on VTA-containing midbrain tissue from wild type mice were performed to assess CLOCK binding at E-box elements (CANNTG) identified in the *TH* promoter. Two primer sets were created to amplify distal and proximal regions of the promoter containing putative E-Boxes. The *TH* distal promoter primers amplified a 143 base pair (bp) product located at -772 containing a canonical E-box (CAGCTG) that deviates slightly from the CLOCK:BMAL1 consensus sequence (CAGCTG) (Figure 2.7A). The *TH*

proximal promoter primers resulted in a 183 bp product starting at -119 from the transcription start site containing a canonical E-box (CAGGTG) that again deviates slightly from the CLOCK:BMAL1 consensus sequence and is in tandem with a second E-box like element (CAGTGG) located 7 base pairs away (Figure 2.7A). This finding was interesting because these E1-E2 tandem sites have been shown to be important for conferring specificity for the CLOCK:BMAL1 complex and driving the circadian amplitude of its targets (Rey et al. 2011; Nakahata et al. 2008). Analysis with the UCSC Genome Browser BLAT alignment tool (www.ucsc.edu/genome) additionally revealed that each of these regions contains a 20-30 bp region of mouse to human evolutionary conservation. The proximal promoter product contains part of a larger region of homology previously termed Conserved Region 2 (CR2) that has been suggested to regulate tissue specificity of the transcript (Kim, Park et al. 2003). ChIP analyses were performed on C57BL/6 mice at 4 time points across the light/dark cycle (ZT 4, ZT 9, ZT 16 and ZT 21). CLOCK was present at both of the *TH* promoter sites assayed during the light phase (distal: Figure 2.7B, C; proximal: E, F), with no enrichment observed above background at either site during the dark phase. CLOCK binding to the *TH* promoter was measured in *Clock*Δ19 mutants compared to WT littermates during the light phase at ZT 4, when binding was expected based on the results obtained in Figures 2.7B and 2.7E. Consistent with the WT data, enrichment of CLOCK at both TH promoter sites was observed in the *Clock*Δ19 mice (distal: Figure 2.7H and proximal: 2.7I).

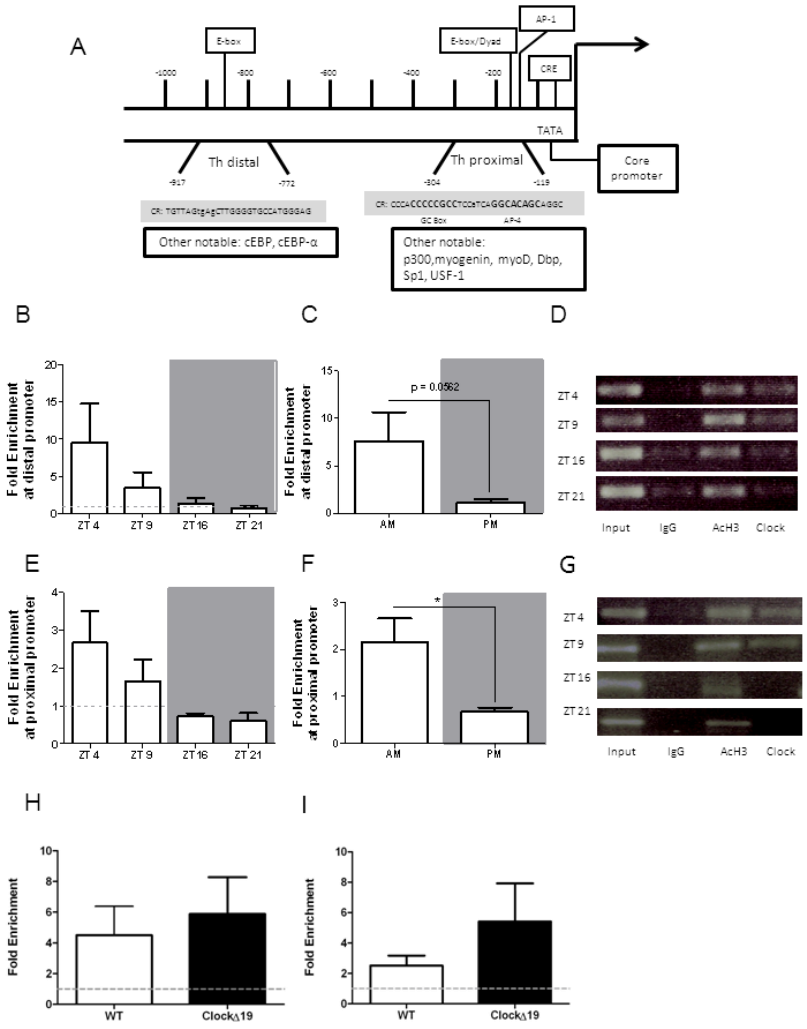

Figure 2.8. CLOCK binding at the *TH* promoter. A. Diagram of *TH* promoter region. Two regions of DNA containing E-Boxes were amplified by quantitative PCR after performing ChIP assays. Important transcription factor binding sites are highlighted. **B.** Fold enrichment, as calculated from Ct values, at distal promoter region across ZT time following ChIP with CLOCK-specific antibody in C57BL/6 mice (n =3-4 per time point). **C.** Comparison of CLOCK binding at the distal TH promoter during the light versus dark phase indicates strong trend toward a diurnal variation in promoter occupancy (t_{13}=2.113, p=0.056). **D.** Representative agarose gels of q-PCR products from ChIP assay showing total input DNA, IgG negative control IPs, AcH3 positive control IPs and CLOCK IPs. **E.-G.** Same as in B-E, but with the proximal TH promoter. **F.** Significant diurnal variation in CLOCK occupancy of the TH proximal promoter (t_{13}=2.713, p=0.02). **H.** Fold enrichment at distal promoter region following ChIP with CLOCK-specific antibody comparing Clock∆19 mutants to wild type (WT) controls; (n =4-6 per time point). **I.** Same as in H, but with the proximal TH promoter.

Importantly, this data indicates that the mutated CLOCK protein is still capable of binding DNA; however the missing exon (exon 19) of the CLOCK protein appears to be critical for conferring proper transcriptional regulation.

As a follow up, it was hypothesized that p-CREB (cAMP responsive element binding protein) may compete with CLOCK for binding at the proximal *TH* promoter given the proximity of the CRE binding site upstream of the proximal CLOCK E-box binding site (Figure 2.7A) and the well-established role of CREB in the activity-dependent regulation of *TH* transcription (Lewis-Tuffin, Quinn et al. 2004). A significant increase in p-CREB binding was found at the *TH* proximal promoter site during the dark phase relative to the light phase that represents an opposite pattern of binding to that observed for CLOCK (Figure 2.8). This suggests an antagonistic relationship between CLOCK and p-CREB in regulation of *TH* transcription.

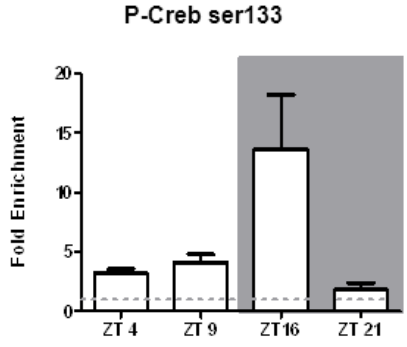

Figure 2.9. P-Creb at the *TH* promoter. Differential levels of p-CREB(s133) binding at the proximal *TH* promoter across ZT time with increased binding observed during the beginning of the dark phase (ZT 16) in C57BL/6 mice.

To investigate the transcriptional role of CLOCK binding at the *TH* promoter, luciferase assays were performed using TH-luc reporter plasmids with either an

intact or mutated E-box to disrupt CLOCK binding. Short and long *TH* promoter reporter plasmids including either the first 250 or first 1000 bp of the promoter inclusive of the E-box sites of interest were cloned. Mutation of either E-box resulted in a significant increase in TH-luc reporter activity (Figure 2.9A).

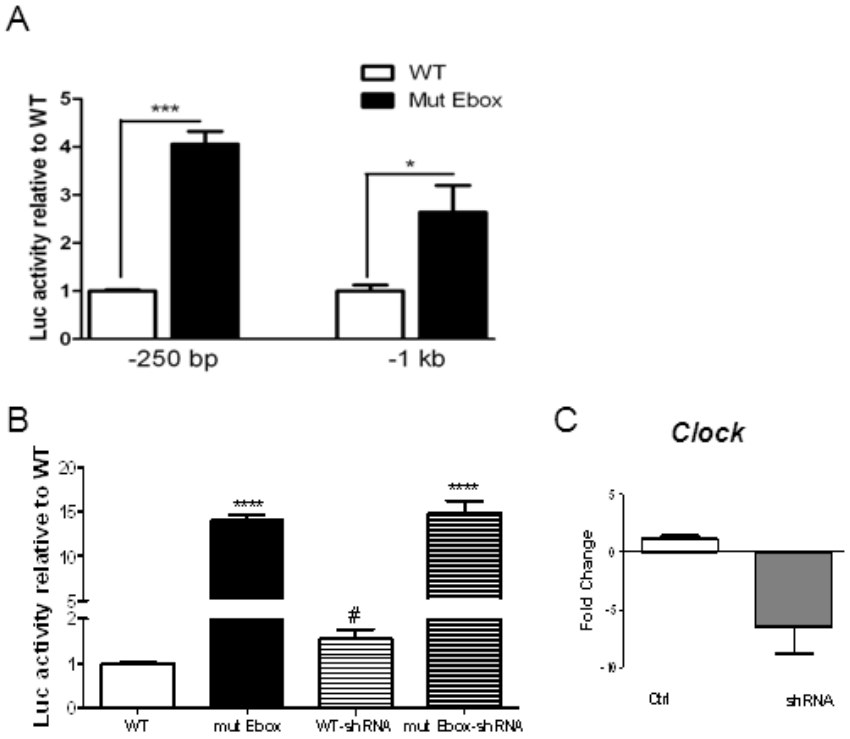

Figure 2.10 E-box dependent TH-luciferase activity. A. Relative luciferase activity in PC12 cells transfected with WT TH-luc constructs (250 bp or 1000 bp) or TH-luc constructs containing mutant E-boxes. Mutating the E-boxes significantly increased luciferase activity at the proximal (t_{16}=11.30, p<0.0001) and distal site (t_9=3.158, p=0.01). **B.** Experiment in A. repeated with *Clock*-shRNA. Cells transfected with WT TH-luc and *Clock*-shRNA have a slight increase in TH-luc activity (T_{22} = 2.744, p = 0.0119). Co-transfection of *Clock*-shRNA with the mut-Ebox TH-luc (250bp) construct does not significantly increase TH-luc activity greater than mutating the E-box alone (Mut Ebox: T_{22} = 20.98, p < 0.0001; Mut Ebox + shRNA: T_{22} = 10.17, p < 0.0001). **C.** Transfection of *Clock*-shRNA in PC12 cells significantly reduces endogenous *Clock* expression (T_7 = 4.733, p = 0.0021).

In order to further evaluate whether CLOCK was contributing to this E-box dependent effect as PC12 cells endogenously express the protein, cultures were co-transfected with the short TH-luc WT and mutant constructs and a shRNA directed against *Clock.* Knockdown of *Clock* with the shRNA was sufficient to increase WT TH-luc activity, yet the modest degree of increase compared to mutation of the E-box leaves room for speculation about other E-box binding transcription factors that may contribute to the regulation of *TH* transcription. Importantly, when the *Clock*-shRNA was co-transfected with the mutant TH-luc construct, it did not affect a greater increase in TH-luc activity. Taken together, these results suggest that E-box sequences in the *TH* promoter are bound by CLOCK and that this is, to some degree, responsible for the reduction of *TH* mRNA expression observed at specific times of day.

Discussion

The current study demonstrates that the disrupted function of the circadian protein CLOCK by the Δ19 mutation leads to large increases in dopaminergic activity at particular times of day. Using optogenetic technology, it was demonstrated that this chronic elevation in daytime VTA dopaminergic activity was sufficient to produce increased exploratory activity, indicative of lowered anxiety levels as observed in the *Clock*Δ19 mutant mice (Roybal, Theobold et al. 2007; Dzirasa, McGarity et al. 2011). A novel mechanism to explain how disruptions in CLOCK function may lead to changes in dopaminergic activity and associated aberrant behavior was uncovered. Here it is

demonstrated that CLOCK acts as a direct negative regulator of *tyrosine hydroxylase* expression and that CLOCK function in the VTA is essential for proper daily rhythms in TH levels and dopamine synthesis. Taken together, this study further defines the role of dopamine in the regulation of complex behavior and underscores the importance of the circadian protein CLOCK in the control of this system

It was found that the *Clock*Δ19 mice exhibit a daytime-specific increase in mean dopaminergic neuronal firing rates in the VTA. Importantly, dopamine neuronal activity was characterized during REM sleep while animals were behaviorally immobile. Thus, these findings provide strong evidence that increased dopamine neuronal firing rates in *Clock*Δ19 mice parallel neurophysiological changes that underlie the behavioral disturbances observed in the mutants, rather than simply reflecting differences in behavioral profiles across the light-dark cycle. Interestingly, the bursting rate of dopaminergic neurons paralleled *TH* expression in WT mice such that both the bursting rate and *TH* expression were increased during the light cycle, while this rhythm was disrupted in *Clock*Δ19 mice. These findings raise the possibility that alterations in CLOCK lead to increases in basal dopamine neuronal firing (most prominently during the light cycle). This enhanced daytime dopamine neural activity would ultimately alter dopamine neuronal bursting and disrupt downstream dopamine-dependent circuits regulating behavior. Indeed, optogenetic stimulation facilitated the direct targeting of VTA dopamine neurons to determine to what extent daytime-specific enhancement of dopamine activity might play a role in

mediating behavioral abnormalities relevant to the behavioral phenotypes of the *Clock*Δ19 mice. It was found that enhanced daytime activity of VTA dopamine neurons in TH::Cre mice led to a reduction in anxiety-related behavior similar to that observed in *Clock*Δ19 mice. This provides compelling evidence that chronic increases in VTA dopamine neural firing may, indeed, underlie the anxiety component of the ClockΔ19 mouse behavioral phenotype. Interestingly, a previous study found that acute optical stimulation of dopamine neurons in the VTA of TH::Cre mice had no impact on anxiety-like behavior (Tsai, Zhang et al. 2009), suggesting that chronic disruptions in neuronal firing are required for alterations to anxiety-related circuitry. Future studies will address the potential long-term plastic changes occurring in mesolimbic circuitry that may be associated with the altered anxiety-related behavior observed as a result of chronic optical stimulation.

It was found that *TH* gene expression and protein levels were altered in a time-dependent manner in *Clock*Δ19 mutants with total TH and phosphorylated-THser40 levels increased in mutants during the light phase at ZT 9 - a time point that lags slightly behind *TH* gene expression. Moreover, there was a specific increase in dopamine synthesis in the NAc of *Clock*Δ19 mutants that was restricted to the light phase. Importantly, these results correlate with the daytime-specific increase in the VTA dopamine neuronal firing rates observed in *Clock*Δ19 mice. This suggests that the increase in dopamine synthesis may act as either a precursor or consequence to increased dopaminergic activity as increased TH expression is known to correlate with increased activity of

dopamine neurons (Aumann, Egan et al. 2011). Furthermore, mice in which the *TH* gene is genetically disrupted have a complete loss of bursting activity in dopamine neurons that can be rescued by L-dopa treatment, suggesting that certain aspects of dopaminergic transmission are indeed dependent upon dopamine synthesis (Paladini, Robinson et al. 2003). Interestingly, no difference in dopamine synthesis was found in the dorsal striatum of *Clock*Δ19 mutants which correlates with previous results that found no differences in TH protein in the substantia nigra of *Clock*Δ19 mice (McClung, Sidiropoulou et al. 2005). Future studies will determine how CLOCK is involved in differentially regulating dopamine synthesis in the VTA compared to the SN.

Another intriguing finding was that *Clock* itself had a diurnal pattern in gene expression in the VTA of WT mice, with higher levels detected during the day than night. This diurnal expression pattern was opposite to what was found for *TH* expression suggesting that CLOCK may act as a transcriptional regulator of *TH.* The finding that *Clock* gene expression was rhythmic in the VTA is surprising given the well-established finding that *Clock* gene expression in the SCN is not rhythmic, but rather its activity is rhythmic due to differential interactions with BMAL1 over the light-dark cycle (Kondratov, Chernov et al. 2003; Maywood, O'Brien et al. 2003). *Clock* gene expression is, however, rhythmic in peripheral tissues such as the liver and heart (Peirson, Butler et al. 2006), and this group has found rhythmic expression of *Clock* in various brain regions (unpublished observations). These findings indicate that *Clock*

expression is differentially regulated across brain regions and suggests that it may have distinct roles within these regions that differ from its role in the SCN.

As direct evidence of CLOCK's role as a transcriptional regulator of *TH*, it was found that CLOCK is present at the *TH* promoter at two separate E-box containing sites. Furthermore, mutation of either E-box element in the proximal or distal promoter of the *TH* gene significantly increased TH-luc activity in reporter assays. There was also identified an E1-E2-like motif in the proximal promoter region of *TH,* but it is unclear what contribution the second E-box like element might make to the transcriptional regulation of the gene. When CLOCK levels were directly knocked down with shRNA, there was a small, but significant increase in TH-luc activity. This data suggests that CLOCK functions as a suppressor of *TH* transcription at one or both of these sites to regulate diurnal patterns in *TH* expression. Indeed, CLOCK binding at the *TH* promoter was greater during the day when *TH* expression was low, and binding was undetectable at night when *TH* levels were high. This finding was surprising given the fact that most studies have found that CLOCK acts as a transcriptional activator at CLOCK-controlled gene promoters. However, a microarray study by Takahashi and colleagues, which examined gene expression *in Clock*Δ19 mice, found that patterns of gene expression in the liver and skeletal muscle of the mutants were complex. Certain genes were found to be downregluated, others were upregulated or had shifted or altered rhythms in expression, suggesting that CLOCK can alter transcription in various ways (Miller, McDearmon et al. 2007). Furthermore, studies have shown that CLOCK can interact with BMAL1 and

Cryptochrome 1 (CRY1) to form a repressive complex at certain gene promoters, and may even disrupt activity of other factors at non-E-box containing regions (Kondratov, Shamanna et al. 2006). In this regard, it is interesting that differential binding of CREB (a known activator of *TH* expression) to the *TH* promoter was detected over the course of 24 hours and in a pattern opposite to that of CLOCK, suggesting an antagonistic relationship between CLOCK and CREB in the regulation of *TH* gene expression.

Conclusions

These data uncover a novel regulation of *TH* directly by CLOCK. Disrupted CLOCK function is associated with loss of diurnal rhythms in *TH* gene expression and enhanced dopaminergic activity at particular times of day. These results also underscore the importance of normal patterns of dopaminergic activity in the regulation of anxiety-related behavior. Thus, the circadian system represents a novel therapeutic avenue to utilize for treatment development for diseases that involve dysfunction in limbic dopaminergic circuitry. Furthermore, the use of optogenetic technology, and particularly the step function opsin employed here, opens the door for a variety of future studies to examine the effects of chronic stimulation of multiple neurotransmitter systems across many brain regions to determine how this impacts complex behavioral phenotypes.

Material and Methods

Animals

*Clock*Δ19 mutant mice were created by N-ethyl-N-nitrosurea mutagenesis and produce a dominant-negative CLOCK protein defective in transcriptional activity as described (King, Vitaterna et al. 1997). For all experiments using *Clock*Δ19 mutants, adult male mutant (*Clock/Clock*) and wild type (+/+) littermate controls on a mixed BALBc; C57BL/6 background were group housed in sets of 2-4 per cage on a 12/12-hour light dark cycle (lights on 6:00 a.m. = Zeitgeber (ZT) 0, lights off at 6:00 p.m. = ZT 12) with food and water provided ad libitum. Optogenetic studies were carried out on 6-8 week old male Tyrosine hydroxylase (TH)::IRES-Cre transgenic mice (EM:00254) (Tsai, Zhang et al. 2009). Adult male C57BL/6 mice (Jackson Laboratories) were used for the chromatin immunoprecipitation assays. All animal use was conducted in accordance with the National Institute of Health guidelines and approved by the Institutional Animal Care and Use Committees of UT Southwestern Medical Center, Duke University, and Stanford University.

Electrophysiology surgeries

Male *Clock*Δ19 and WT littermate controls, 20-30 weeks old, were used for electrophysiological experiments. Animals were surgically implanted with recording electrodes and experiments initiated following a two-week recovery. For surgery, mice were anesthetized with ketamine (100mg/kg) and xylazine (10mg/kg), placed in a stereotaxic device, and metal ground screws were

secured to the cranium. A total of 14 tungsten microwires were arranged in bundle arrays of 4-10 wires (each wire separated by at least 250mm), and implanted to target the dorsal hippocampus and VTA. Implanted coordinates were as follows (all coordinates are measured from bregma): dorsal hippocampus, AP-2.3mm, ML +1.63mm, DV-1.3mm; VTA, -3.2mm, ML+0.3mm, DV -4.25mm. Implanted electrodes were anchored to ground screws using dental acrylic. After recovery, mice were then separated into individual cages and their cage placed into the recording chamber. Following a two-day habituation period, neurophysiological data was recorded throughout the entire 24 hour light-dark cycle of each mouse.

Neuronal and LFP data acquisition

Neuronal activity was sorted online and recorded using the Multi-Neuron Acquisition Processor system (Plexon Inc, TX). Local field potentials (LFPs) were pre-amplified (500X), filtered (0.7–170 Hz), and digitized at 500 Hz using a Digital Acquisition card (National Instruments, Austin, TX) and a Multi-Neuron Acquisition Processor (Plexon, Dallas, TX). Bursting and firing rate analyses were performed using Neuroexplorer (Nex Technologies, Littleton, MA). All electrophysiological recordings were referenced to two ground screws located above the cerebellum and anterior cortex. Notably, ground wires tested from the two screws were iso-electric, demonstrating that ground loops were not introduced by this design. VTA channels were thresholded to select for dopaminergic neurons based on standard physiological criteria including

waveforms > 2ms in length and bursting (Grace and Bunney 1983; White 1996; McClung, Sidiropoulou et al. 2005). At the end of the recording, cells were sorted again using an offline sorting algorithm (Plexon, Dallas, TX) to confirm the quality of recorded cells. For firing analysis of dopaminergic neurons, data was collected during 60 sec epochs of REM sleep occurring during each of the 6 hour intervals corresponding with ZT0-6, ZT6-12, ZT12-18, and ZT18-24. As several mutant mice failed to display a 60 sec epoch of REM sleep during each of the four time windows and not all neurons remained stable during the entire 24 hour recording even when REM epochs were identified, additional criteria were applied such that neurons had to display a minimum firing rate of 1.5Hz and at least 1 bursting episode during the 60 sec period in order to be included in analysis. Burst events were initiated by a pair of spikes having an interspike interval of 80 ms and terminated by interspike intervals of 160 ms. Following the initial analysis, within neuronal firing rate and bursting analysis were performed where only neurons recorded during the first 6 hours of the light cycle and the first 6 hours of the dark cycle were included.

Behavioral state identification

Behavioral states were identified using a two-dimensional state map as previously described (Dzirasa, Ribeiro et al. 2006). The state map generated cluster separation based on the high amplitude theta (4-9Hz) and gamma (33-55Hz) oscillations characteristic of REM sleep, the absence of gamma oscillations and high amplitude delta (1-4Hz) characteristic of SWS, and the high

amplitude gamma oscillations and theta oscillations characteristic of waking. Behavioral state maps were generated from each of the 2-4 hippocampal LFPs acquired; the map that produced the best cluster separation was utilized for behavioral state identification.

Optogenetics

Virus construction and packaging. The recombinant AAV-DIO-Ef1a-ChR2 (C128S)-eYFP vector was constructed by cloning DIO-Ef1a-ChR2 (C128S)-eYFP into an AAV backbone using MluI and EcoR1 restriction sites. The resulting plasmid DNA was serotyped with AAV_5 coat proteins and packaged by the viral vector core at the University of North Carolina.

Stereotactic surgery

TH::Cre mice were anaesthetized with 1.5-3.0% isoflurane and kept on a self-regulating heating pad throughout the duration of the sterotactic surgery. Purified AAV_5 virus was unilaterally injected into the VTA at AP -3.3, ML 0.44, DV -4.1 and -4.7 (relative to Bregma) using a 33-gauge metal beveled needle facing medial. A 10µl Hamilton microsyringe (nanofil; WPI, Sarasota, FL) and its controller (Micro4; WPI, Sarasota, FL) delivered 1µl of virus at each DV coordinate at a rate of 0.1 µl/min. The needle was left in place for 10 min between injections and slowly withdrawn. Immediately following, a Doric optical fiber (NA=0.22, Doric Lenses Inc., Quebec, Canada) was permanently implanted unilaterally over the VTA at -4.1mm DV. Adhesive cement (C&B metabond,

Parkell, Edgewood, NY) and cranioplastic cement (Dental cement, Stoelting, Wood Dale, IL) were used to secure the Doric implant to the skull and the incision was closed and sealed with tissue adhesive (Vetbond; Fisher, Pittsburgh, PA). All surgeries were performed using strict aseptic techniques. Mice were administered 0.9% saline and buprinex sub-cutaneously immediately following surgery. After recovery, mice were left undisturbed for 3 weeks to allow for sufficient viral expression prior to behavioral testing.

Chronic optical stimulation paradigm and Behavioral testing

TH::Cre mice injected with a light sensitive step-function opsin (SFO) received seven days of one hour bouts of optical stimulation between ZT8-10 followed by behavioral testing. Behavioral tests were separated by 48 hours with a "booster" optical stimulation given between test days to sustain alterations in VTA dopamine neural activity. Prior to optical stimulation, mice were individually placed into a clean cage and allowed to acclimatize to the new environment for 5 min. A multi-mode patchcord (NA 0.22, 200μm core, Doric Lenses Inc. Quebec, Canada) was used to deliver 473nm laser light (OEM Lasers Systems, East Lansing, MI) to the permanent implanted optical fiber. Laser output was controlled using a Master-8 pulse generator (A.M.P.I, Jerusalem, Israel) delivering 1 sec pulses of 473nm light (minimum 5mW at fiber tip) every 10 sec for a period of 1 hour. Control mice underwent identical handling procedures but received no optical stimulation. Commutators (Doric Lenses Inc., Quebec,

Canada) were useful during this longer stimulation paradigm in reducing torque on the patch cords that result from movement of the animal.

Behavioral Assays

Behavioral testing took place between ZT 6-12 and was performed on days when no optical stimulation was administered. Animals were habituated to the testing room for a minimum of 30 min. Behavioral tests were conducted in order of increasing stress to avoid potential stress confounds on subsequent testing. All behavior was manually scored by a trained, blinded observer.

Elevated plus maze

The plus maze consisted of two plastic open arms perpendicular to two closed arms (arms: 25 X 5cm) and was elevated from the ground at a height of 30cm. Mice were placed into the center of the plus-maze facing a closed arm and were allowed to explore the maze for 5 min.

Open field

The open field consisted of a large $60cm^3$ plastic box. Mice were individually placed into a corner of the open field box and allowed to explore the arena for 30 min. A trained blinded observer scored both time spent in, and entries into, the center of the arena. The center was designated as a $20cm^2$ area in the center of the open field. Distance travelled in the open field was calculated by uploading video to the online video tracking software, Actual Analytics

(www.actualanalytics.com). Verification as to the accuracy of the online software was initially confirmed by comparing automated against observer-derived data.

Immunohistochemical verification of opsin expression

Mice were perfused with 4% paraformaldehyde in 1XPBS (pH 7.4) and the brains transferred to a 30% sucrose solution. 40 mm sections were taken and processed for TH and DAPI. Briefly, floating sections were rinsed in 1XPBS to remove the cryoprotectant/fixative. Sections were then blocked in PBS++ (3% Normal Donkey Serum, 0.3% Triton-X in PBS) for 30 min and incubated with an anti-tyrosine hydroxylase primary antibody (1:500, Aven Labs) overnight at 4°C on a rotary shaker. The following day, sections were rinsed in 1XPBS and incubated in a secondary conjugated to Cy5 (1:500, Jackson Laboratories, West Grove, PA) for 3 hours at room temperature on a rotary shaker. Sections were then incubated with DAPI (1:50,000) for 20 min, washed, and mounted on microscope slides with PVA-DABCO.

Confocal microscopy and analysis

Confocal fluorescence images were acquired on a Leica TCS SP5 scanning laser microscope using a 40X/1.25NA oil immersion objective to visualize the fiber placements and viral-mediated expression. Serial stack images covering a depth of 10μm through multiple sections were acquired using equivalent settings. The Volocity image analysis software (Improvision / PerkinElmer, Waltham, MA)

was used for identifying co-localization of DAPI, eYFP and TH staining. Imaging and analysis were performed blind to experimental conditions.

Gene expression

Animals were sacrificed at six time points over the circadian cycle corresponding to Zeitgeber time (ZT) 0, 4, 8, 12, 16 and 20 (ZT0 corresponds to lights on; lights go off at ZT12) and brains were frozen on dry ice. VTA punches were made on a frozen stage from 300 µM slices taken on a cryostat (Leica). RNA isolation and cDNA synthesis was carried out as previously described (McClung, Sidiropoulou et al. 2005). RNA was isolated using TRIzol reagent (Invitrogen) according to the manufacturer's instructions. Any remaining DNA was digested by using the DNA free system (Ambion, Austin, TX.). cDNA was synthesized with an oligo dT primer and superscript III reverse transcriptase enzyme (Invitrogen). Real-time PCR was performed in duplicate on the ABI 7500 Real-Time PCR system (Applied Biosystems) using the Fast start SYBR green PCR master mix (Roche Applied Science, Indianapolis) according to the manufacturer's instructions with specific *TH, Gapdh, Clock, Per2* and *Cryptochrome 2 (Cry2)* primers (Table 2.1). The relative levels of each mRNA were calculated by the $2^{-\Delta\Delta Ct}$ method and normalized to the corresponding *Gapdh* mRNA levels (Maywood, Fraenkel et al. 2010). Each Ct value used for these calculations is the mean of 2-5 biological replicates of the same reaction.

Table 2.1 ChIP and Gene Expression Primers

Chromatin Immunoprecipitation Primers		
	Forward	**Reverse**
***Th* distal**	5'-TGGGTGTGGATGCTCACTGGA-3'	5'-ACTCCCTGCATCATGGTCTCGAG-3'
***Th* proximal**	5'-GATGTCTCCTGTCCCAGAACACC-3'	5'-CCACGCCTGCTGTGCCTGAG-3'
Gene expression primers		
Gapdh	5'-AACGACCCCTTCATTGAC-3'	5'-TCCACGACATACTCAGCAC3'
TH	5'-TGCAGCCCTACCAAGATCAAAC-3'	5'-CGCTGGATACGAGAGGCATAGTT-3'
Clock	5'-CAGAACAGTACCCAGAGTGCT-3'	5'-CACCACCTGACCCATAAGCAT-3'
Per2	5'-GAGTGTGTGCAGCGGCTTAG-3'	5'-GTAGGGTGTCATGCGGAAGG-3'
Cry2	5'-GGAAGACCTCAGTCACCCTGTG-3'	5'-TCTTCACCAGGAGGTTCCTCG-3'

Tissue collection and SDS-PAGE

Mice were placed in a plexiglass restrainer and euthanized by microwave irradiation aimed at the head (5 kW, 1.2 s, Murimachi Kikai Co., LTD. Tokyo, Japan). VTA tissue was dissected from 1-2mm slices with a 16-gauge tissue punch and immediately frozen for later use. For protein extraction, tissue samples were homogenized by sonication on wet ice in a buffer containing 320mM sucrose, 5mM HEPES, phosphatase inhibitor cocktail I and II (Sigma, St. Louis, MO), protease inhibitor (Sigma, St. Louis, MO), 5% SDS, and 50mM NaF. Protein homogenate was spun at 12,000 RPM for 10 minutes at 4°C and the supernatant carefully removed. DC assays (Biorad, Hercules, CA) were performed to quantitate protein levels. Aliquots of sample were combined in Laemmli SDS sample buffer (Bio-World, Dublin, OH), and heated at 65°C for 20

minutes. Samples were loaded (10µg total protein per lane) and run on a pre-cast 4-15% Tris-glycine (TG) extended gel (Biorad, Hercules, CA) at 100V for ~ 90 minutes in 1X TGS buffer (Biorad, Hercules, CA). Proteins were transferred overnight at 4°C onto Immobilon PVDF membranes (Millipore, Bedford, MA) at 35V in 1XTG buffer.

Quantitative Immunoblotting

Membranes were re-wet briefly in a series of methanol, MilliQ water and 1XPBS and blocked in Odyssey Blocking Buffer (LI-COR Biosciences, Lincoln, NE) for 1 hour at room temperature (RT). Membranes were incubated overnight at RT with the following primary antibodies diluted in blocking buffer + 0.2% Tween20: mouse anti-TH (1:2000, Sigma, St. Louis, MO), rabbit anti-phospho-ser31 TH (1:400, Millipore, Bedford,MA), rabbit anti-phospho-ser40 TH (1:1000, Millipore, Bedford, MA) and mouse anti-GAPDH (1:20,000, Fitzgerald, Acton, MA). Blots were stripped between application of the two rabbit phospho-antibodies and re-probed (NewBlot Stripping buffer, LI-COR Biosciences, Lincoln, NE). Blots were washed in 1XPBS + 0.1% Tween20 and incubated for 1 hour at RT with infrared (IR)Dye 680 conjugated goat anti-rabbit (1:5000, LI-COR Biosciences, Lincoln, NE) and IRDye 800 conjugated goat anti-mouse secondary (1:5000, LI-COR Biosciences, Lincoln, NE) antibodies diluted in 0.2% Tween20 + 0.02% SDS. Blots were washed in 1XPBS + 0.1% Tween20 with a final wash in 1XPBS. Blots were scanned using the Odyssey Infrared Imaging System (LI-COR Biosciences, Lincoln, NE) interfaced to a PC running Odyssey 2.1 software for quantification.

Proteins bands were quantified using an integrated intensity and mean band background subtraction method. These values were then expressed as a ratio to the corresponding GAPDH integrated intensity to control for potential discrepancies in amount of protein loaded between samples.

Dopamine synthesis

Mice were injected with the amino acid decarboxylase inhibitor NSD-1015 (Sigma, 100 mg/kg, i.p.) and euthanized by cervical dislocation 60 min later. On a cold plate, the nucleus accumbens and dorsal striatum were punched out from separate tissue slabs (approximately +1.7-1.0 and +1.0-0.0 mm according to Bregma for nucleus accumbens and dorsal striatum, respectively) using 2 mm diameter circular tissue punches. Tissue punches were frozen and stored at –80^{o}C.

Tissue L-DOPA High-Performance Liquid Chromatography Electrochemical Detection (HPLC-EC) analysis

Tissues were weighed, frozen, and homogenized by sonication in 99 volumes (w/v) of ice-cold 100 mM $HClO_4$. Homogenate was centrifuged for 20 min at 15,000 g, 4°C. Supernatants were recovered and passed through 0.2 µm filters and L-DOPA was quantified in the filtrates by HPLC-EC. The HPLC system consisted of a BASi (West Lafayette, IN) LC-4C detector coupled to a BASi LCEC radial flow cell. Flow was provided by a Shimadzu (Columbia, MD) LC-20AD solvent delivery module, preceded by an online degasser series 1100 from

Agilent (Santa Clara, CA). The chromatograms were analyzed using PowerChrom software (eDAQ, Colorado Springs, CO). Monoamines in 10 µl tissue filtrate were separated on a 1 x 100 mm UniJet microbore 5 µm C-8 column (BASi). The mobile phase consisted of 24 mM Na_2HPO_4, 3 mM sodium octyl sulfate, 27.4 mM citric acid, 107 µM EDTA and 18.75 % (v/v) MeOH, pH adjusted to 2.4 with NaOH. The flow was set at 50 µl/min and the potential was set at + 750 mV relative to an Ag/Cl reference electrode. Elution time for L-DOPA was 7 min.

Chromatin immunoprecipitation

ChIP assays were performed according to the methods described previously (Tsankova, Kumar et al. 2004). Briefly, 2 mm VTA containing midbrain dissections from C57BL/6 mice or *Clock*Δ19 mutant mice and their wild type littermates were cross-linked with 1% formaldehyde for 15 minutes. Cross-linking was quenched with 2 M glycine for 5 minutes. The chromatin was sheared to approximately 200-1000 bp fragments by 8 rounds of sonication and cleared with Protein A beads (Thermo Scientific, Rockford, IL). Between 60 and 100 µg of chromatin was used for each pull-down with 5–12 µg of each of the following primary antibodies: CLOCK-H276x (Santa Cruz Biotechnology, Santa Cruz, CA); acetylated H3, no. 06-599 (Millipore, Bedford, MA); IgG no. 12-370 (Millipore, Bedford, MA); anti-phospho-Creb s133 no. 06-519 (Millipore, Bedford, MA). Antibody–chromatin complexes were immunoprecipitated with Protein A beads according to the manufacturer's instructions. Following reverse cross-linking of

input and precipitated samples, levels of protein binding at each promoter of interest were determined by measuring the amount of associated DNA by quantitative PCR (Applied Biosystems Prism 7700, Foster City, CA) with primer sets for the *TH* proximal and distal site promoters (sequences are listed in Table 2.1). Input DNA and immunoprecipitated DNA were amplified in duplicate in the presence of SYBR Green on the ABI 7500 Real-Time PCR system (Applied Biosystems, Carlsbad, CA). Relative quantification of template DNA was performed using the fold enrichment method.

Construction of WT and E-box mutant TH luciferase reporter gene constructs

The TH promoter reporter genes were prepared by inserting promoter fragments (containing the putative transcriptional start site) into the pGL3-luc vector. An initial TH promoter fragment (~1 kb) was generated by PCR from mouse genomic DNA with primers: 5'-TCCTGAACCATTGCCTGAAGGAAG-3' upstream and 5'-GGTCCCGAGTTCTGTCTCCA-3' downstream. This fragment was then inserted into pGEM-T Easy vector (Promega cat. #A1360) and subsequently digested with EcoR1 to release the 1 kb promoter or SacI and SalI to liberate the 250 bp fragment. These were cloned into pGL3-luc to generate -1 kb and -250 bp reporter constructs. Mutagenic primers were designed to produce point mutations at the putative E-boxes of the TH-luc constructs. The proximal E-box sequence of the -250 TH luc construct was changed from CAGGTG to CCCGGG (this resulted in production of a diagnostic XmaI site), using complementary primers

(coding sequence: 5'-CCCTTACATGGGGGCcccgggAGAATGGGGCTGCC-3'). The distal E-box sequence of the -1 kb TH luc construct was changed from CAGCTG to CCCGGG (this resulted in a production of a diagnostic XmaI site), using complementary primers (coding sequence: 5'-CCCTTACATGGGGGCcccgggAGAATGGGGCTGCC-3'). The manufacturer's recommended protocol was followed for QuikChange II Site-Directed Mutagenesis (Stratagene cat. # 200555) using a 6.5 min extension time. WT and mutant E-box TH-luc constructs were confirmed by DNA sequencing.

Luciferase assay

Cell culture and performance of the luciferase assay were carried out as described previously (Enwright III, Wald et al. 2010). Briefly, rat pheochromocytoma (PC12) cells were cultured in Dulbecco's modified Eagle's Medium F-12 supplemented with 10% horse serum, 5% fetal bovine serum, and 1% penicillin/streptomycin in a 37°C, 5% CO_2 incubator. The assay was performed using PC12 cells transfected by electroporation (BTX 360) with 5 µg of either construct. Three days post-transfection, cells were collected in lysis buffer (25 mM glycylglycin, 15 mM $MgSO_4$, 4 mM EGTA, 1% Triton X-100, pH 7.8, 1 mM DTT) and centrifuged to clear cellular debris. Thirty microliters of the resulting lysate was combined with 140 µl of luciferase assay buffer (25 mM glycylglycin, 15 mM $MgSO_4$, 4 mM EGTA, 1 mM DTT, 1 mM ATP, 1 mM potassium phosphate, 1 mM coenzyme A, pH 7.8). Luminescence was measured using an FLx-800 microplate fluorescence reader after an automated injection of

40 µL of 1 mM luciferin per well. Luciferase activity was normalized to total protein levels measured by Bio-Rad protein assay. qPCR was performed on PC12 lysates to verify endogenous expression of CLOCK (data not shown). Luciferase assays involving co-transfection of *Clock*-shRNA were performed with the Dual-Glo Luciferase Assay system kit components (Promega) according to the manufacturer's instructions. PC12 cells were cultured as described above, but Lipofectamine LTX with Plus Reagent (Invitrogen) was used to transfect 3.5 µg total DNA per well of a 12-well plate. Tk-Renilla (0.035 µg) was transfected in all wells to allow for normalization of the firefly luminescence to the renilla signal. Cells were harvested 48 hours post-transfection with Dual-Glo lysis buffer. Firefly luciferase activity was measured on a microplate luminometer after an automated injection of 100 µl of luciferase assay buffer II. Renilla luciferase activity was recorded after automated injection of 100 µL of Stop & Glo Reagent. Firefly luciferase enzyme activity was normalized to renilla luciferase activity.

Statistics

Data were analyzed by unpaired student's t-test or an ANOVA followed by a Bonferonni post-hoc test where appropriate. Analyses over time were conducted using a two-way ANOVA followed by a Bonferonni post-hoc test for multiple comparisons. Analyses were conducted using the GraphPad Prism 5 statistical software for Windows. The CircWave v1.4 software (courtesy of Dr. Roelof Hut, http://www.euclock.org/) was used to analyze rhythmicity of gene expression and protein level patterns. All data are presented as means ± standard error of the

mean with p< 0.05 considered statistically significant. *p<0.05, **p<0.01, ***p<0.001.

CHAPTER 3
Results

A MUTATION IN CLOCK LEADS TO ALTERED DOPAMINE RECEPTOR FUNCTION

(In preparation)

Sade Spencer, Melissa Torres-Altoro, Edgardo Falcon, Rachel Arey, Marian Marvin, Matthew Goldberg, James Bibb, and Colleen A. McClung

Introduction

The circadian rhythm, evolution's innate timekeeping system, plays a central role in the regulation of the normal physiology and behavior of nearly every living organism (Ko and Takahashi 2006). The desynchronization of one's "clock" in the form of genetic mutations, disruptions in sleep/wake cycle, or dysregulation of circulating hormones is a shared feature of numerous health problems including many psychiatric diseases (Barnard and Nolan 2008; Takahashi, Hong et al. 2008). Numerous studies have found alterations in physiological rhythms including sleep/wake activity, body temperature, blood pressure and hormones in major depression and bipolar disorder (BD) (Atkinson 1975; Linkowski, Mendlewicz et al. 1987; Linkowski, Kerkhofs et al. 1994). Indeed, the cycling nature of BD (including seasonal variations in mood states) led to the first postulations that there was a circadian component to the pathology of the disease (Sayer, Marshall et al. 1991; Cassidy and Carroll 2002; McClung 2007).

More recently, human genetics studies have identified SNPs and haplotypes in various circadian genes which associate with psychiatric disorders. For example, *cryptochrome 1 (Cry1)* and *neuronal PAS domain-containing 2 (Npas2)* have a statistically significant association with major depression while *circadian locomotor output cycles kaput (Clock)* and *vasoactive intestinal peptide (Vip)* are associated with BD (Soria, Martinez-Amoros et al. 2010). Finally, many of the common treatments for these conditions including mood stabilizing agents and antidepressants appear to alter or synchronize the internal clock (Welsh and Moore-Ede 1990; Possidente, Lumia et al. 1992).

The circadian clock is set by a core loop of proteins which usually cycle over a period of approximately 24 hours. Essential elements of this core loop include the transcription factors CLOCK and brain and muscle Arnt-like protein-1 (BMAL1) which heterodimerize and bind to E-box elements within a number of genes regulating their transcription (Ko and Takahashi 2006; Takahashi, Hong et al. 2008). The CLOCK-BMAL1 dimer positively regulates the *Period (Per)* and *Cryptochrome (Cry)* genes. The PER and CRY proteins themselves can form a complex, and upon re-entry into the nucleus inhibit their own transcription by repressing the function of CLOCK-BMAL1 in a negative feedback loop (Ko and Takahashi 2006). In addition to this core loop, there are a number of other proteins implicated in regulating the timing mechanism through diverse modifications (Cardone, Hirayama et al. 2005; Grimaldi, Nakahata et al. 2009; Katada and Sassone-Corsi 2010; Tataroglu and Schafmeier 2010). Though the master pacemaker lies within the suprachiasmatic nucleus (SCN) of the

hypothalamus, virtually every cell in the body possesses an auxiliary clock which can be synchronized to the SCN or in some cases oscillate semi-autonomously (Ko and Takahashi 2006).

Mounting evidence supports a role for the regulation of diverse neurotransmitter systems by the circadian clock. Dopamine and other neurotransmitters implicated in mood disorders have diurnal rhythms in their levels, levels of related enzymes, receptor expression or activity (Wirz-Justice 1987; Ozaki, Duncan et al. 1993; Akhisaroglu, Kurtuncu et al. 2005). Mice with a mutation in the *Clock* gene (*Clock*Δ19 mutants) display changes in dopaminergic transmission consistent with a disruption in the normal rhythm of dopaminergic activity (McClung, Sidiropoulou et al. 2005; Dzirasa, Coque et al. 2010; Spencer Submitted). Moreover, these mice show a behavioral phenotype that closely models human bipolar mania including disrupted circadian rhythms, hyperactivity, decreased depression-related behavior, less anxiety, and increased preference for multiple drugs of abuse (King, Vitaterna et al. 1997; Gekakis, Staknis et al. 1998; McClung, Sidiropoulou et al. 2005; Roybal, Theobold et al. 2007; Ozburn 2012). Aberrant monoamine function has been proposed to contribute to the pathology of many psychiatric diseases partially because drugs that act on transporters or receptors are effective treatments (Barchas 1999). As a result, numerous studies have examined the association between dopamine signaling and psychiatric disease. For example, a recent study provided evidence for an interaction between the catechol-O-methyltransferase (COMT) Val158Met allele and the dopamine D3 receptor (DRD3) Ser9Gly genotypes in bipolar I disorder

(Lee, Chen et al. 2011). Interestingly, *Clock*Δ19 mice have a defect in the ability of neurons in limbic circuits of the brain to synchronize as animals are performing behavioral tasks which likely contributes to their overall manic-like profile (Dzirasa, Coque et al. 2010; Dzirasa, McGarity et al. 2011). It is possible that this lack of synchronization in striatal regions is due to changes in dopamine receptor function in response to an altered dopaminergic tone. Thus, in this study, we examined the influence of the *Clock*Δ19 mutation on dopaminergic transmission in the striatum.

Results

Dopaminergic transmission is altered in the striatum of *Clock*Δ19 mice

Since the locomotor hyperactivity in the *Clock*Δ19 mice suggests an increase in dopaminergic signaling in dorsal striatum, we decided to measure levels of dopamine and metabolites in this region. To determine if there were significant changes in dopamine transmission in the striatum, we performed high performance liquid chromatography (HPLC) on tissue preparations from *Clock*Δ19 mice compared to controls. Here we found no significant difference in total dopamine levels between wild type and *Clock*Δ19 mutants; however, when dopamine metabolites and dopamine turnover were analyzed, significant differences emerged. There was an increase in DOPAC ($T(22) = 2.983$; $p < 0.01$) and HVA ($T(23) = 4.858$; $p < 0.0001$) in the mutant mice. When dopamine turnover was assessed, no change in the ratio of DOPAC/DA was observed but there was a significant enhancement in the HVA/DA ratio ($T(23) = 3.486$; $p <$

0.01). These changes in the levels of dopamine metabolites are reflective of alterations in dopamine neurotransmission within the dorsal striatum. As both the intraneuronal metabolite DOPAC and the extraneuronal metabolite HVA are augmented, it can be inferred that there is an increase in dopamine release and turnover although there is no significant net change in total dopamine levels.

Table 3.1 HPLC Analysis of Dopamine and Metabolites in Dorsal Striatum

	Dopamine	HVA	DOPAC	HVA/DA	DOPAC/DA
WT	129.19 ± 4.50	12.49 ± 0.31	7.25 ± 0.40	9.37 ± 0.26	5.69 ± 0.39
Clock∆19	138.66 ± 4.78	15.55 ± 0.53****	8.78 ± 0.32**	11.35 ± 0.49**	6.24 ± 0.25

Table 3.1 HPLC Analysis of Dopamine and Metabolites in Dorsal Striatum
Levels of dopamine (DA), HVA and DOPAC were measured in dorsal striatum tissue by HPLC. Values shown are the average pM/mg tissue ± the standard error. Dopamine levels were not significantly changed in the *Clock∆19* mice compared with wild type controls ($T_{(23)}$ = 1.435, p = 0.1646). There were significant differences in the metabolites and metabolite ratios. HVA, DOPAC and the ratio of HVA/DA were increased in the *Clock∆19* mice (**p<0.01 and ****p<0.0001, n = 12-13 animals per group).

Clock∆19 mice have an altered response to dopamine receptor antagonists

To explore the functional consequences of elevated striatal dopamine levels and metabolism in the *Clock*∆19 mice, the locomotor response to dopamine receptor antagonists was evaluated. Importantly, locomotion in response to these agents provides information about levels of the endogenous ligand, dopamine, in the extracellular space. The ability of the D2 antagonist raclopride to inhibit locomotor activity was assessed across a limited range of doses from 0.03 to 0.3 mg/kg (Figure 3.1A-D). We found a significant effect of dose ($F(3,40) = 11.81$; $p < 0.0001$) but no effect of genotype (Figure 3.1B).

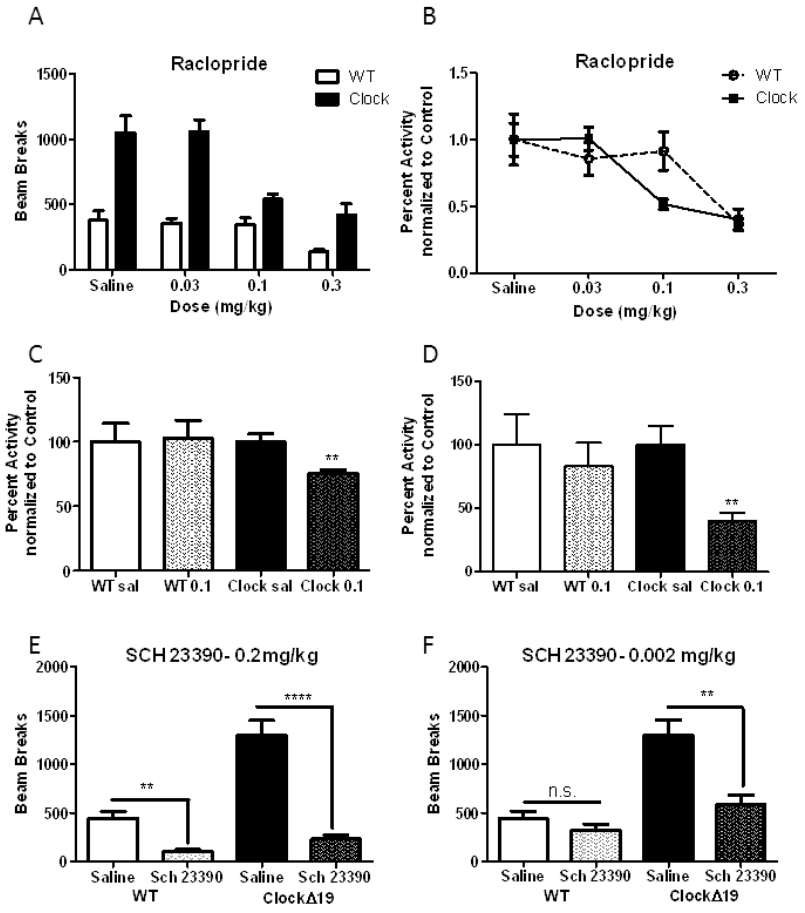

Figure 3.1. Locomotor response to dopamine antagonists A. Mean ± SEM for total beam breaks in a locomotor activity chamber for 60 minutes immediately following an i.p. injection of the indicated dose of raclopride. N = 5-6 per group. **B.** Data in A normalized to saline controls within each genotype for comparison of percent change in activity. There was a main effect of dose ($F_{(3,40)} = 11.81$; $p < 0.0001$). **C** and **D.** Percent activity at the 0.1 mg/kg dose of quinpirole separated into fine C. and ambulatory D. motor activity. The Student's t-test found differences in fine ($T_{(9)} = 3.393$; $p = 0.008$) and ambulatory ($T_{(10)} = 3.75$; $p = 0.0038$) components of locomotion exclusively in the *Clock*Δ19 mutants. **E.** Mean ± SEM for total beam breaks for 60 minutes immediately following an i.p. injection of 0.2 mg/kg SCH 23390. Activity was significantly decreased for WT ($T_{(15)} = 3.938$; $p = 0.0013$) and *Clock*Δ19 mice ($T_{(15)} = 5.636$; $p < 0.0001$). N = 7-10 per group. **F.** Mean ± SEM for total beam breaks for 60 minutes immediately following an i.p. injection of 0.002 mg/kg SCH 23390. Activity was significantly decreased in *Clock*Δ19 mutants ($T_{(15)} = 3.481$; $p = 0.0033$) but not controls. N = 7-10 per group.

However, closer evaluation of the dose-response curves suggested that there might be a leftward shift in responding to raclopride indicating a possible increase in sensitivity to the drug specifically at the 0.1 mg/kg dose. When a separate analysis of fine and ambulatory movement was performed at this dose, it revealed that the *Clock*Δ19 mutants display a significant decrease in percent activity in both fine (Figure 3.1C, $T(9) = 3.393$; $p < 0.01$) and ambulatory (Figure 3.1D, $T(10) = 3.75$; $p < 0.01$) movements compared to saline controls. Furthermore, this effect was not detected in the wild type animals suggesting increased sensitivity in the *Clock*Δ19 mutants. A similar increase in sensitivity was observed when the D1 antagonist SCH 23390 was administered. At a 0.02 mg/kg dose, a significant decrease in locomotor activity independent of genotype was found (Figure 3.1E) (WT: $T(15) = 3.938$, $p = 0.0013$; *Clock*Δ19*:* $T(15) = 5.636$, $p < 0.0001$). At the lower 0.002 mg/kg dose, the activity of the wild type mice was not significantly attenuated while the *Clock*Δ19 mutant mice displayed a significant 56% reduction in total locomotor activity (Figure 3.1F) ($T(15) = 3.481$, $p = 0.0033$). Taken together, these results are consistent with an increase in functional dopamine receptor protein and/or an increase in extracellular dopamine.

*Clock*Δ19 mutant mice have an altered behavioral response to a D2R agonist

Given that *Clock*Δ19 mice have altered dopaminergic transmission, we evaluated the influence of dopamine receptor agonists in their locomotor

responses. Low doses of a D2 agonist act preferentially on dopamine neurons (Shi, Smith et al. 1997), therefore D2-type autoreceptor function was assayed by administering i.p. injections of the D2 agonist quinpirole-hcl at doses ranging from 0.1 to 50 µg/kg (Figure 3.2A and B). As has been reported previously, the *Clock*Δ19 mutants display hyperactivity in response to a novel environment, therefore data was normalized within genotype to saline controls in order to directly compare changes in percent activity in response to the drug (Roybal, Theobold et al. 2007). As expected, there was a highly significant main effect of quinpirole dose ($F(4,93) = 7.31$; $p < 0.0001$) but no effect of genotype on the total locomotor response to quinpirole at any of these lower doses (Figure 3.2A and B). The quinpirole locomotor dose response study was then repeated with higher doses ranging from 1 to 24 mg/kg to ascertain whether there were any differences in postsynaptic responses (Figure 3.2C and D). Once again, a significant main effect of quinpirole dose on total locomotor activity was observed ($F(4,83) = 25.89$; $p < 0.0001$) with no effect of genotype. However, when total activity was subdivided into fine versus ambulatory motor behavior, there was a significant effect of genotype ($F(1,87) = 7.73$; $p < 0.01$) and dose ($F(4,87) = 19.27$; $p < 0.0001$) for fine motor movements (Figure 3.2E) with only an effect of dose for ambulations ($F(4,85) = 25.95$; $p < 0.0001$) (Figure 3.2F). This suggests that the *Clock*Δ19 mice are more sensitive to the locomotor inhibiting effects of quinpirole as demonstrated by the potentiation of the decrease in levels of fine or stereotyped motor movements produced in response to postsynaptic D2 receptor stimulation.

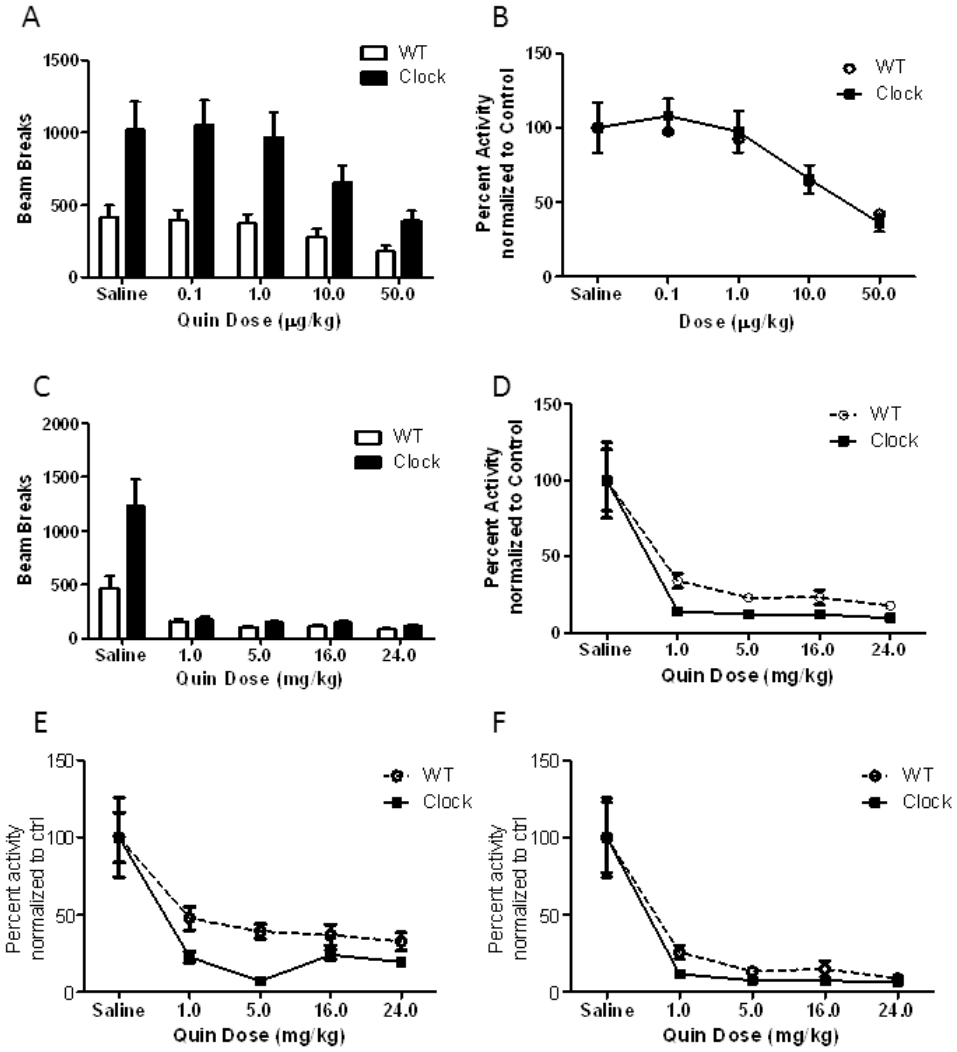

Figure 3.2. Locomotor dose response to D2 agonist. A. and **C.** Mean ± SEM for total beam breaks in a locomotor activity chamber for 60 minutes immediately following an i.p. injection of the indicated dose of quinpirole-hcl (n = 9-14 per group). **B.** Data in A normalized to saline controls within each genotype for comparison of percent change in activity. There is a main effect of quinpirole dose ($F_{(4,93)} = 7.31$; $p < 0.0001$) with no difference between genotypes. **D.** Data in C normalized to saline controls within each genotype for comparison of percent change in activity. There was a main effect of quinpirole dose ($F_{(4,93)} = 25.89$; $p < 0.0001$) with no effect of genotype. Subdividing this data into fine **E.** and ambulatory **F.** motor movements revealed a significant effect of genotype ($F_{(1,87)} = 7.73$; $p = 0.0067$) and dose ($F_{(4,87)} = 19.27$; $p < 0.0001$) for fine motor movements in E with only an effect of quinpirole dose for ambulations in F ($F_{(4,85)} = 25.95$; $p < 0.0001$).

D2 stimulation normally blocks horizontal locomotion while increasing stereotyped behaviors, but the in *Clock*Δ19 mutants there was a more complete suppression of movement.

*Clock*Δ19 mice are insensitive to the locomotor stimulating effects of a D1 agonist

We next assessed the locomotor response to the highly selective full D1-type agonist SKF 81297 which consistently elevates locomotor activity in wild type animals (Desai, Terry et al. 2005). Analysis by two-way ANOVA revealed a significant genotype x dose interaction ($F(4,40) = 4.97$; $p = 0.0024$) with a main effect on both genotype ($F(1,40) = 53.45$; $p < 0.0001$) and dose ($F(4,40) = 4.55$; $p < 0.01$) (Figure 3.3C and D). Bonferroni post-hoc analysis showed a significant increase in total percent activity in the wild type mice compared to the *Clock*Δ19 mutants at the 0.625, 2.5 and 5.0 mg/kg doses ($p < 0.05$, $p < 0.0001$ and $p < 0.0001$, respectively) (Figure 3.3D). To ensure that the lack of locomotor activation was not a function of reaching a ceiling effect, a set of wild type and *Clock*Δ19 mutant animals were challenged with a 15 mg/kg dose of the psychostimulant cocaine-hcl. A similar 30% increase in total locomotion was observed in both wild type and mutant mice (Figure 3.3E). These data suggest a significant perturbation of D1-type functional receptors in the *Clock*Δ19 mutants.

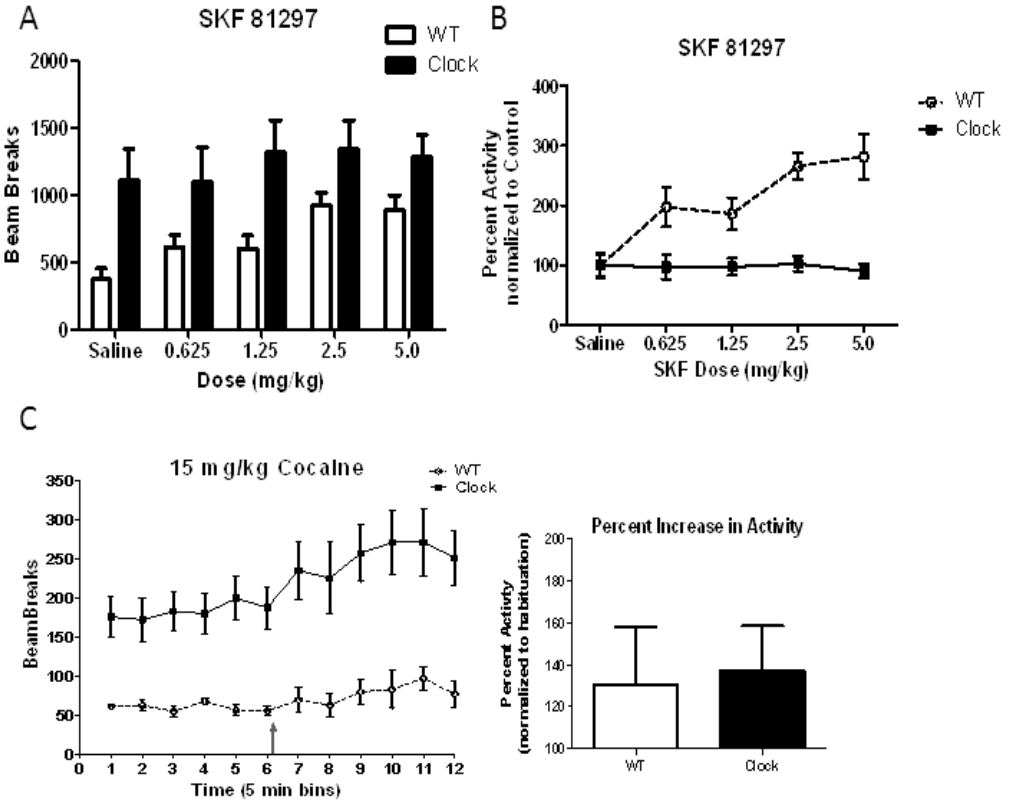

Figure 3.3. Locomotor response to D1 agonist A. Mean ± SEM for total beam breaks in a locomotor activity chamber for 60 minutes immediately following an i.p. injection of the indicated dose of SKF 81297 (n = 5 per group). **B.** Data in A normalized to saline controls within each genotype for comparison of percent change in activity. Analysis by two-way ANOVA revealed a significant genotype x dose interaction ($F_{(4,40)} = 4.97$; $p = 0.0024$) with a main effect of genotype ($F_{(1,40)} = 53.45$; $p < 0.0001$) and a main effect of dose ($F_{(4,40)} = 4.55$; $p = 0.004$). Bonferroni post-hoc analysis showed a significant difference between the means at the 0.625 ($p < 0.05$), 2.5 ($p < 0.0001$) and 5.0 mg/kg ($p < 0.0001$) doses. **C.** Beam break activity over time. Arrow indicates i.p. injection of 15 mg/kg cocaine. WT and *Clock*Δ19 mutant mice showed a 30% increase in locomotor activity to this dose of cocaine.

*Clock*Δ19 mice have an altered D1/D2 ratio in striatum

Since the results from the locomotor experiments with D1 and D2 receptor agonists and antagonists demonstrated a functional change in

dopamine receptor activity, we next set out to determine if there were changes in dopamine receptor protein levels in dorsal striatum.

Surprisingly, evaluation of total protein levels revealed a slight but significant increase in total D1 receptor levels in the *Clock*Δ19 mice ($T(8) = 2.739$; $p = 0.0255$) (Figure 3.4A). These data were acquired during the same time of the day in which the locomotor activity assays were performed. When D2 protein levels were measured there was a much more robust increase ($T(8) = 3.775$; $p = 0.0054$) (Figure 3.4B) which resulted in a dramatic decrease in the D1/D2 ratio in the striatum ($T(8) = 2.553$; $p = 0.034$) (Figure 3.4C). A biotinylation assay was used to determine whether these changes in total protein levels were reflective of the membrane-bound population of dopamine receptors. There was not a substantial difference in surface levels of the D1 dopamine receptor, but again surface D2 receptors were significantly upregulated in *Clock*Δ19 mice ($T(8) = 2.99$; $p = 0.0173$). Thus, the altered response to dopaminergic drugs is associated with an improper D1/D2 receptor composition in the striatum.

D1/D2 receptor signaling is altered in the *Clock*Δ19 mice

To further define the effects of the altered D1/D2 protein ratio observed in the *Clock*Δ19 mice on striatal dopamine signaling, we evaluated the responsiveness of the cAMP/protein kinase A (PKA) cascade to forskolin, a potent adenylate cyclase activator. The D1 dopamine receptor family is coupled to Gαs which increases cAMP formation, thus enhancing PKA activity whereas the Gαi-coupled D2 dopamine receptors antagonize this pathway (Herve 2011).

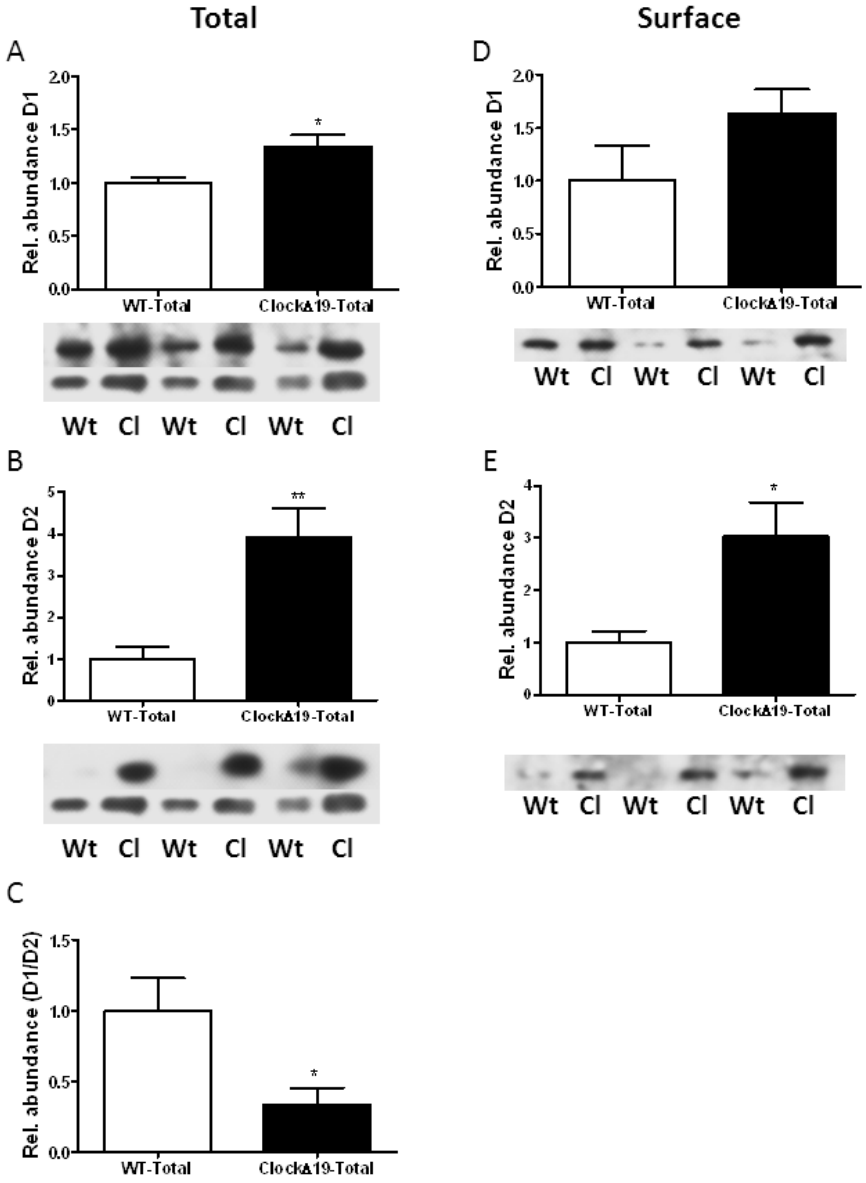

Figure 3.4. Dopamine receptor protein levels in the dorsal striatum. A. Total D1DR protein levels in the striatum were increased in *Clock*Δ19 mutants ($T_{(8)}$ = 2.739; p = 0.0255). **B.** Total D2DR protein levels in the striatum were increased in *Clock*Δ19 mutants ($T_{(8)}$ = 3.775; p = 0.0054) **C.** The ratio of D1DR protein to D2DR protein was significantly altered in the *Clock*Δ19 mutants ($T_{(8)}$ = 2.553; p = 0.034). **D.** No difference in surface D1DR protein. **E.** Surface D2DR protein levels in the striatum were increased in *Clock*Δ19 mutants ($T_{(8)}$ = 2.99; p = 0.0173). N= 4-5 animals per genotype.

We assessed the PKA-dependent phosphorylation of two important downstream effectors of dopamine signaling, the GluR1 subunit of the AMPA receptor and extracellular signal-regulated kinase (ERK) following treatment with forskolin. Treatment of striatal slices with forskolin increased the PKA-dependent phosphorylation of GluR1 at Ser845 in wild type (Figure 3.5A, $T(13) = 5.359$, $p = 0.0001$) and *Clock*Δ19 mice ($T(12) = 11.05$, $p < 0.0001$) without affecting total levels of GluR1 (Figure 3.5B), however the response in wild type mice was much larger than that seen in the *Clock*Δ19 mice ($T(9) = 2.288$, $p = 0.0479$). A similar effect was observed for phospho-ERK2-T183/Y185. Forskolin significantly enhanced the phosphorylation of ERK2 in the wild type ($T(13) = 3.527$, $p = 0.0037$), but the induction did not reach significance in the *Clock*Δ19 mutants (Figure 3.5C). Thus, there was a significantly reduced level of induction in the *Clock*Δ19 mutants compared to that observed in the wild type ($T(9) = 2.24$, $p = 0.05$). The drug treatments had no effect on total ERK levels in either genotype (Figure 3.5D) and there were no baseline differences in total ERK (Figure 3.5D) or phospho-ERK2 between genotypes (Figure 3.5C). These results suggest a blunted response in the *Clock*Δ19 mutants to cAMP stimulation.

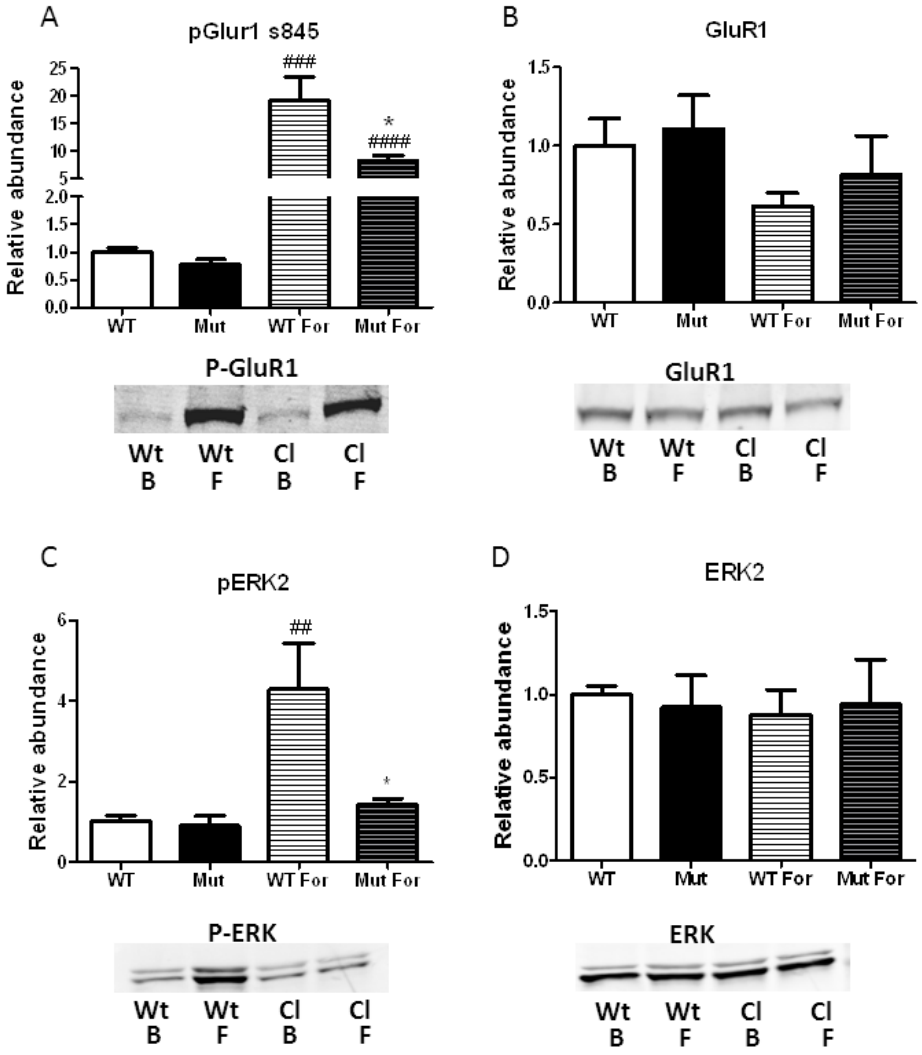

Figure 3.5. cAMP signaling. Effects of treatment of striatal slices with forskolin (10 μM, 5 min) or KREB's buffer. Representative blots with quantification. N = 3 animals per genotype with 2-3 biological replicates per n. **A.** Treatment of striatal slices with forskolin increased p-GluR1 Ser845 in wild type ($T_{(13)}$ = 5.359; p = 0.0001) and *Clock*Δ19 mice ($T_{(12)}$ = 11.05; p < 0.0001), but the induction in the mutant mice was significantly weaker than that observed in controls ($T_{(9)}$ = 2.288; p = 0.0479). **B.** Treatments did not affect total GluR1 levels. **C.** Treatment of striatal slices with forskolin increased phospho-ERK2 T183/Y185 in wild type mice ($T_{(13)}$ = 3.524; p = 0.0037) but not in *Clock*Δ19 animals resulting in a significant difference between genotypes with this treatment ($T_{(9)}$ = 2.24; p = 0.05). **D.** Treatments did not affect total levels of ERK2.

Discussion

These results show that loss of function of the circadian transcription factor CLOCK results in robust changes in dopaminergic transmission and dopamine receptor function. Mice with the dominant-negative *Clock*Δ19 mutation display altered responses to dopamine receptor antagonists which suggest increased dopaminergic tone. This is consistent with the increased dopamine cell firing and bursting previously reported in these mutants (McClung, Sidiropoulou et al. 2005; Coque, Mukherjee et al. 2011). Interestingly, our previous studies found that these mice have an increase in total tissue dopamine content but no change in metabolite levels in the nucleus accumbens (Coque, Mukherjee et al. 2011). Here we find that in the dorsal striatum there is no significant difference in total dopamine levels, but rather an increase in DOPAC which could indicate greater MAO-A enzymatic activity. This is interesting since previous studies have found that the circadian proteins BMAL1, NPAS2 and PER2 can regulate the transcription of MAO-A (Hampp, Ripperger et al. 2008). However the DOPAC/DA ratio was not significantly different between genotypes because the mutants displayed a parallel trend toward augmented dopamine levels. Both total levels of HVA and the HVA/DOPAC ratio were increased in the mutants which could be suggestive of an overall increase in transmitter release and extracellular dopamine. This interpretation is consistent with the observation of increased sensitivity to D1 and D2 receptor antagonists. These differences in dopamine levels between the ventral and dorsal striatum could be due to the fact that the rate limiting enzyme in dopamine synthesis, tyrosine hydroxylase is

increased in the *Clock*Δ19 mice selectively in the VTA and not in the substantia nigra (SN) (McClung, Sidiropoulou et al. 2005). Future studies will determine if there are similar differences in dopaminergic activity in the SN as seen in the VTA.

The *Clock*Δ19 mutants failed to produce a locomotor activating response to a D1-type agonist. However they show a normal locomotor response to cocaine. This suggests that D1 receptor signaling is impaired in the *Clock*Δ19 mice while D2-type responses might be heightened. The change in D1 receptor activity could represent an attempt of the circuit to compensate for the increased dopaminergic tone in these mice. A decrease in D1 receptor protein was not observed, rather a slight increase in D1 protein was reported in the striatum. Thus the absence of response to the D1 agonist is not due to a lack of protein translation. It is possible that there are differences in receptor affinity which underlie the difference in response as both D1 and D2 receptors have been shown to occupy high and low affinity states (Richfield, Penney et al. 1989). Additionally, it is now increasingly clear that dopamine receptor heteromers represent a biologically relevant subpopulation within the brain with unique pharmacological and signal transduction profiles (Hasbi, O'Dowd et al. 2011). A change in the proportion of D1-D2 heteromers might be expected to change the profile of the response to individual dopamine receptor agonists. Interestingly, the D1-D2 heteromer has already been implicated in both addiction and schizophrenia (Hasbi, O'Dowd et al. 2011). Similarly, there may be changes in the fraction of receptors which are synaptic versus extra-synaptic accounting for

discrepancies between D1 protein levels and activity. Curiously, a lack of response to a D1 agonist is similarly seen in both D1R knock-out mice and in mice in which the D1 receptor is overexpressed (Xu, Moratalla et al. 1994; Dracheva, Xu et al. 1999). Studies involving independently generated D1DR knockout mice have generated conflicting results with reports of no change in horizontal locomotor activity or slight locomotor depression (Drago, Gerfen et al. 1994; Smith, Striplin et al. 1998) and other reports of hyperactivity (Xu, Moratalla et al. 1994). This discrepancy could be attributed to multiple factors ranging from differences in targeting strategy, background strain, and experimental conditions. D1 receptors are prominent not only in striatum but also in prefrontal cortex and these receptors are thought to have opposing roles in the regulation of locomotor activity in these brain regions (Wilkinson 1997), therefore future studies will be necessary to assess changes in cortical dopamine transmission in the *Clock*Δ19 mice.

It is likely that a change in the D1/D2 ratio in striatum is involved in the aberrant response profile. Indeed there is a robust increase in D2 receptor expression in the *Clock*Δ19 mice and an increased response to a D2-type agonist. Moreover, the pharmacological studies performed in slice preparations demonstrate that there is a decrease in the level of PKA induction by forskolin in the mutants. For instance, while forskolin stimulated GluR1 ser845 phosphorylation in both wild types and mutants, the increase was four-fold higher in the wild type. These results point towards a possible increase in antagonism of cAMP stimulation by D2-type receptors. Interestingly, increased D2 receptor

signaling has been implicated in bipolar disorder. Analysis of post-mortem brain samples of the pre-frontal cortex from diseased brains and healthy controls found *DRD2* expression increased in BD patients and decreased in schizophrenics relative to controls (Zhan, Kerr et al. 2011). Moreover, data collected from *in vivo* imaging studies of D2 receptor occupancy within the basal ganglia have reported an increase in binding in bipolar psychotic patients (Wong, Pearlson et al. 1997; Nikolaus, Antke et al. 2009).

It is increasing clear that the coupling of diverse neuronal populations throughout the brain is involved in encoding higher order cognitive processes. For example, the phase relationship of striatal and hippocampal theta rhythms has previously been correlated with goal-directed learning in a T-maze task (DeCoteau, Thorn et al. 2007). Previously we found that the *Clock*Δ19 mice have serious defects in the ability of limbic regions of the brain to synchronize activity as the mice explore certain anxiety-related environments (Dzirasa, Coque et al. 2010; Dzirasa, McGarity et al. 2011). The changes in striatal dopamine transmission reported here including altered dopamine turnover and D1/D2 ratios in the *Clock*Δ*19* mutants likely contribute to the defects in proper synchronization that are necessary for the animal to make important decisions regarding their level of exploratory behavior. The nigrostriatal dopamine system and the dorsal striatum have traditionally been studied in terms of sensorimotor function while the mesolimbic dopamine system and the nucleus accumbens has been investigated for its role in motivation and addiction, but just as the anatomical boundaries between these brain regions are imprecise so too are the functional

distinctions. There is significant overlap in terms of contributions to brain stimulation reward, habitual behavior, reward prediction and reinforcement of memory consolidation (Wise, 2009). Accordingly, it would not be surprising if the alterations in dopaminergic transmission reported here resulted in disrupted circuit level activity, and contributed significantly to the *Clock*Δ19 mutant phenotype beyond the observed hyperactivity. Future studies will more specifically determine the role of altered striatal dopaminergic signaling in neuronal synchronization and related behaviors.

Conclusions

In summary, normal CLOCK function appears to be involved in the regulation of dopamine transmission in the dorsal striatum. Loss of CLOCK function increases dopamine release and turnover in the striatum as indicated by increased levels of metabolites HVA and DOPAC. Moreover, this increased dopaminergic tone results in downstream changes in levels of dopamine receptor protein with a surprising augmentation of both D1DR and D2DR protein levels but a significant shift in the ratio of D1 to D2 receptors in favor of D2DR. Finally, these effects have functional consequences at both the level of behavior and cellular signaling with alterations in locomotor responses to both D1 and D2-type specific agonists, and a blunted activation of cAMP signaling in the *Clock*Δ19 mutants. Taken together, these studies further define the defects in dopaminergic transmission which result from a nonfunctional CLOCK protein, and help

elucidate the changes in dopaminergic transmission which are responsible for the regulation of activity, reward, and mood.

Materials and Methods

Animals

*Clock*Δ19 mutant mice were created by *N*-ethyl-*N*-nitrosurea mutagenesis and produce a dominant-negative CLOCK protein defective in transcriptional activation activity as described (King, Vitaterna et al. 1997). For all experiments using *Clock*Δ19 mutants, adult male mutant (*Clock/Clock)* and wild type (+/+; WT) littermate controls on a mixed BALBc/C57BL/6J background were group housed in sets of 2-4 per cage on a 12/12-h light dark cycle (lights on at 6:00 a.m. = Zeitgeber time (ZT) 0, lights off at 6:00 p.m. = ZT 12) with food and water provided *ad libitum*. All animal use was conducted in accordance with the National Institute of Health guidelines and approved by the Institutional Animal Care and Use Committees of UT Southwestern Medical Center.

Drugs

(-)-Quinpirole hydrochloride (LY 171,555), R(+)-SKF 81297 hydrobromide, S(-)-Raclopride (+)-tartrate salt, R(+)-SCH 23390 hydrochloride, and forskolin were purchased from Sigma-Aldrich. Cocaine hydrochloride was provided by the National Institute on Drug Abuse (NIDA).

High-Performance Liquid Chromatography

Dorsal striatum dopamine measurements were performed as described previously (Goldberg, Fleming et al. 2003). Briefly, fresh brains were dissected from adult animals and 1 mm coronal slices taken using a mouse brain matrix. One millimeter tissue punches of the dorsal striatum were placed in 1.5 ml microcentrifuge tubes, weighed, and frozen on dry ice. The samples were stored at −80°C until further processing. The tissue punches were homogenized by sonicating in 49 volumes of 0.1 N perchloric acid and 0.2 mM sodium bisulfite. The homogenate was centrifuged at 20 000 *g* for 10 min at 4°C to pellet the debris. Twenty-five microliters of the resulting homogenate was loaded into an autosampler connected to an high-performance liquid chromatography with an electrochemical detector (ESA CoulArray with Model 5014B Microdialysis Cell) to measure the levels of dopamine and dopamine metabolites homovanillic acid (HVA) and 3,4-dihydroxyphenylacetic acid (DOPAC). Neurotransmitter levels were normalized to tissue weight.

Locomotor activity

Mice were individually placed in automated locomotor activity chambers equipped with infrared photobeams (San Diego Instruments) and measurements began immediately. Fine and ambulatory motor activity of the animals was continuously measured with the data collected in 5-min bins. Locomotor activity dose response studies were performed in a randomized Latin-square design. Mice were moved to the behavioral testing room 1 hour prior to the habituation

period each day. The first hour of each locomotor activity session was measured as baseline activity. After this time, the animals received an injection of vehicle or the indicated dose of each drug and locomotor activity was measured for an additional hour.

Surface biotinylation assays

Surface dopamine receptor levels were detected using a biotinylation assay followed by quantitative immunoblot analysis. Animals were sacrificed by cervical dislocation, their brains removed, and slices prepared with 1 mm brain block. Fresh dorsal striatum tissue punches were dissected and frozen on dry ice for later processing. The tissue punches were thawed and chopped into smaller fragments. Each sample was then incubated in 1X PBS containing 1 mg/ml EZ-Link sulfo-NHS-Biotin (Pierce) for 40 min at 4°C with rotation. After a further 10 minute incubation on ice, the biotinylation reaction was quenched by a 10 minute incubation in ice-cold 100 mM glycine in 1X PBS on ice. Then the tissue was washed 3 times in PBS and homogenized by sonication in RIPA buffer (Pierce) containing protease inhibitors and phosphatase inhibitor cocktails I and II (Sigma-Aldrich). A DC protein assay (Biorad) was performed on these total homogenates to ascertain protein concentrations. From each sample, 100 µg of total protein was removed to a separate eppendorf tube and the biotinylated fraction was precipitated with 100 µl of Neutravidin Agarose slurry (Pierce) for 2 hours at 4°C with rotation. After this incubation, the samples were centrifuged for 3 minutes at 10,000xg and the supernatant collected was the non-biotinylated intracellular

fraction. The biotinylated surface proteins were eluted from the neutravidin beads by boiling for 10 minutes at 90°C in 50 µl of loading buffer with DTT. Total protein fractions and biotinylated proteins were separated on 12% SDS-PAGE gels and detected by western blot using specific antibodies for D1 (1:2000, GeneTex) and D2 (1:1000, Millipore) dopamine receptors, gapdh (1:10000, Fitzgerald) and n-cadherin (1:5000, millipore). Horseradish peroxidase-conjugated secondary antibodies (Jackson ImmunoResearch) were used in combination with the Supersignal West Dura system (Promega) to detect the signal on film. Densitometry was conducted by using NIH IMAGE software. These values were expressed as a ratio to the corresponding gapdh band to control for potential discrepancies in amount of protein loaded among samples.

Acute slice pharmacology and quantitative immunoblotting

Preparation and incubation of striatal slices was performed as reported previously (Hamada, Higashi et al. 2004). Wild type and *Clock*Δ19 mutant mice were sacrificed by decapitation. Their brains were rapidly dissected and placed in ice-cold oxygenated Krebs buffer (124 mM NaCl, 4 mM KCl, 26 mM $NaHCO_3$, 10 mM D-glucose, 1.5 mM $CaCl_2$, 1.5 mM $MgSO_4$, 1.25 mM KH_2PO_4). The striatum was microdissected from 350 µm coronal sections prepared on a vibratome. Individual slices were placed in polypropylene incubation tubes with 2 ml of fresh Krebs buffer containing 10 µg/ml adenosine deaminase (Sigma) and pre-incubated at 30°C with continuous oxygenation with 95% O_2/5% CO_2 for 60 minutes. The Krebs buffer was replaced with fresh solution after the first 30

minutes. Slices were then treated with Krebs buffer alone, or buffer containing forskolin (10 µM) for 5 minutes. After the treatments, slices were transferred to eppendorf tubes, quickly frozen on dry ice, and stored at -80°C until processed for immunoblotting. The samples were sonicated in boiling lysis buffer (1% SDS with 50 mM sodium fluoride) and boiled for an additional 10 minutes. The protein concentration of each sample was determined by the DC protein assay (Biorad). Aliquots of sample were combined in Laemmli SDS sample buffer (Bio-Rad), and boiled at 95°C for 5 minutes. Equal amounts of protein (~75 µg) were loaded onto 10% polyacrylamide gels and separated SDS/PAGE electrophoresis at 150 V for 5 hours. Proteins were transferred overnight at 4°C onto Immobilon PVDF membranes (Millipore,) at 35V in 1XTG buffer. Membranes were incubated overnight at 4°C with the following primary antibodies diluted in blocking buffer: mouse anti-GluR1 (1:3000), and rabbit anti-phospho-GluR1 ser845 (1:2000) from Millipore Corporation, mouse anti-p44/42 MAPK (ERK1/2) (1:1000), and rabbit phospho-p44/42 (Thr202/Tyr204) (1:2000) from Cell Signaling Technology, and tubulin as loading control (Epitomics). Blots were probed simultaneously for total and phosphorylation state-specific antibodies using infrared IR-Dye 680 conjugated goat anti-rabbit and IR-Dye 800 conjugated goat anti-mouse secondary (1:10,000, LI-COR Biosciences) antibodies for two-color detection. Blots were scanned using the Odyssey Infrared Imaging System (LI-COR Biosciences) interfaced to a PC running Odyssey 2.1 software for quantification. Proteins bands were quantified using an integrated intensity and mean band background subtraction method. These values were then expressed as a ratio to

the corresponding tubulin integrated intensity to control for potential discrepancies in amount of protein loaded among samples. Phospho-protein levels were normalized to total protein values.

Statistics

All data were analyzed using an unpaired student's t-test or ANOVA followed by a Bonferonni post-hoc test, unless otherwise specified. Analyses were conducted using the GraphPad Prism 5 statistical software for Windows. All data are presented as means ± standard error of the mean with $p < 0.05$ considered statistically significant. *$p<0.05$, **$p<0.01$, ***$p<0.001$, and ****$p<0.0001$.

CHAPTER 4

CONCLUSIONS

Accumulating evidence indicates that disruptions in the molecular circadian clock contribute to a number of central nervous system disorders. Prominently, bipolar disorder has been suggested to have an association with a number of circadian genes. In fact, the circadian mutant *Clock*Δ19 mice have been identified as a promising tool for modeling the manic phase of bipolar disorder. The manic-like behavior of these mice seems to be associated with changes in dopaminergic transmission in the ventral tegmental area which sends prominent projections to the nucleus accumbens and prefrontal cortex. Significantly, altered mesocorticolimbic dopamine function is attributed to a variety of psychiatric diseases including substance abuse disorders, mania, depression, and schizophrenia. Importantly, there is a growing body of evidence indicating important cross-talk between the dopamine and circadian systems. Thus the *Clock*Δ19 mutants are a useful tool for investigating the influence of the circadian system on dopamine transmission and potentially discovering the molecular mechanisms underlying various mood and reward-related disturbances.

This thesis work studied the role of CLOCK in regulation of dopamine transmission in the context of the *Clock*Δ19 model of mania. *In vivo* VTA dopamine cell firing and bursting, measured by surgically implanted electrode arrays, was elevated in the mutants during REM sleep across the 24 hour cycle

with the most significant differences observed during the first half of the light cycle. The earlier finding that knock-down of *Clock* in the VTA by shRNA is sufficient to increase dopamine cell firing in a cell autonomous fashion suggests that this change in physiology is at least partially intrinsically facilitated by alterations in the intracellular gene expression program (Mukherjee, Coque et al. 2010). Microarray analysis of LCM dissected knock-down cells versus control samples revealed the dysregulation of a number of genes involved in dopamine transmission including some in common with the constitutive *Clock*Δ19 mutant like *TH* and *preproenkephalin* as well as a number of different ion channels (Mukherjee, Coque et al. 2010). On the other hand, dopamine cell bursting is believed to be driven by afferent projections because dopamine neurons do not spontaneously fire bursts in slice (Floresco, West et al. 2003), but alterations in the excitability of dopamine cells can make them more or less prone to burst firing. Therefore, it will be interesting to determine what mechanisms within the VTA itself in addition to circuit-level alterations differentially contribute to the enhancement in firing and bursting seen in the VTA of *Clock*Δ19 mutants.

The firing of dopaminergic neurons was measured during REM sleep as opposed to in anesthetized animals, because REM sleep is a normal physiological state characterized by dopamine release comparable to that observed during the waking state and greater than in the more quiescent state of slow wave sleep (SWS) as measured in multiple VTA projections (Lena, Parrot et al. 2005). REM sleep is also termed paradoxical sleep because the discovery of this third distinct behavioral state was contrary to the previously held notion that

sleep was a wholly passive process marked by a lack of significant neuronal activity. In fact, it is well known that many brain regions are significantly more active during REM sleep (Jones 1991). Although extracellular dopamine levels display a clear diurnal rhythm, dopamine containing neurons of the VTA and SN actually do not normally display significant differences in their mean firing rate across sleep-wake transitions (Miller 1983; Trulson and Preussler 1984). Other evidence suggests, however, that other important sleep-state related changes in dopaminergic activity occur during the REM phase within these regions. C-fos immunoreactivity, a molecular marker of cellular activity, is increased in rat dopamine neurons concentrated in the VTA but not the SN during REM sleep rebound after REM deprivation (Maloney, Mainville et al. 2002). Moreover, dopamine release in the nucleus accumbens and prefrontal cortex is elevated during REM sleep compared to SWS (Léna, Parrot et al. 2005). Differences in firing pattern rather than firing rate are hypothesized to contribute to these differences. It is notable that when the bursting rate of dopaminergic neurons in WT mice was compared during the ZT0-6 versus ZT12-18 epochs, it was found that these neurons displayed a significantly increased bursting rate during the light cycle at the peak of REM sleep time. It is beyond the scope of this study, but it would be informative to examine both firing and bursting rate parameters across all three behavioral states in both wild types and mutants.

The mutants displayed significant deficits in REM sleep time during the light phase, the normal inactive period. Previously, an analysis of sleep parameters in the coisogenic C57BL/6J *Clock*Δ19 mutant mouse revealed

deficits specifically in SWS sleep with no baseline differences in REM sleep as well as a 51% lower increase in rebound REM sleep after 6 hours of sleep deprivation (Naylor, Bergmann et al. 2000). The Naylor et al study compared total time spent in each behavioral state between wild type, heterozygote, and *Clock*Δ19 mutant mice whereas the present analysis was more sensitive to light-cycle dependent changes because it compared time spent in REM sleep in four separate periods across the light-dark cycle. Indeed, total REM sleep time is not different between genotypes in the present study if pooled across time. It has been shown that alterations in REM sleep can contribute significantly to neurobiological disease. For example, a relative increase in REM sleep has been associated with mood disturbances like major depression and a decrease in REM sleep has been correlated with neurodegeneration such as Parkinson's disease (ACNP 2008). It is unclear how a disturbance in REM sleep pattern rather than deviation in total REM sleep time, as is described in the *Clock*Δ*19* mutants might contribute to mood-related behavior. Importantly, sleep disturbances in general are a common risk for mood and substance use disorders. Between 60-84% of patients with major depressive disorder and anywhere from 23-78% of bipolar manic patients report symptoms of insomnia (Harvey 2011).

Remarkably, a chronic elevation of neuronal activity in the VTA of wild type mice through optogenetic manipulations resulted in an increase in exploratory activity and a decrease in anxiety-related behavior analogous to the behavior of the *Clock*Δ19 mutants. Conversely, it was previously demonstrated

that decreasing dopamine cell firing in the *Clock*Δ19 mutants with a potassium channel virus (HSV Kir2.1) had an anxiety inducing effect (Coque, Mukherjee et al. 2011). Another recent study examined the contribution of dopamine neuron activity to aversive conditioning and generalized anxiety in a transgenic model that utilized genetic inactivation of NMDA receptors by expressing a mutated form of the essential NR1 subunit specifically in DAT expressing cells to prevent glutamatergic activation of DA neurons in response to aversive stimuli. These researchers found that cue-dependent fear conditioning was impaired in these mutants and anxiety-related behavior was enhanced following but not prior to foot-shock conditioning (Zweifel, Fadok et al. 2011). Importantly, this behavior was rescued by restoration of NMDAR signaling in the VTA (Zweifel, Fadok et al. 2011). The Zweifel study highlighted the contribution of stimulated dopamine release to anxiety related behavior compared to the Coque at al report which involved modulation of inherent excitability of VTA dopamine neurons by expressing a potassium channel virus. This difference likely accounts for the lack of a baseline difference in the NR1 mutant. Similarly, the optical stimulation paradigm employed here with the slower off kinetics of the step-function opsin results in a constant state of depolarization over an extended period of time that would be expected to increase both intrinsic and evoked responses of the VTA dopamine cells. A single *in vivo* dose of a benzodiazepine agonist, a pharmaceutical commonly prescribed for the treatment of anxiety disorders, results in a long-lasting increase in the AMPA/NMDA ratio in VTA dopamine neurons (Heikkinen, Moykkynen et al. 2008). These findings point to a prominent

involvement of VTA dopaminergic neurotransmission and plasticity in the development and treatment of anxiety-related disorders.

Apart from anxiety-related behavior, changes in the activity of dopamine neurons has also been linked to depression-related behavior and activation of stress pathways. An acute restraint stress increases mean firing and bursting rate in VTA dopamine neurons which persists 24 h after a single exposure to stress (Anstrom and Woodward 2005). A chronic 10 day social defeat stress paradigm similarly results in an increase in VTA dopamine cell firing when measured immediately after termination of the defeats selectively in mice that have been categorized as susceptible (Krishnan, Han et al. 2007). The neuroadaptation of increased burst firing in the VTA is persistent up to 3 weeks after social defeat (Razzoli, Andreoli et al. 2011). It is unclear how increased VTA dopamine cell firing leads to a decrease anxiety-related behavior on the one hand, but increased depression-related behavior on the other, and it is difficult to integrate these VTA firing rate findings in terms of the anxiety and depression-related behavior and the phenotype of *Clock*Δ19 mutants. It seems clear that overlapping, but distinct brain circuits are involved in regulating these behaviors.

In the search for molecular mechanism underlying the mood and reward-related phenotypes of the ClockΔ19 mutants, it was previously reported that many genes involved in dopaminergic transmission are dysregulated in the VTA of these mice including tyrosine hydroxylase, the rate limiting enzyme in dopamine synthesis (McClung, Sidiropoulou et al. 2005). In the past, comprehensive microarray studies have examined gene expression changes in

the *Clock*Δ19 mice in the SCN as well as peripheral tissues such as the liver and skeletal mouse and found that levels and patterns of gene expression are modulated in diverse ways as a result of the loss CLOCK function including general upregulations or downregulations as well as shifts in rhythms suggesting that CLOCK can alter transcription in various ways (Miller, McDearmon et al. 2007) (Panda, Antoch et al. 2002). These studies have largely not been extended to brain regions outside of the SCN like the VTA, but a recent study used laser capture microdissection and ultra-low mRNA amplification (LCM-ULI) to profile the transcriptome in a variety of brain regions, including the VTA, at two time points across the light-dark cycle (Winrow, Tanis et al. 2009). Interestingly, the VTA had the highest number of light-dark regulated genes compared to the other brain regions profiled including the locus coeruleus (LC), SCN and ventrolateral preoptic nucleus (VLPO) (Winrow, Tanis et al. 2009). The present report may be the first to elucidate the mRNA expression profile of tyrosine hydroxylase as well as a number of circadian genes at multiple time points across the light-dark cycle within the VTA. Significant diurnal variations in *TH, Clock, Per2* and *Cry2* expression were reported in the VTA of wild type mice with these rhythms being blunted in the *Clock*Δ19 mutants. Both *Per2* and *Cry2* mRNAs were predictably downregulated in the ClockΔ19 mutants as they are direct downstream targets of CLOCK transactivation. Appropriately, expression of *Bmal1* which is not a CLOCK target was observed to be largely intact in the VTA of *Clock*Δ19 mutants (unpublished observations). *TH* mRNA was upregulated in the mutants consistent with previously published results

(McClung, Sidiropoulou et al. 2005), but this modulation occurred in a time-dependent manner. Interestingly, the levels of the *TH* and *Clock* transcripts were inversely correlated in the wild type mice perhaps consistent with CLOCK acting as a negative regulator of *TH* expression. Only a few other studies have examined circadian gene expression within midbrain structures. In a study comparing bHR (high responder) and bLR (low responder) rats selectively bred on the basis of their locomotor response to novelty, investigators did not detect a diurnal variation in *Clock* expression in the VTA measured at ZT2 and ZT14 by in situ hybridization while *Per2* mRNA was reported to be oppositely regulated in bHR versus bLR rats (Kerman, Clinton et al. 2012). Few conclusions can be drawn from this study as they did not analyze expression within a control group of rats. Additionally, while in situ hybridization has the benefit of increased brain region selectivity, it is far less sensitive compared to quantitative RT-PCR methods further limiting the interpretation of their results in comparison to present findings.

The *Clock*Δ19 mutants display a time-dependent increase in total TH protein in the VTA at ZT9. This time point lags slightly behind the peak difference in mRNA expression. The overall diurnal pattern of total TH protein expression in WT mice is consistent with previous findings in rodents, demonstrating peak levels of TH during the light phase that decrease during the dark phase (Webb, Baltazar et al. 2009). In this same study, investigators also examined TH protein in the NAc and found that peak levels occurred out of phase with the VTA during the dark phase. Additionally, the peak in TH protein levels in the VTA

corresponded to the peak in preference for a drug reward (measured by amphetamine CPP) while the peak in TH protein in the NAc corresponded to the peak in preference for a natural reward (Sex CPP) (Webb, Baltazar et al. 2009). Interestingly, the *Clock*Δ19 mutants have been reported to have an increased preference for cocaine and an increase in cocaine self-administration compared to WTs during the light phase when their TH protein levels are significantly elevated (McClung, Sidiropoulou et al. 2005; Ozburn Revision reviewed). The *Clock*Δ19 mutants also exhibit an increase in phosphorylated TH protein at ser40 at this time. Phosphorylation of tyrosine hydroxylase at ser31 or at ser40 has been shown to increase TH enzyme activity both *in vivo* and *in vitro* with ser31 being a target of ERK while ser40 is prominently phosphorylated by PKA among others (Dunkley, Bobrovskaya et al. 2004). A recent study examining the phosphorylation-state dependent regulation of TH activity *in vivo* reported that basal enzyme activity is likely to be regulated by ser31 phosphorylation, but that the ser40 site may be preferentially responsive in the mesoaccumbens pathway or under circumstances of abnormally elevated dopamine signaling (Salvatore and Pruett 2012). This may explain why phospho-TH at ser40 is selectively increased in the mutants but ser31 is unchanged. The study by Salvatore at al further attempted to demonstrate a certain level of autonomy between somatodendritic versus terminal field dopaminergic compartments in terms of dopamine regulation to the extent that local infusion of AMPT into the VTA reduced tissue dopamine content in the VTA without affecting levels in the nucleus accumbens (Salvatore and Pruett 2012). This result, to some extent,

calls into question the suitability of making correlations between measures of VTA TH levels and dopamine function downstream in the nucleus accumbens. However, we find that the increase in TH phosphorylation in the VTA of the *Clock*Δ19 mutants does parallel the daytime increase in dopamine synthesis measured in the nucleus accumbens. There is no difference in dopamine synthesis during the dark phase between wild type and *Clock*Δ19 mutants mirroring the lack of change in TH mRNA or protein at this time. The wild type animals displayed a significant diurnal increase in dopamine synthesis, but TH phosphorylation in the VTA did not mirror this effect. Interestingly there were no significant alterations in synthesis in the dorsal striatum which is consistent with an earlier finding of a lack of change in TH protein levels in the substantia nigra of *Clock*Δ19 mice (McClung, Sidiropoulou et al. 2005). It is clear that the dopamine neurons in the SN and VTA are fundamentally different in terms of anatomy, function, regulation, and gene expression programs (Greene 2006). This may extend to the role of the circadian genes in regulation of dopamine function in these two brain regions.

TH mRNA expression is tightly controlled by a number of epigenetic, transcriptional, and posttranslational mechanisms (Lenartowski and Goc 2011). The *TH* promoter region contains a large number of potential transcription factor interaction sites, but there is a profound lack of inter-species sequence homology within the proximal promoter aside from the first 200 base pairs upstream of the transcriptional start site (Kim, Park et al. 2003). There are two E-box elements, the binding site for bHLH transcription factors like CLOCK, within the first 1 kb 5'

to the transcription start site including one within the proximal conserved region. In midbrain tissue taken from wild type mice, CLOCK was discovered to be present at the *TH* promoter selectively during the light phase. This pattern of enrichment fits well with the mRNA expression data demonstrating that CLOCK binding at the *TH* promoter is high when *TH* mRNA is low and *Clock* mRNA is at its highest. This finding of CLOCK acting as a negative regulator is fairly provocative as the transcription factor is traditionally thought of as an activator, but there is some precedent for CLOCK behaving as a transcriptional repressor. *In vitro* studies have shown that CLOCK can interact with BMAL1 and Cryptochrome 1 (CRY1) to form a repressive complex at certain gene promoters, and may even disrupt activity of other factors at non-E-box containing regions (Kondratov, Shamanna et al. 2006). Transcriptional repression by the CLOCK/NPAS2:BMAL1 dimer has previously been reported for specific genes *activating transcription factor 5 (Atf5), c-myc*, and *transcription termination factor 1 (TTF-1)* (Fu, Pelicano et al. 2002; Kim, Hur et al. 2002; Lemos, Goodspeed et al. 2007). The Lemos et al report, which demonstrated the interaction between CLOCK:BMAL1 and *Atf5,* asserts that *TH* is likely not a target of circadian transcriptional regulation because its mRNA expression did not oscillate in response to serum shock in PC12 and it did not interact with the transcription factors in electrophoretic mobility shift assays (Lemos, Goodspeed et al. 2007). The discrepancy between the EMSA data and the present ChIP data might be due to a lack of endogenous interaction partners that are needed to facilitate the association between CLOCK:BMAL1 and the *TH* promoter. Indeed the required

amount of *TH* promoter to drive proper expression of genes in dopamine neurons is extremely large, indicating that multiple factors are involved in its transcription. Such in vitro studies of transcription factor regulation of a gene product are traditionally hampered by the necessity of using various in vitro techniques (including small promoter fragments) and non-neuronal cell lines. Moreover, *TH* mRNA has a clear and reproducible diurnal rhythm in expression in dopamine neurons *in vivo* (Weber, Lauterburg et al. 2004) (Figure 2.4A). The chromatin immunoprecipitation assay is advantageous because it should reflect the *in vivo* situation within the brain when performed in tissue preparations, however optimization is difficult and the technique depends heavily upon the quality of the antibody used. It is believed that the collective evidence supports a role for CLOCK in the direct regulation of *TH,* but alternatively CLOCK dysfunction may mediate the gene expression changes by some secondary mechanism. Lending further credibility to the present findings, there is a report that a similar bHLH dimer NPAS3:ARNT is able to negatively regulate *TH* expression in the ventral midbrain during development (Teh, Loh et al. 2007). It does seem to be clear, that the E-box element is an important regulatory sequence within the proximal *TH* promoter although reports are conflicting as to the magnitude and direction of its regulatory effect.

The discovery of increased tyrosine hydroxylase levels and activity in the VTA was hypothesized to result in increased dopamine content within the ventral tegmental area as well as in its projection areas like the nucleus accumbens. This question was assessed by performing HPLC analysis on tissue punches

from dorsal and ventral striatum where a significant increase was expected, at least at certain times of day, within the nucleus accumbens but not in the dorsal striatum. A small but significant increase in total tissue dopamine content with no differences in metabolites was reported in the nucleus accumbens (Coque, Mukherjee et al. 2011); however this was a transient effect (reported at ~ZT 0-2) which was not found at other times of day. It may be that the greatest changes in dopamine levels in the NAc will be identified in the extracellular compartment rather than total tissue content and future studies using microdialysis techniques are warranted. Surprisingly, when HPLC analysis was performed on dorsal striatum tissue, there was a non-significant trend towards an increase in DA, but significant increases in the levels of dopamine metabolites DOPAC and HVA (~ZT 0-6). This finding was somewhat surprising because, up to this point, there had been no indication that there were any changes in the nigrostriatal dopaminergic pathway. The result was suggestive of alterations in the activity of catabolic dopamine enzymes. Dopamine clearance is mediated by reuptake through the dopamine transporter (DAT) as well as by enzymatic degradation. Dopamine is catabolized into major products 3-methoxytyramine (3MT), DOPAC and HVA by the enzymes monoamine oxidase (MAO) and catechol-O-methyltransferase (COMT) as shown in figure 4.1 (Quaak, van Schayck et al. 2009).

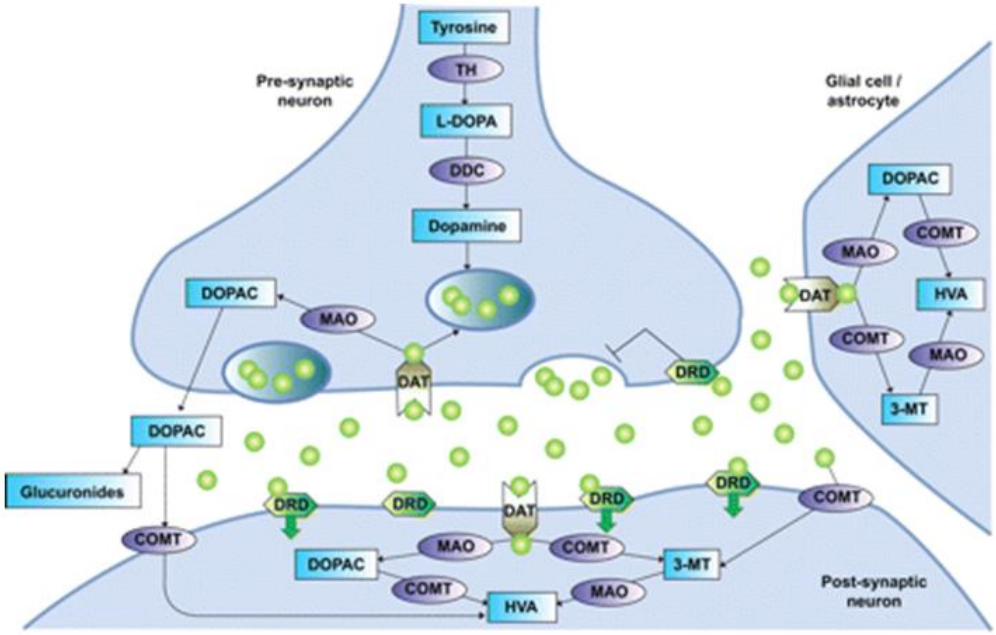

Figure 4.1 Dopamine Metabolism Pathways TH: tyrosine hydroxylase; L-DOPA: L-3,4-di-hydroxy-phenylalanine; DDC: 3,4-dihydroxyphenylacetic acid (DOPAC) decarboxylase; MAO: monoamine oxidase; DAT: dopamine transporter; DRD: dopamine receptor; COMT: catechol-O-methyltransferase; HVA: homovanillic acid; 3-MT: 3-methoxytyramine. Green circles: dopamine. Adapted fromQuaak 2009.

Research indicates that the DAT and these enzymes play different roles in dopamine clearance and metabolism in various brain regions. It is known that the expression of the DAT is much higher in the striatum in comparison to the prefrontal cortex (Sesack, Hawrylak et al. 1998). Thus COMT has a less important role in mediating extracellular dopamine clearance within the striatum due to the presence of the DAT, and MAO acts as the primary catabolic enzyme (Yavich, Forsberg et al. 2007). The observation of elevated DOPAC in the dorsal striatum indicated that MAO enzymatic activity might be enhanced. Interestingly, there is evidence that *Mao-a* expression is regulated by circadian clock genes

(Hampp, Ripperger et al. 2008). In a preliminary effort to test the theory of augmented MAO function, a non-significant trend toward an increase in enzyme activity was uncovered (Appendix A1, Figure A1.4). Because performance of the enzyme assay required subcellular fractionation to isolate the mitochondrial fraction, the dorsal and ventral striatum were pooled, and as a consequence, any brain region specific changes may have been diluted. Additional experiments will be necessary to determine if significant differences in enzymatic activity exist in either the dorsal striatum or nucleus accumbens. A finding of increased MAO levels in the mutants would actually be counterintuitive based on the behavioral data of the *Clock*Δ19 mice and findings in MAO mutants. An increase in MAO activity would be predicted to decrease monoamine levels and result in behavioral phenotypes like decreased open field locomotor activity, increased anxiety, and increased aggression unless it was present in the context of an abundant upregulation of monoamine synthesis (Bortolato, Chen et al. 2008). Levels of HVA were increased in the mutants as well which might be suggestive of an overall increase in neurotransmitter release and extracellular DA in the dorsal striatum. Indeed, an increase in DA synthesis without a change in MAO activity could also account for the increase in metabolite levels. If this is the case, it is unclear what mechanisms might be mediating the augmentation of DA synthesis in this region.

Based on the hypothesis that extracellular DA levels were elevated, it was expected that dopamine receptor function would be changed in the *Clock*Δ19 mutants. The ClockΔ19 mutants showed a lack of locomotor activating response

to the D1 agonist SKF 81297 and an increased locomotor depression to a D1 antagonist. This data is difficult to interpret because it can be explained by both a loss and a gain of function. For example, a lack of responding to a D1 agonist is similarly seen in both D1R knock-out mice and in mice in which the D1 receptor is overexpressed (Xu, Moratalla et al. 1994; Dracheva, Xu et al. 1999). Similarly, the enhancement in the locomotor suppressing effects of the D1 antagonist SCH 23390 can be attributed to either increased D1DR function or an augmentation of extracellular dopamine levels. Evidence collected at the protein level is equivocal because a slight increase in D1DR protein is observed in the dorsal striatum and a trend toward a decrease is observed in the nucleus accumbens selectively during the dark phase. Slice pharmacology experiments were initiated in an effort to clarify these results. When cAMP signaling was generally stimulated with forskolin, there was a significant induction of GluR1 ser845 phosphorylation in both wild types and mutants, but the increase was four-fold higher in the wild type. These results may again point towards a decrease in D1 function or possibly an increase in antagonism of cAMP stimulation by D2-type receptors of which protein levels were observed to be upregulated in both the dorsal and ventral striatum. Interestingly, increased D2 receptor signaling has been implicated in bipolar disorder. Analysis of post-mortem brain samples of the pre-frontal cortex from diseased brains and healthy controls found *DRD2* expression increased in bipolar patients and decreased in schizophrenics relative to controls (Zhan, Kerr et al. 2011). Moreover, data collected from *in vivo* imaging studies of D2 receptor occupancy within the basal ganglia have reported an increase in

binding in bipolar psychotic patients (Wong, Pearlson et al. 1997; Nikolaus, Antke et al. 2009).

These data uncover a novel regulation of *TH* directly by CLOCK in the mesoaccumbens dopamine circuit whereby disrupted CLOCK function is associated with loss of diurnal rhythms in *TH* gene expression and a time-dependent enhancement of dopaminergic activity. Likewise normal CLOCK function appears to be involved in the regulation of dopamine transmission in the dorsal striatum, although the precise function of CLOCK within the nigrostriatal circuit is less clear. A summary of the present findings in the context of the individual dopamine circuits is illustrated in Figure 4.2 below. Loss of CLOCK function appears to increase dopamine release and turnover in the striatum as indicated by increased levels of HVA and DOPAC. Additionally, there are downstream changes in levels of dopamine receptor proteins. Finally, these changes have functional consequences at both the level of behavioral and cellular signaling with altered locomotor responses to dopaminergic agonists and antagonists, and a blunted activation of cAMP signaling in the *Clock*Δ19 mutants. Taken together, these studies further define a newly discovered role for the clock in the regulation of midbrain dopamine transmission. Thus, the circadian system may represent a novel therapeutic avenue to utilize for treatment development of diseases that involve dysfunction in dopaminergic circuitry like addiction, depression, mania, or Parkinson's disease. These studies may additionally contribute to our understanding of the molecular mechanisms underlying the time-dependent effects of both recreational and therapeutic drugs.

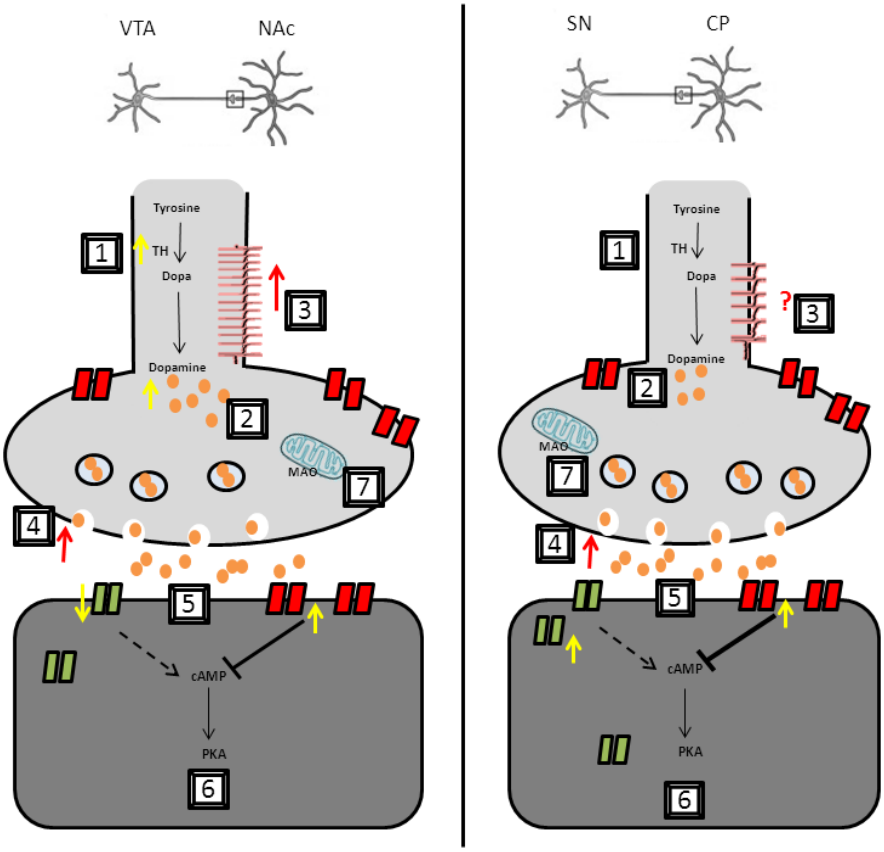

Figure 4.2. Projected model of pathway specific changes in DA transmission in the *Clock*Δ19 mutants. Left: In the VTA-NAc pathway, there is an increase in TH protein **(1)** which mediates an increase in DA synthesis (orange) **(2).** These changes are coincident with an increase in DA cell firing **(3)** and bursting resulting in a likely increase in DA release **(4)** possibly due to augmented quantal size**.** Increased extracellular DA over an extended period of time results in adaptations at the receptor level **(5)** with decreased D1DR (green) and increased D2DR (red) observed (at specific time points) resulting in D1/D2 imbalance favoring the D2 receptor and altering downstream signaling **(6)**. Increased DA synthesis may also lead to increased MAO activity **(7). Right:** In the SN-CP pathway, TH protein **(1)** and DA synthesis **(2)** changes have not been detected at any of the time points thus far measured**.** DA cell firing **(3)** and bursting has not been investigated. Extracellular DA concentrations may be elevated, by an unknown mechanism, **(4)** based on increased sensitivity to antagonists and increased metabolite levels. Here again, the hypothesized increase in extracellular dopamine over an extended period of time results in adaptations at the receptor level **(5)** with a slight increase in D1DR levels but a suspected decrease in D1 function (perhaps due to increased sequestering of the D1DR in the cytoplasm) and a substantial increase in D2DR protein ultimately resulting in D1/D2 imbalance favoring the D2 receptor and similarly altering downstream signaling **(6)**.

CHAPTER 5

FUTURE DIRECTIONS

While these studies have significantly contributed to the understanding of the influence of the circadian clock on dopamine transmission in the *Clock*Δ19 mutants, they still leave many questions left unanswered. A major finding of this present report is an elevation of dopamine cell firing and bursting across the light-dark cycle in the VTA of *Clock*Δ19 mutants. It is known that dopamine neurons display 3 main activity states *in vivo*: an inactive hyperpolarized state, tonic single-spike firing, and phasic burst firing (Grace, Floresco et al. 2007). While it has been shown that the rates of both tonic and phasic dopamine cell activity is increased in the VTA of the mutants, it is unclear whether the population dynamics have been altered. In the future, it would be interesting to determine whether the relative percentages of inactive, tonic, and phasic dopamine neurons are changed. Microelectrode arrays can be used to identify the number of spontaneously active dopamine neurons within a population and this measure can be compared between wild type and *Clock*Δ19 mutants (Floresco, West et al. 2003). Similarly, it is unclear whether there are changes to the functional inputs to the VTA such as the LDTg and PPTg which gate VTA dopamine cell burst firing.

There is reason to believe that the CLOCK in some way regulates the intrinsic excitability of VTA dopamine cells because the *Clock*-shRNA increases dopamine cell firing in slice (Mukherjee, Coque et al. 2010). An attractive

candidate for mediating this effect is the hyperpolarization-activated cyclic nucleotide gated channels (HCN channels) which are pacemaker channels that are directly regulated by cAMP and cGMP. The current mediated by these channels (I*h*) is part of the electrophysiological signature used to identify dopamine neurons in slice or culture preparations (Chu and Zhen 2010). Interestingly, the Mukherjee et al study identified a 1.60 fold down-regulation in HCN1 expression in the VTA cells in which *Clock* was knocked down (Mukherjee, Coque et al. 2010); however HCN1 is not commonly believed to be significantly expressed within the VTA, but an early study profiled the expression of HCN1-HCN4 mRNAs by *in situ* hybridization within the adult rat brain and detected all four genes (Monteggia, Eisch et al. 2000). It would be informative to confirm the colocalization of particular HCN proteins with TH within the VTA, and if present investigate whether levels or activity of HCN subunits are altered in the *Clock*Δ19 mutants.

The preponderance of the evidence suggests that the *Clock*Δ19 mutants are a model of altered extracellular dopamine within the mesoaccumbens circuit, but the confirmatory evidence is incomplete. In future studies, it will be crucial to examine extracellular levels of dopamine within the nucleus accumbens, prefrontal cortex, and dorsal striatum by *in vivo* microdialysis across the light-dark cycle. Such studies have been performed successfully in rats (Castañeda, de Prado et al. 2004), but they will be more technically challenging in the much smaller mouse. Additionally, due to the rapidity of clearance mechanisms in play

at the dopaminergic synapse, it may be possible that this technique is still not sensitive enough to detect differences.

Originally, many of these studies were proposed to be performed both with and without lithium treatment. Lithium has been demonstrated to rescue many of the behavioral phenotypes of the *Clock*Δ19 mutant mice as well some of the neurophysiological changes observed in the mutants (Roybal, Theobold et al. 2007; Dzirasa, Coque et al. 2010; Coque, Mukherjee et al. 2011). It would be interesting to determine if lithium's therapeutic actions in the *Clock*Δ19 mutant mice were mediated through normalization of the midbrain dopamine system or whether other dopaminergic modulators are able to improve their behavioral profile. The efficacy of antipsychotics that target D2 receptors should be investigated in the *Clock*Δ19 mutants given the enhanced D2 receptor function observed. Dopaminergic drugs are rife with side-effects; therefore modifying the altered signaling pathways downstream of the dopamine receptors may offer an even better avenue for targeting treatment.

Additional pharmacological studies may offer the best opportunity for dissecting the mesocorticolimbic versus nigrostriatal circuit level changes. For example, a bilateral guide cannula directed at each of these targets can be chronically implanted to administer dopaminergic agonists and antagonists and again measure locomotor output. Additionally, the agonist studies can be repeated in the context of dopamine depletion with a pretreatment of α-methyl-p-tyrosine which will further expose changes in dopamine receptor function without interference of endogenous dopamine. Finally, there is ample information left to

be gleaned from pharmacological signaling studies. The slice pharmacology studies, demonstrated with forskolin in chapter 3, can be conducted with specific D1 and D2 agonists. A preliminary study using SKF 81297 was inconclusive, but these experiments should be repeated upon optimization of incubation time and concentration parameters. The results of these biochemical studies may guide future experiments to determine how specific alterations in dopamine pathways contribute to changes in motivation and reward-related behavior in the mutants.

APPENDIX A1.

ALTERED DOPAMINE RECEPTOR EXPRESSION IN THE NUCLEUS ACCUMBENS OF *CLOCK*Δ19 MUTANTS

Introduction

The neurotransmitter dopamine widely innervates many central nervous system circuits and is one of the most extensively studied signaling molecules in the brain. Dopamine is involved in regulating diverse physiological functions including control of motor coordination, learning and memory processes, and regulation of motivated behaviors and mood (Mogenson, Jones et al. 1980; Bressan and Crippa 2005; Cools 2008; Wise 2009). Midbrain dopamine cells in the ventral tegmental area and substantia nigra centrally coordinate many of the aforementioned functions through their projections to various brain structures. The selective loss of substantia nigra pars compact dopamine neurons innervating the dorsal striatum famously causes Parkinson's disease (Barzilai and Melamed 2003). Moreover, anomalous dopamine function is hypothesized to contribute to the pathology of a variety of psychiatric diseases including bipolar disorder, substance abuse, schizophrenia, and depression (Binder, Kinkead et al. 2001; Cousins, Butts et al. 2009). Alterations in mesocorticolimbic dopaminergic transmission are largely credited with triggering these mood and reward related pathologies.

Dopamine is a monoamine neurotransmitter derived from the two-step conversion of the amino acid tyrosine. Dopamine mediates so-called slow

synaptic transmission through intracellular signaling cascades activated by interaction with its G-protein coupled receptors (GPCRs) (Thompson, Burnham et al. 2005). There are two distinct sub-types of dopamine receptors within the brain, the D1 and D2 class, of which there are several family members for each (D1: D1, D5 and D2: D2, D3, D4). The D1 class of receptors couple to Gαs/olf and activate adenylyl cyclase (AC) and cAMP signaling. Conversely, the D2 class couple to Gαi/o to inhibit AC activity and decrease cAMP signaling (Beaulieu and Gainetdinov 2011). D2-type receptors can also serve as autoreceptors on dopamine neurons mediating autoregulatory feedback inhibition of further dopamine cell firing, synthesis, and release.

There are multiple levels of regulation governing the initial development and maintenance of dopamine neurons as well as the later synthesis, release, and homeostasis of dopamine at its targets. A specific program of transcription factors believed to regulate the patterning and specification of midbrain dopamine neurons has been identified including NURR1, PITX3, FOXA1/2 and LMX1a/b (Flames and Hobert 2011). Biochemical and functional analyses have demonstrated that PITX3 and NURR1 cooperatively interact to activate *TH* and *Dat (dopamine transporter)* expression directly and induce maturation of midbrain dopamine cells (Martinat, Bacci et al. 2006; Jacobs, van Erp et al. 2009). There has recently been identified a novel negative regulation of *TH* by the circadian transcription factor CLOCK which may represent a normal homeostatic mechanism to control levels of dopamine synthesis in the mature brain across the 24-hour day (Spencer (Submitted)) . Mice with a mutation in the

Clock gene (*Clock*Δ19 mutants) display multiple changes in dopaminergic transmission consistent with a disruption in the normal rhythm of dopaminergic activity (McClung, Sidiropoulou et al. 2005; Dzirasa, Coque et al. 2010; Spencer Submitted). Moreover, these mice show a behavioral phenotype that closely models human bipolar mania, a disorder theorized to be caused by hyperactivity of dopaminergic circuits, including disrupted circadian rhythms, hyperactivity, decreased depression-related behavior, less anxiety, and increased preference for drugs of abuse (King, Vitaterna et al. 1997; Gekakis, Staknis et al. 1998; McClung, Sidiropoulou et al. 2005; Roybal, Theobold et al. 2007). As such, these mice represent a unique model in which to study alterations in the midbrain dopamine system, in particular the consequences of a hyperdopaminergic state.

In the present study, the regulation of D1 and D2 dopamine receptors in the nucleus accumbens was assessed across the light-dark cycle in *Clock*Δ19 mutants and whether there might be additional mechanisms contributing to alterations in dopamine homeostasis in addition to previously identified diurnal dysregulation of dopamine synthesis.

Results

Altered mRNA expression of DA receptors in *Clock*Δ19 mutants

It has been reported that *Clock*Δ19 mutant mice display a moderate increase in total tissue homogenate levels of dopamine in the NAc (Coque, Mukherjee et al. 2011). It is clear from the work of others that increased dopaminergic tone can result in compensatory changes in dopamine receptor

expression and function (Jones, Gainetdinov et al. 1999; Fauchey, Jaber et al. 2000). Thus, it was hypothesized that diurnal dopamine receptor mRNA expression might be altered in the VTA or NAc of *Clock*Δ19 mutant mice compared to their wild type littermates. *D1DR, D2DR,* and *D3DR* mRNA expression was measured at six time points over the circadian cycle corresponding to ZT 0, ZT 4, ZT 8, ZT 12, ZT 16 and ZT 20. The expression levels of *D2DR* and *D3DR* were evaluated in the VTA because D2 type receptors can act as autoreceptors on presynaptic dopamine neurons inhibiting neurotransmitter release, therefore increased D2-type receptor expression might represent a compensatory mechanism aimed at limiting dopamine release (Feuerstein 2008). No difference was observed between genotypes in *D2R* mRNA expression, and no significant diurnal variation in expression was detected over time (Figure A1.1A). There was a significant effect of genotype on *D3R* mRNA expression with an overall effect of increased expression in the *Clock*Δ19 mutants as compared to the wild type ($F(1,37) = 5.85$; $p = 0.0206$) (Figure A1.1B). Here again, no significant diurnal variation in *D3DR* expression over time was detected in either genotype. The expression of *D1DR, D2DR,* and *D3DR* was then examined in the NAc. Here a similar regulation of all three receptors was observed in the *Clock*Δ19 mutants compared to wild type. There was a main effect of genotype ($F(1,48) = 9.56$; $p = 0.0033$) and time ($F(5,48) = 5.76$; $p = 0.0003$) on *D1DR* mRNA expression with a tendency for decreased expression in the mutants (Figure A1.2A).

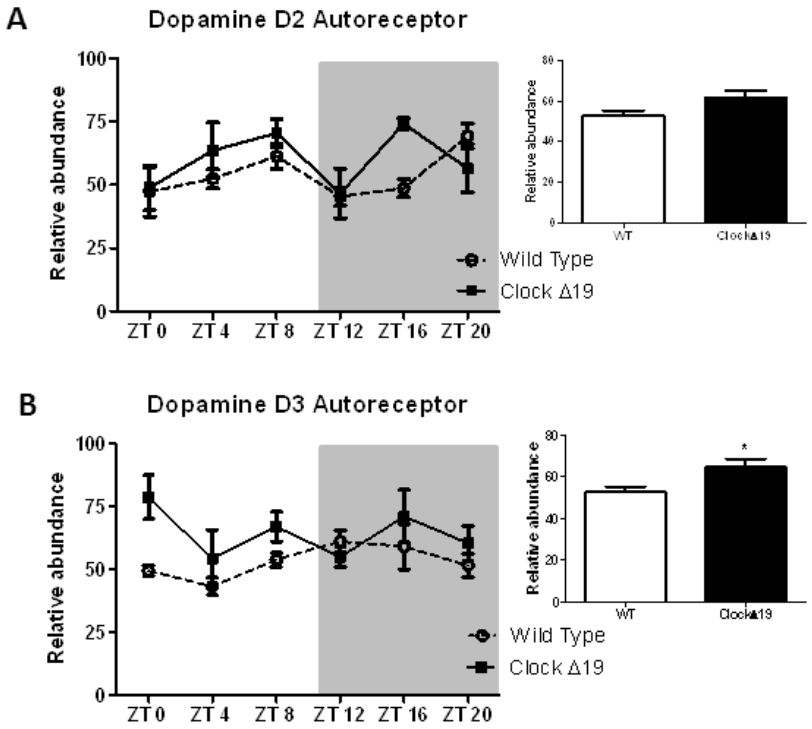

Figure A1.1 Dopamine autoreceptor mRNA expression. A. Plotted is the relative abundance of *D2DR* mRNA from VTA tissue normalized to the expression of an internal control, *Gapdh*. **B.** Plotted is the relative abundance of *D3DR* mRNA from VTA tissue normalized to the expression of an internal control, *Gapdh*. Analysis by two-way ANOVA revealed a main effect of genotype ($F_{(1,37)}$ = 5.85; p = 0.0206). Inset depicts overall increase in total averaged *D3DR* expression in mutants compared to wild type ($T_{(47)}$ = 2.629; p = 0.0115).

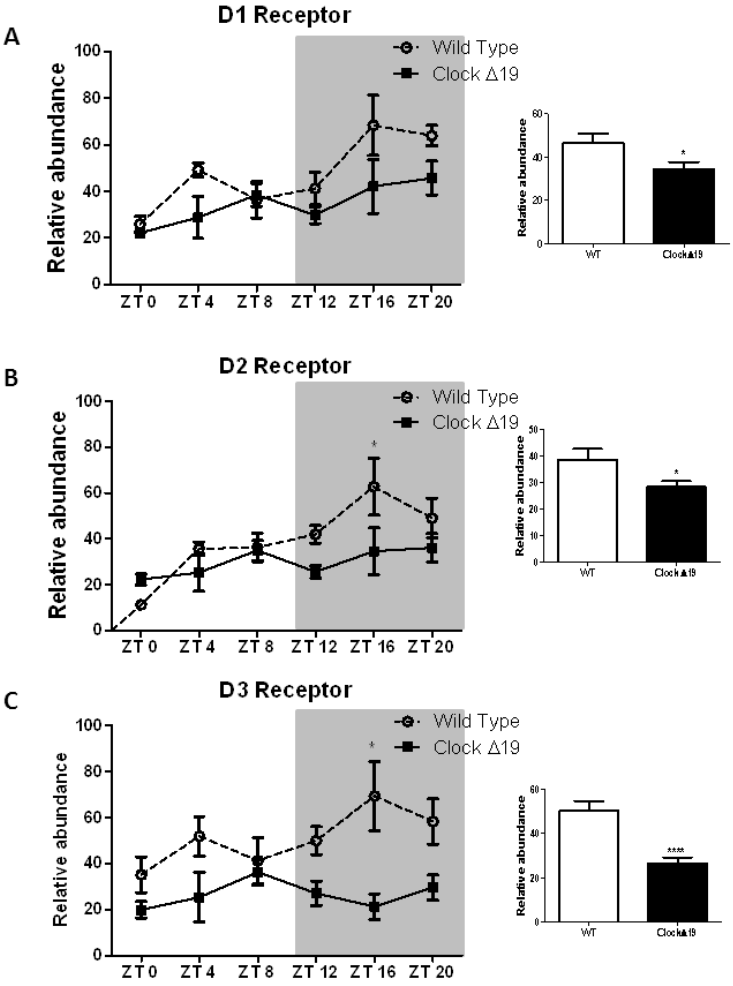

Figure A1.2 Dopamine receptor mRNA expression. A. Relative abundance of *D1DR* mRNA from NAc tissue normalized to the expression of *Gapdh*. Analysis by two-way ANOVA revealed a main effect of genotype ($F_{(1,48)} = 9.56$, $p = 0.0033$) and a main effect of time ($F_{(5,48)} = 5.76$; $p = 0.0003$). Diurnal variation was statistically significant in wild type (WT) animals ($F_{(5,24)} = 5.366$; $p = 0.0019$), while *Clock*Δ19 mutants displayed none. Inset depicts overall decrease in total averaged *D1DR* expression in mutants compared to wild type ($T_{(58)} = 2.44$; $p = 0.0178$). **B.** Relative abundance of *D2DR* mRNA from NAc tissue normalized to *Gapdh*. Analysis by two-way ANOVA revealed a main effect of genotype ($F_{(1,48)} = 6.26$; $p = 0.0158$) and a main effect of time ($F_{(5,48)} = 5.66$; $p = 0.0004$). Bonferroni post-hoc tests revealed a significant difference between the means at ZT 16 ($p < 0.05$). Diurnal variation was statistically significant in wild type (WT) animals ($F_{(5,24)} = 6.633$; $p = 0.0005$) but not *Clock*Δ19 mutants. Inset depicts overall decrease in total averaged *D2DR* expression in mutants compared to wild type ($T_{(57)} = 2.241$; $p = 0.029$). **C.** Relative abundance of *D3DR* mRNA from NAc tissue normalized to the expression of *Gapdh*. Analysis by two-way ANOVA revealed a main effect of genotype ($F_{(1,48)} = 25.06$ $p < 0.0001$). Bonferroni post-hoc tests reveal a significant difference between the means at ZT 16 ($p < 0.05$). Inset depicts overall decrease in total averaged *D3DR* expression in mutants compared to wild type ($T_{(58)} = 4.76$; $p < 0.0001$). n = 3-5 animals per genotype per time point for all mRNA expression.

There was a significant diurnal variation in *D1DR* expression detected in the wild type ($F(5,24) = 5.366$; $p = 0.0019$). Similarly, a main effect of genotype ($F(1,48) = 6.26$; $p = 0.0158$) and time ($F(5,48) = 5.66$; $p = 0.0004$) was observed for *D2DR* mRNA expression again with an overall decrease in levels in the mutants (Figure A1.2B). Bonferroni post-hoc analysis revealed a significant difference between the means specifically at ZT 16 ($p < 0.05$). There was a significant diurnal variation in *D2DR* expression detected in wild type animals which was again blunted in *Clock*Δ19 mutants ($F(5,24) = 6.633$; $p = 0.0005$). Finally, there was a significant main effect of genotype ($F(1,48) = 25.06$; $p < 0.0001$) in *D3DR* mRNA expression between wild type and *Clock*Δ19 mutants with decreased expression in the mutants (Figure A1.2C). Post-hoc tests show a significant difference between the means specifically at ZT 16 ($p < 0.01$). No significant diurnal variation was detected in *D3DR* expression independent of genotype. These results are consistent with the expectation that the altered dopaminergic environment of the *Clock*Δ19 mutants would have an effect on the expression of these dopamine-responsive genes.

Time-dependent changes in DA receptor protein in the NAc of *Clock*Δ19 mice

As the results from the expression studies indicated that there were diurnal differences in dopamine receptor expression with the largest differences observed during the dark phase, it was next set out to determine whether these changes extended to dopamine receptor protein levels.

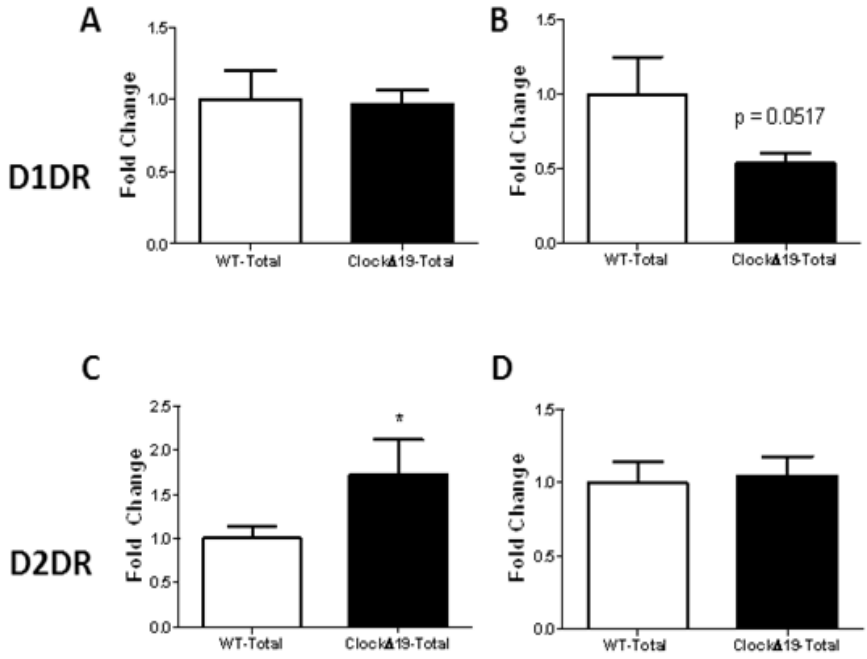

Figure A1.3. Dopamine receptor protein levels in the nucleus accumbens. A. D1DR protein levels in the NAc were unchanged in *Clock*Δ19 mutants during the light phase. **B.** D1DR protein levels in the NAc displayed a trend toward a decrease in *Clock*Δ19 mutants during the dark phase. ($T_{(10)}$ = 1.792; p = 0.0517) **C.** D2DR protein levels in the NAc were increased in *Clock*Δ19 mutants during the light phase. ($T_{(11)}$ = 1.807; p = 0.0491) **D.** D2DR protein levels in the NAc were unchanged in *Clock*Δ19 mutants during the dark phase.

When protein was examined from total NAc homogenates during the light phase, no significant difference in D1DR protein levels were observed (Figure A1.3A); however when protein levels were quantified during the dark phase there was a strong trend towards a decrease in D1DR protein in the *Clock*Δ19 mutants consistent with the mRNA expression pattern (T(10) = 1.792; p = 0.0517) (Figure

A1.3B). When D2DR levels were assayed, there was a surprising increase in D2DR protein during the light phase ($T(11) = 1.807$; $p = 0.0491$) (Figure A1.3C) with no significant differences detected during the dark phase (Figure A1.3D). This result was unexpected because it did not match the gene expression data, but it might be attributed to a compensatory increase in D2-autoreceptor protein from the VTA projections which cannot be differentiated from the post-synaptic pool by immunoblotting.

*Clock*Δ19 mutants display locomotor hyperactivity to novelty across the light-dark cycle

Notably, the largest changes in dopamine receptor gene expression occurred during the dark phase as well as a strong trend toward a decrease in D1 receptor protein. Previously it was demonstrated that the *Clock*Δ19 mutants display significant hyperactivity when placed in a novel home cage environment compared to wild type controls (Roybal, Theobold et al. 2007). Largely, they show a failure to habituate normally after prolonged exposure to this environment. It has been demonstrated that this hyperactivity is associated with a daytime increase in *TH* mRNA, TH protein, and dopamine synthesis (Spencer et al, submitted). It is unclear if this hyper-locomotive response to novelty is dependent on those molecular correlates or whether the hyperactivity is maintained during the dark phase when these factors appear to normalize and D1 receptors seem to be down-regulated.

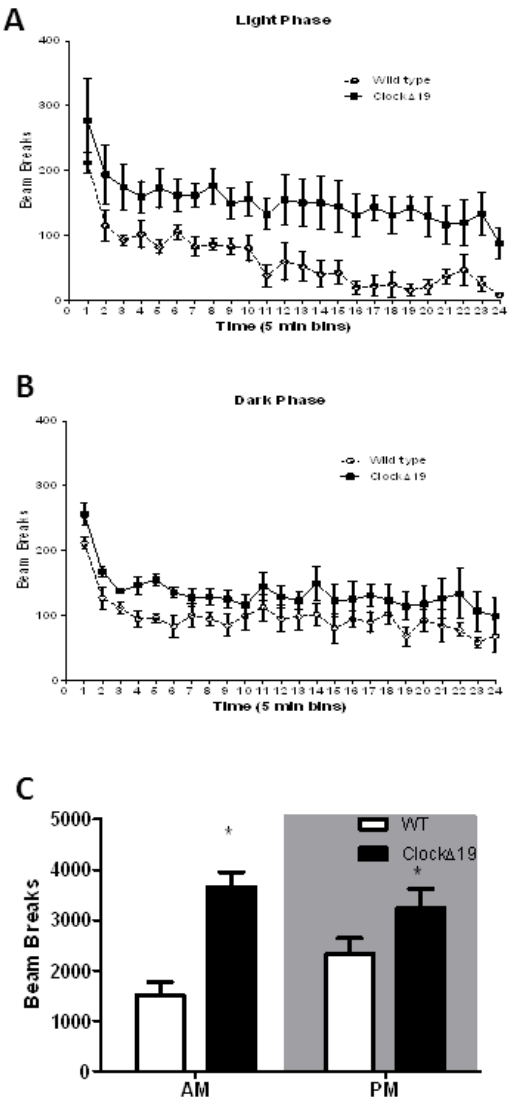

Figure A1.4. Locomotor hyperactivity to novelty across the light-dark cycle. *Clock*Δ19 mutants displayed significant locomotor hyperactivity in response to novelty compared to controls during both the light phase (A) and the dark phase (B). **A.** Analysis by two-way ANOVA revealed a main effect of genotype ($F_{(1,192)} = 143.25$, $p < 0.0001$) and a main effect of time ($F_{(23,192)} = 4.55$; $p < 0.0001$) for locomotor activity tested during the light phase. **B.** Analysis by two-way ANOVA revealed a main effect of genotype ($F_{(1,192)} = 47.95$, $p < 0.0001$) and a main effect of time ($F_{(23,192)} = 4.50$; $p < 0.0001$) for locomotor activity tested during the dark phase. **C.** Cumulative beam break activity over the one-hour test. Analysis by Student's T-test indicates that the *Clock*Δ19 mutants had elevated total activity during the light phase ($T_{(8)} = 5.53$, $p = 0.0003$) and dark phase ($T_{(8)} = 1.9192$, $p = 0.0456$). Wild type mice displayed a significant increase in activity in the dark phase compared to the light phase ($T_{(8)} = 2.084$; $p = 0.03535$) but the mutants did not.

WT and *Clock*Δ19 mutants were tested in locomotor activity chambers during both the light and dark phase and once again the previous finding of significant hyperactivity during the light phase was confirmed ($F(1,192) = 143.25$; $p < 0.0001$). Interestingly, when a separate set of animals was tested during the dark phase, this hyperactivity persisted in the *Clock*Δ19 mutants ($F(1,192) = 47.95$; $p < 0.0001$), but the magnitude of the difference was diminished due to the normal diurnal increase in locomotor activity of the wild type mice ($T(8) = 2.084$; $p = 0.03535$). The locomotor activity of the *Clock*Δ19 mutants did not differ significantly from levels observed during the light phase.

*Clock*Δ19 mutants do not have differences in MAO activity

Because there was a persistence of the locomotor hyperactivity to novelty during the dark phase when differences in dopamine synthesis were not detected between wild types and mutants, alternative mechanisms that might contribute to their elevated activity were investigated. In another circadian mutant, the *Per2* mutants who exhibit increased dopamine synthesis and altered striatal neuronal activity, augmentation of the dopamine system is attributable to a decrease in dopamine metabolism by the catabolic enzyme monoamine oxidase A (Hampp, Ripperger et al. 2008). In a cell culture system, researchers determined that circadian clock components BMAL1, NPAS2, and PER2 function as positive regulators of *Mao* transcription (Hampp, Ripperger et al. 2008).

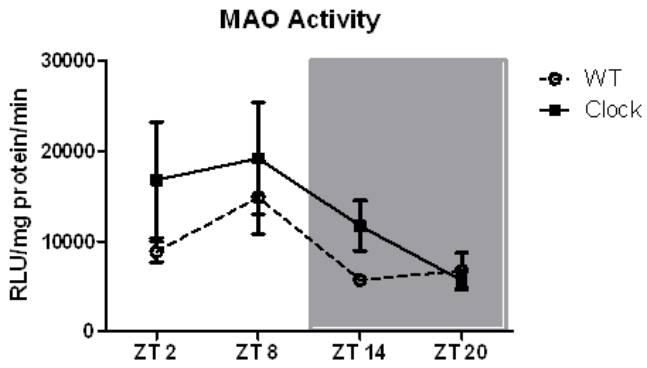

Figure A1.5. Monoamine oxidase enzyme activity across the LD cycle. Analysis by two-way ANOVA revealed a main effect of time ($F_{(3,41)} = 2.92$; $p = 0.0452$) for MAO enzyme activity.

A similar type of phenomenon was investigated in the *Clock*Δ19 mutants across the light-dark cycle. Luminescent enzyme assays were performed on tissue homogenates of the dorsal and ventral striatum in wild type and *Clock*Δ19 mutants. Contrasting with the *Per2* mice, no decrease in MAO activity was observed in the *Clock*Δ19 mutants compared to wild types across the light dark cycle although there was a trend towards an increase during the dark phase. These results suggest that changes in dopamine metabolism do not contribute significantly to the altered dopaminergic transmission in the *Clock*Δ19 mutants.

Discussion

These results show that loss of function of the circadian transcription factor CLOCK results in robust changes in dopamine receptor mRNA and some changes at the protein level in the nucleus accumbens. Mice with the dominant-negative *Clock*Δ19 mutation displayed dysregulation in the gene expression of *D1DR, D2DR,* and *D3DR* with a decrease in levels of all three in the nucleus

accumbens as well as a loss of diurnal rhythmicity in *D1DR* and *D2DR.* There was also an increase in the expression levels of the *D3DR* mRNA in the VTA of mutants. As a collective, these changes are in line with what might be expected as compensatory mechanisms activated in response to an increase in dopaminergic tone. For example, it is known that the dopamine transporter null (DAT -/-) mice which exhibit increased extracellular dopamine show a decrease in the mRNA and protein of *D1DR* and *D2DR* in both the dorsal and ventral striatum (Fauchey, Jaber et al. 2000; Ghisi, Ramsey et al. 2009).
These results are consistent with the manifestation of a similar phenomenon in the *Clock*Δ19 mutants.

It is unclear whether the gene expression changes in dopamine receptors are due to direct transcriptional control of CLOCK or merely representative of compensatory responses to dopaminergic activity in the *Clock*Δ19 mutants. As noted, CLOCK normally acts as a transcription factor regulating the expression of core circadian components as well as a myriad of other non-circadian clock controlled genes. A recent study suggests a novel negative regulation of tyrosine hydroxylase, the rate-limiting enzyme in dopamine synthesis, by CLOCK (Spencer (Submitted)). Promoter analysis of the D1, D2, and D3 receptors reveals the presence of multiple E-box sites, the canonical binding site for the CLOCK/NPAS2:BMAL1 heterodimer, upstream of the transcriptional start sites. In studies that are ongoing, it has been demonstrated by ChIP assays that both CLOCK and NPAS2 are enriched at the promoters of the *D1* and *D2* receptor and that this promoter occupancy is sensitive to the psychostimulant cocaine

which increases dopamine in the synapse (unpublished observations). Future studies are necessary to determine what contribution, if any, CLOCK may make directly to the basal and stimulated transcriptional activity of the dopamine receptor genes.

Total dopamine receptor protein levels were also significantly altered in the nucleus accumbens of *Clock*Δ19 mutants in a time-dependent manner with a strong trend towards a decrease in D1DR protein during the dark phase which corresponded to a time of day when the largest differences in *D1* mRNA were detected in the mutants. In the analysis of D2DR protein, a significant increase was detected in the *Clock*Δ19 mutants during the light phase. It is conceivable that the dopamine receptor changes reported in the NAc of the *Clock*Δ19 mutants may contribute to their manic-like behavioral profile (Roybal, Theobold et al. 2007). A recent study generated a mouse with a forebrain specific overexpression of CK1δ, touted as a potential ADHD model, which displays a significant decrease in both D1 and D2 protein levels in the striatum and shares a number of behavioral abnormalities in common with the *Clock*Δ19 mutants including hyperactivity, reduced anxiety, and similar responses to systemic administration of dopaminergic agonists and antagonists (Zhou, Rebholz et al. 2010). This finding is intriguing because CK1δ is a kinase prominently implicated in posttranslational regulation of the circadian clock. It is noteworthy that dopamine receptor signaling, especially through D2 pathways, has been linked to psychiatric diseases such as schizophrenia and bipolar disorder. Analysis of post-mortem brain samples of the pre-frontal cortex from diseased brains and

healthy controls found *DRD2* expression increased in bipolar patients and decreased in schizophrenics relative to controls (Zhan, Kerr et al. 2011). These contrasting results seem to indicate that dopaminergic imbalance, irrespective of the direction of change, has important consequences for mood-related behavior.

In the present study, WT and *Clock*Δ19 mutants were tested in locomotor chambers during both the light and dark phase because strong trends or significant changes in dopamine receptor protein were noted during both phases of the 24-hour cycle. It has repeatedly been confirmed that the *Clock*Δ19 mutants display significant hyperactivity in response to a novel environment, but these studies have been performed during the light phase or the normally inactive period for laboratory mice (McClung, Sidiropoulou et al. 2005; Roybal, Theobold et al. 2007).Here the previous finding of hyperactivity during the light phase was confirmed and it persisted during the dark phase but with a smaller magnitude because wild type animals increased their locomotion. The wild type animals exhibited a diurnal variation in their locomotor response while the *Clock*Δ19 mutants did not. The *Clock*Δ19 mutants have been reported to display a host of other mood-related behavioral abnormalities, and at some point it should be determined whether these behaviors are stable or variable across the light-dark cycle.

An MAO enzyme assay was performed on striatal homogenates to determine if changes in dopamine metabolism by this enzyme could contribute to the altered dopamine function observed, but no difference in MAO activity was detected in the *Clock*Δ19 mutants compared to wild types across the light dark

cycle. There was a trend towards an increase specifically at ZT14 which was opposite to what had been anticipated. Analysis by two-way ANOVA detected a significant main effect of time suggesting that there is a diurnal variation in MAO activity in both wild types and mutants. The diurnal variation in MAO activity appears to be inversely correlated to the normal pattern of extracellular dopamine levels in the striatum (Smith, Olson et al. 1992). It was hypothesized that there might be differences in MAO activity in the *Clock*Δ19 mutants because transcriptional regulation of *Mao-a* has, at least partially, been attributed to circadian clock proteins BMAL1 and NPAS2. However, BMAL1 and NPAS2 are circadian proteins which are not direct transcriptional targets of CLOCK, and when *Bmal1* expression was examined in various brain regions in the *Clock*Δ19 mutant mice, little to no modulation of its levels or rhythms were detected perhaps explaining the lack of modulation of MAO activity (unpublished observations). A second possible justification for the lack of an effect may be that brain region specific alterations were overlooked because the dorsal and ventral striatum were pooled to conduct the assay. HPLC analysis of the dorsal striatum indicated that dopamine metabolites DOPAC and HVA were increased in the *Clock*Δ19 mutant which is suggestive of altered activity of the metabolic enzymes. Thus the present MAO activity result is limited in its interpretation.

Conclusions

These studies reveal compensatory alterations in dopamine receptor gene expression in the *Clock*Δ19 mutants accompanied by changes at the

protein level. Furthermore, the data suggest that dopaminergic dysregulation contributes to locomotor hyperactivity in the *Clock*Δ19 mutants across the entire light-dark cycle. An improved understanding of the diverse mechanisms diurnally regulating dopamine transmission both in a normal (wild type) and pathologic state (*Clock*Δ19 mutants) has many benefits including a better understanding of dosing time-dependent effects of dopaminergic drugs which are commonly used to treat a number of psychiatric diseases.

Material and Methods

Animals

*Clock*Δ19 mutant mice were created by *N*-ethyl-*N*-nitrosurea mutagenesis and produce a dominant-negative CLOCK protein defective in transcriptional activation activity as described (King, Vitaterna et al. 1997). For all experiments using *Clock*Δ19 mutants, adult male mutant (*Clock/Clock)* and wild type (+/+; WT) littermate controls were group housed in sets of 2-4 per cage on a 12/12-h light dark cycle (lights on at 6:00 a.m. = Zeitgeber time (ZT) 0, lights off at 6:00 p.m. = ZT 12) with food and water provided *ad libitum*. All experimental subjects have been backcrossed at least 5 generations. All animal use was conducted in accordance with the National Institute of Health guidelines and approved by the Institutional Animal Care and Use Committees of UT Southwestern Medical Center.

Gene expression

Animals were sacrificed at six time points over the circadian cycle corresponding to Zeitgeber time (ZT) 0, 4, 8, 12, 16 and 20 (ZT0 corresponds to lights on; lights go off at ZT12) and brains were frozen on dry ice. NAc and VTA punches were made on a frozen stage from 300 µm slices taken on a cryostat (Leica). RNA isolation and cDNA synthesis was carried out as previously described (McClung, Sidiropoulou et al. 2005). Briefly, RNA was isolated using TRIzol reagent (Invitrogen) according to the manufacturer's instructions. Any remaining DNA was digested by using the DNA free system (Ambion) and cDNA was synthesized with an oligo dT primer and superscript III reverse transcriptase enzyme (Invitrogen). Real-time PCR was performed in duplicate on the ABI 7500 Real-Time PCR system (Applied Biosystems) using the Fast start SYBR green PCR master mix (Roche Applied Science) according to the manufacturer's instructions with primers specific for *gapdh* and dopamine receptors.

Table A1.1 Gene Expression Primers

	Forward	Reverse
Gapdh	5'-AACGACCCCTTCATTGAC-3'	5'-TCCACGACATACTCAGCAC-3'
D1DR	5'-TGGCATACCTAAGCCACTGGAGAA-3'	5'-ATTCAGGTTGAATGCTGTCCGCTG-3'
D2DR	5'-TCTTCTGGTGGCCACACTGGTTAT-3'	5'-ACAGGTTCAAGATGCTTGCTGTGC -3'
D3DR	5'-AGACACATGGAGAGCTGAAACGCT-3'	5'-TTCAGGGATGTGGATAACCTGCC-3'

The relative levels of each mRNA were calculated by the $2^{-\Delta\Delta Ct}$ method and normalized to the corresponding *Gapdh* mRNA levels (Maywood, Fraenkel et al.

2010). Each Ct value used for these calculations is the mean of 2-5 biological replicates of the same reaction.

Tissue Collection, SDS-PAGE and Western Blot

Animals were sacrificed by cervical dislocation, their brains removed, and slices prepared with 1 mm brain block. Fresh nucleus accumbens tissue punches were dissected and frozen on dry ice for later processing. For protein extraction, tissue samples were homogenized by sonication on wet ice in a buffer containing 320mM sucrose, 5mM HEPES, phosphatase inhibitor cocktail I and II (Sigma, St. Louis, MO), protease inhibitor (Sigma, St. Louis, MO), 5% SDS, and 50mM NaF. Protein homogenate was spun at 12,000 RPM for 10 minutes at 4°C and the supernatant carefully removed. DC assays (Biorad, Hercules, CA) were performed to quantitate protein levels. Aliquots of sample were combined in Laemmli SDS sample buffer (Bio-World, Dublin, OH), and heated at 95°C for 5 minutes. Samples were loaded (75µg total protein per lane) and run on 10% Tris-glycine (TG) gel at 140 V for ~ 90 minutes in 1XTGS buffer (Biorad, Hercules, CA). Proteins were transferred overnight at 4°C onto Immobilon PVDF membranes (Millipore, Bedford, MA) at 35V in 1XTG buffer. Membranes were blocked in 5% Milk diluted in TBST for 1 h at room temperature (RT). Membranes were incubated overnight at RT with the following primary antibodies diluted in blocking buffer: rabbit anti-D1DR (1:2000, GeneTex), rabbit anti-D2DR (1:1000, Millipore), and mouse anti-GAPDH (1:20,000, Fitzgerald, Acton, MA).

Horseradish peroxidase-conjugated secondary antibodies (Jackson ImmunoResearch) were used in combination with the Supersignal West Dura system (Promega) to detect the signal on film. Densitometry was conducted by using NIH IMAGE software.

Locomotor response to novelty

The mice were moved to the behavioral testing room 1 hour prior to the testing period. Mice were individually placed in automated locomotor activity chambers equipped with infrared photobeams (San Diego Instruments) and measurements began immediately. Fine and ambulatory motor activity of the animals was continuously measured with the data collected in 5-min bins for 2 hours.

MAO-Glo Enzyme Assay

The MAO-Glo Assay (Promega) was performed according to the manufacturer's instructions. Mice were sacrificed by cervical dislocation at 4 ZT times and fresh tissue slices containing whole striatum were flash frozen until ready for use. Tissue was homogenized in 500 µl homogenization medium (0.32 M sucrose, 1 mM EDTA, 10 mM Tris-HCL, pH 7.8) followed by a series of sequential centrifugation steps performed at 4° C to isolate the mitochondrial fraction. The final pellet was resuspended in 100 µl MAO Buffer (Promega). Total MAO activity was assayed by incubation of 25 µl of mitochondrial protein extract with 25 µl MAO substrate, an aminopropylether analog of methyl ester luciferin (Promega), for 1 hour at room temperature. The luminescent signal was then read after the

subsequent addition of the luciferin detection reagent which is an esterase that converts the methyl ester luciferin into luciferin. Total MAO activity was plotted as RLU/mg protein/min. Protein concentrations are estimated with the DC assay (Biorad, Hercules, CA).

Statistics

All data were analyzed using an unpaired student's t-test or an ANOVA followed by a Bonferonni post-hoc test, unless otherwise specified. Analyses over time were conducted using a repeated two-way ANOVA followed by a Bonferonni post-hoc test to control for multiple comparisons. Analyses were conducted using the GraphPad Prism 5 statistical software for Windows. All data are presented as means ± standard error of the mean with $p < 0.05$ considered statistically significant. *$p<0.05$, **$p<0.01$, ***$p<0.001$, and ****$p<0.0001$.

APPENDIX A2.

CIRCADIAN GENES *PERIOD 1* AND *PERIOD 2* IN THE NUCLEUS ACCUMBENS REGULATE ANXIETY-RELATED BEHAVIOR

(In preparation for submission to Genes, Brains, and Behavior)

Edgardo Falcon, Sade Spencer, Jaswinder Kumar, Vaishnav Krishnan, Shibani Mukherjee, Shari G. Birnbaum, and Colleen A. McClung

Introduction

Circadian rhythms are prominent in virtually every species on this planet and nearly all bodily and cognitive functions in humans follow a 24 hour cycle (Ko and Takahashi 2006). Several studies have found that disruptions in normal rhythms in the sleep/wake cycle can lead to a variety of health problems such as jet lag, shift workers syndrome, and even increase the risk for cancer and heart disease (Moser, Penter et al. 2006). It has become increasingly clear that circadian rhythms also contribute to differences in mood state, reward and motivation. Abnormal rhythms are strongly associated with psychiatric diseases like seasonal affective disorder (SAD), bipolar disorder, major depression, and drug addiction (McClung 2007; Falcon and McClung 2008). Moreover, many of the treatments used for these illnesses are known to modulate the circadian clock. Nonetheless, the exact role of rhythm disruptions in these diseases still remains elusive, as does the contribution of specific circadian genes in individual brain regions in the regulation of mood.

The circadian clock in mammals is regulated by a core transcriptional/ translational loop which cycles over the course of 24 hrs (Ko and Takahashi

2006). The suprachiasmatic nucleus (SCN) is the location of the central pacemaker in the brain, however most circadian genes are widely expressed throughout the brain and in other organs. The central components are the Circadian Locomotor Output Cycles Kaput (CLOCK) and Brain and Muscle ARNT-like Protein 1 (BMAL1) proteins which dimerize and induce the expression of the *Period* (*Per1, Per2,* and *Per3*) and the *Cryptochrome* (*Cry1* and *Cry2*) genes. The CRY and PER proteins can inhibit the activity of CLOCK and BMAL1, thus creating a negative feedback loop. Several other proteins such as Rev-erbα, Retinoid-Related Orphan Receptor Beta (RORβ, Casein kinase 1 epsilon (CK1ε, Glycogen Synthase Kinase 3 Beta (GSK3β, are also involved in regulating the timing of these rhythms. It was shown previously that the three *Period* genes have differential functions in the regulation of circadian rhythms (Shearman, Jin et al. 2000; Bae, Jin et al. 2001). Mice with a mutation in either *mPer1* or *mPer2* have disrupted free running rhythms with lower amplitude in constant darkness (DD). However, most mice retain a significant period of approximately 22-23 hours for several days in DD before losing all rhythmicity (Bae, Jin et al. 2001). Animals with mutations in both *mPer1* and *mPer2* have a much more dramatic and immediate loss of rhythmicity in DD, suggesting that PER1 and PER2 can compensate for one another to some extent when one protein is lost to help maintain circadian rhythms (Bae, Jin et al. 2001). In contrast, mice with a mutation in *mPer3* have surprisingly few disruptions in circadian locomotor activity. Indeed, mice with double mutations in *mPer3* and *mPer1* or *mPer2* do not have an increase in circadian rhythm disruption over the

single *mPer1* or *mPer2* mutations alone, suggesting that this gene has a minimal role in core circadian clock function even though it displays rhythmic expression levels in the SCN (Shearman, Jin et al. 2000; Bae, Jin et al. 2001). However, recent studies suggest a more tissue-specific role for *mPer3* in circadian timekeeping of peripheral oscillators throughout the body, like the liver, lung, and esophagus, among others (Pendergast, Niswender et al. 2012)

Several human genetic studies have identified SNPs and haplotypes in individual circadian genes that associate with various psychiatric disorders. For example, variations in *Clock*, *Bmal1*, *GSK3β*, *Per3*, *RORβ* and *Rev-erbα* have all been linked to a bipolar disorder diagnosis or various aspects of bipolar disorder (Benedetti, Bernasconi et al. 2004; Nievergelt, Kripke et al. 2006; Benedetti, Dallaspezia et al. 2007; Kishi, Kitajima et al. 2008; Kripke, Nievergelt et al. 2009; McGrath, Glatt et al. 2009). Moreover, polymorphisms in *Per2* are associated with vulnerability to major depression and seasonal depression (Partonen, Treutlein et al. 2007; Lavebratt, Sjoholm et al. 2010) and levels of *Clock*, *Period 1* and *Bmal1* mRNA are elevated in blood leukocytes of people with a history of depression (Gouin, Connors et al. 2010). Recently, SNPs in *Bmal2* (a functional homologue to *Bmal1*) have been identified that associate with social phobia anxiety-related disorders (Sipilä, Kananen et al. 2010). Work in animal models has found that mice with a mutation in the *Clock* gene (*Clock*Δ19) (King, Zhao et al. 1997; Vitaterna, Ko et al. 2006) have a complete behavioral profile which is strikingly similar to human bipolar patients in the manic state, including hyperactivity, lowered levels of anxiety or increased “risk taking”

behavior, lowered levels of depression-like behavior, and an increase in the reward value for a variety of stimuli (McClung, Sidiropoulou et al. 2005; Roybal, Theobold et al. 2007). A few studies have similarly begun to examine the influence of the *Per* genes on mood and reward related behavior in mice. (Abarca, Albrecht et al. 2002; Spanagel, Pendyala et al. 2005; Halbout, Perreau-Lenz et al. 2011). Here we wanted to examine the influence of the *Per* genes on anxiety-related behavior and start to understand the mechanisms by which these genes are involved in the response to stress.

Results

mPer1 and *mPer2* are involved in regulating anxiety-related behavior

To determine if mice deficient in *mPer1*, *mPer2*, or both have any anxiety-related behavioral abnormalities, three behavioral paradigms were utilized (the dark/light test, open field and the elevated plus maze). Each of these tests has been validated extensively as a measure of anxiety-related behavior and for their sensitivity to anxiolytic and anxiogenic drugs (Belzung and Griebel 2001). Compared to WT animals, there was a significant decrease in the activity on the light side of the dark/light chamber in mice deficient in *mPer1* and a more sizeable decrease in activity in mice lacking *mPer1*and *mPer2* (Figure A2.1A). Mice deficient in *mPer2* alone were similar to WT animals. In the elevated plus maze there was a significant decrease in the frequency of open arm entries in *mPer1;mPer2* mutant mice with non-significant reductions in each single mutant alone (Figure A2.1B).

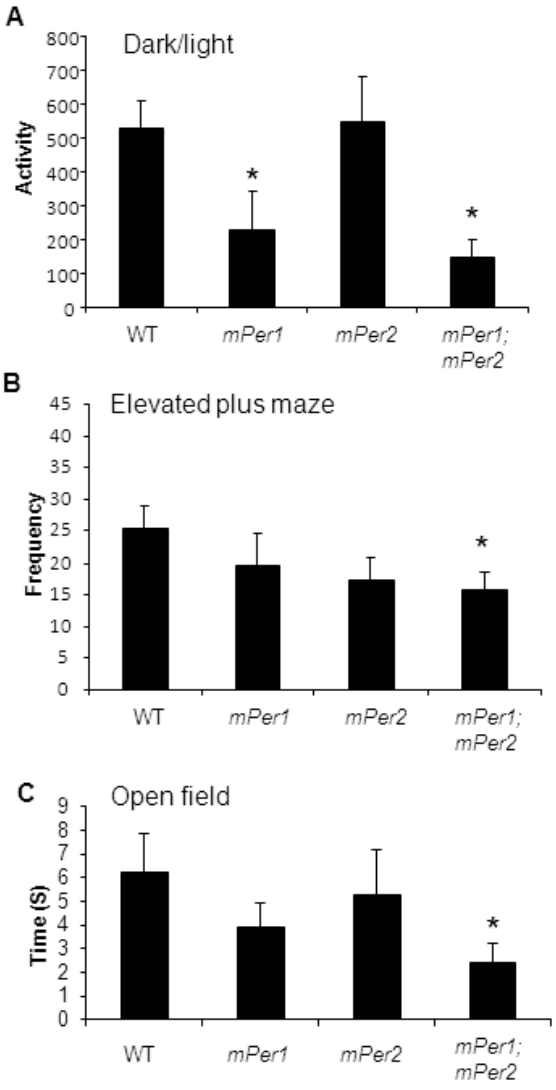

Figure A2.1 *mPer1;mPer2* mutant mice are more anxious. Mice were subjected to the multiple measures of anxiety-related behavior. **A.** *mPer1* mutant mice and *mPer1;mPer2* mutant mice had less activity in the lit compartment of a dark/light box compared to WT mice. **B.** *mPer1;mPer2* mutant mice had less frequent entries into the open arm of the EPM. **C.** *mPer1;mPer2* mutant mice spent less time in the center of the OF (n=12-24, *P<0.05).

In the open field test, *mPer1;mPer2* mutant mice spent less time in the center compared with WT mice (Figure A2.1C). Again animals deficient in only *mPer1* or *mPer2* were not significantly different than WT. Taken together, these results suggest that *mPer1;mPer2* mutant mice have an increase in anxiety-related behavior. Since the single *mPer1* and *mPer2* deficient lines showed inconsistent or non-significant results in these measures, this suggests that each protein is likely able to compensate to some extent for the loss of the other.

Mutations in the *Period* genes do not alter the locomotor response to novelty

Mice with a mutation in the *Clock* gene are hyperactive in response to a novel environment (Roybal, Theobold et al. 2007). Thus, it was set out to determine if mice with a mutation in either *mPer1*, *mPer2*, or *mPer1;mPer2* have any differences in novelty-induced activity. Mice were placed in an unfamiliar chamber for two hours and beam breaks were counted in 5 minute bins. Loss of *Period* gene function did not lead to a significant change in total locomotor activity across the 2 hour span (Figure A2.2) in any of the lines tested. These results suggest that *mPer1* and *mPer2* are not involved in the regulation of the locomotor response to novelty. These results also confirm that the decreased exploratory behavior seen in the anxiety-related tests are not due to an overall decrease in locomotor activity.

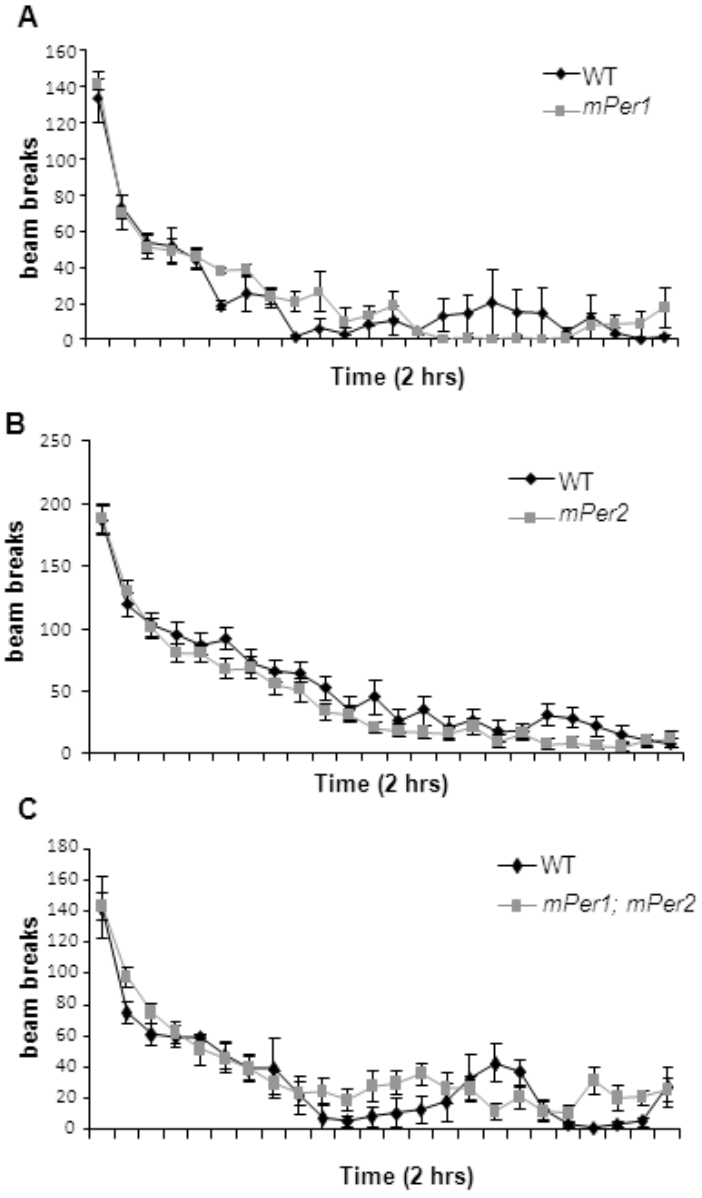

Figure A2.2. **Mice with mutations in the *Per* genes have a normal locomotor response to novelty.** *mPer1* mutant mice **A.** *mPer2* mutant mice **B.** and *mPer1;mPer2* mutant mice **C.** all were not significantly different than wild type mice in the locomotor response to a novel environment over 2hrs (n=13-24).

Chronic social defeat and antidepressant treatment alter *Period* gene expression in the NAc

Since mice with mutations in both *Per* genes have significant behavioral phenotypes in anxiety-related measures, it was sought to determine if chronic stress or anxiolytic/ antidepressant treatment would alter *Per* gene expression in the nucleus accumbens (NAc). The social defeat paradigm, in which mice are subjected to attacks by an aggressive mouse once a day for 10 days, was used as a model of chronic stress. The defeat mice were also housed in an environment where they had constant visual and sensory contact with the aggressor at all times during the 10 day protocol. Previous studies have found that in the majority of mice, this paradigm leads to a profound increase in social avoidance behavior and anxiety-related behavior which is extremely long lasting, but can be reversed with chronic imipramine treatment (Berton, McClung et al. 2006; Tsankova, Berton et al. 2006). Changes in *Per* gene expression were examined in the nucleus accumbens (NAc) which is highly involved in both depression and anxiety-related behavior because previous studies have found that social defeat leads to specific gene expression changes in this region (Nestler and Carlezon 2006; Krishnan, Han et al. 2007). Furthermore, *Per* gene expression is strong in striatal regions, and can be altered in these regions by other behavioral paradigms such as those that employ chronic exposure to drugs of abuse (Nikaido, Akiyama et al. 2001; Iijima, Nikaido et al. 2002). After 10 days of defeat followed by 28 days of vehicle or imipramine treatment, mice which had vehicle treatment had no significant changes in expression of either *mPer1* or

mPer2 (Figure A2.3A). However, mice that received imipramine treatment following defeat had a significant upregulation of both *mPer1* and *mPer2* (Figure A2.3A). Interestingly, control mice which did not experience the social defeat but did have chronic imipramine treatment had no significant changes in *mPer1* or *mPer2* (Figure A2.3B). This suggests that the induction of the *Per* genes with anxiolytic/antidepressant treatment is specific to animals in an anxious/depressed state.

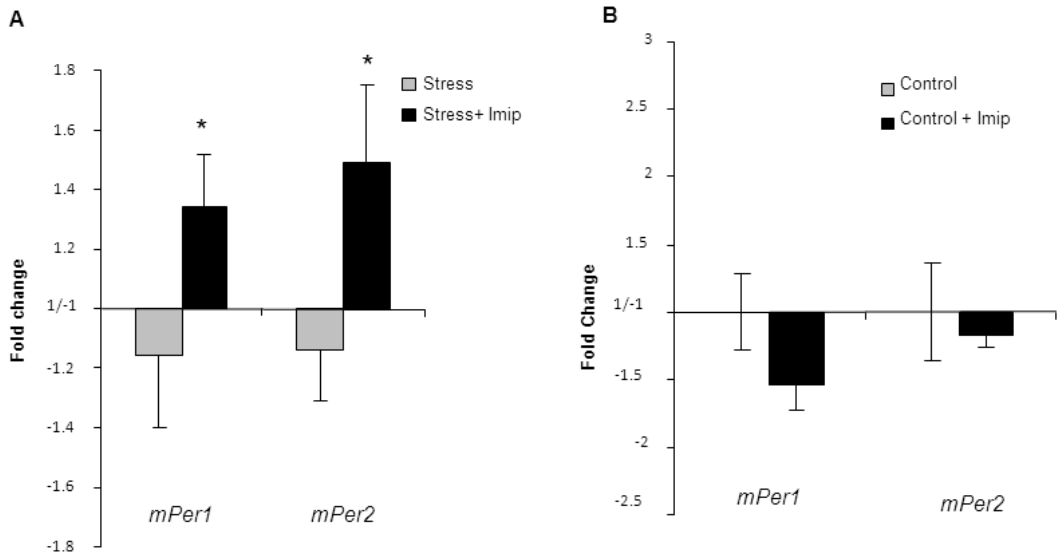

Figure A2.3. Chronic stress followed by imipramine treatment leads to an increase in *mPer1* and *mPer2* expression in the NAc. WT mice were subjected to 10 days of social defeat stress followed by 28 days of vehicle or imipramine treatment. Control mice were only subjected to the 28 days of vehicle or imipramine but not the stress. *mPer1* and *mPer2* mRNA expression was significantly increased in the NAc following chronic stress and imipramine treatment **A.** but not with imipramine treatment alone **B.** (n=5 *p<0.05). The decrease in *mPer1* and *mPer2* expression in the vehicle treated group either with or without defeat stress was not significant.

Disruption in PER1/PER2 function globally disrupts gene expression in the NAc

The PER proteins are known to influence gene transcription via binding to other transcription factors (Ko and Takahashi 2006). Therefore microarray analysis of *mPer1;mPer2* was undertaken in an effort to identify changes in gene expression in the NAc that might underlie the anxiogenic phenotypes of the *mPer1;mPer2* mutant mice, and identify any molecular pathways that seem to be controlled by these proteins. Using Affymetrix microarrays comparing NAc tissue from *mPer1;mPer2* mutant mice versus WT controls, a large number of genes were found to be differentially regulated in this region (Table A2.S1). Many of the fold changes were extremely high (up to a fold change of 163) compared to the modest changes in expression (less than 2 fold) most often identified in microarray studies of the NAc (McClung and Nestler 2003; Berton, McClung et al. 2006). Moreover, Gene Set Enrichment Analysis (GSEA) (Mootha, Lindgren et al. 2003; Subramanian, Tamayo et al. 2005) found the highest concordance with genes involved in oxidative stress, macrophage function, response to DNA breaks and major depression (Table A2.S2), as well as a number of genes found to be differentially regulated in various forms of cancer. These results demonstrate the importance of the *Period* genes in the regulation of gene expression in the NAc and point towards a crucial role for these genes in the cellular response to stress.

Knockdown of mPer1 and mPer2 in the nucleus accumbens contributes to anxiety-related behavior

To determine if a knock-down of *mPer1* and *mPer2* gene expression specifically in the NAc would be sufficient to increase anxiety, an AAV virus with a short hairpin RNA which targeted a common sequence in both *mPer1* and *mPer2* was microinjected into the NAc. This leads to a decrease in the expression of both genes via RNA interference (RNAi) mechanisms. In mouse embryonic fibroblast cells, this AAV-shRNA led to large decreases in *mPer1* and *mPer2* expression (7.2 fold and 13.3 fold respectively, data not shown) when compared to expression of an AAV-scrambled control shRNA (AAV-scr) which does not match the sequence of any known gene. Infection with the AAV-*mPer1/mPer2* shRNA virus in the NAc of intact mice lead to a more modest 3 fold decrease in *mPer1* and a 2.4 fold decrease in *mPer2* compared with controls (Figure A2.4C). To ensure that this decrease was specific to *mPer1* and *mPer2,* levels of *mPer3* were measure and no change in expression was found (data not shown). After waiting two weeks for full viral expression in the NAc, AAV-*mPer1/mPer2* shRNA infected mice and mice expressing the AAV-Scr shRNA were subjected to the elevated plus maze and the open field. Even with this modest decrease in *mPer1* and *mPer2* expression in the NAc, there was a significant decrease in the frequency of open arm entries in the EPM and time spent in the center of the open field (Figure A2.4D, E). These data suggest that *mPer1* and *mPer2* expression in the NAc is important in the regulation of anxiety-related behavior.

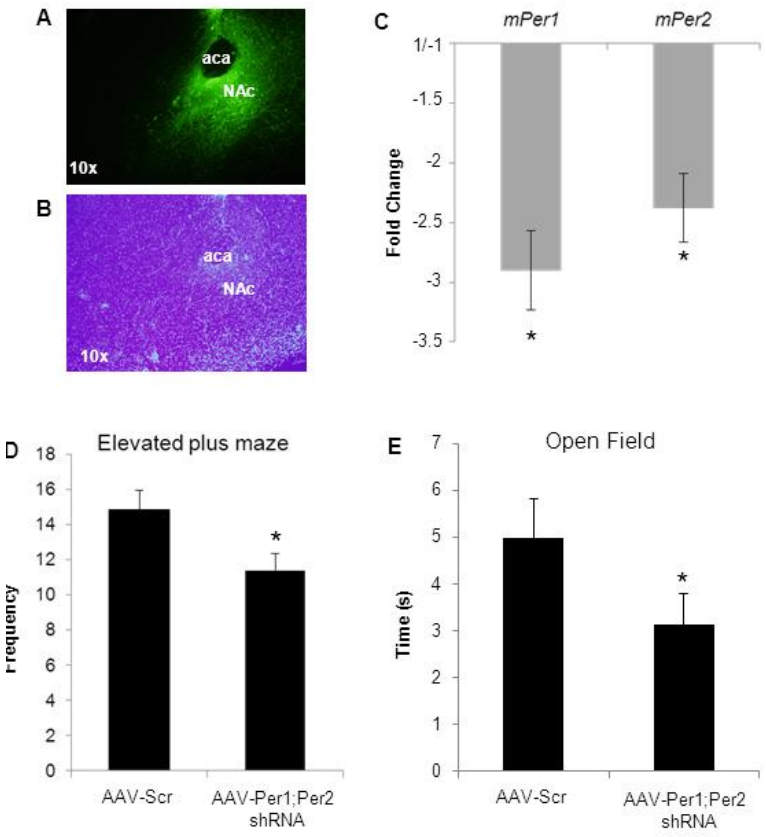

Figure A2.4. Knock-down of *mPer1/mPer2* in the NAc increases anxiety. Mice were infused with the AAV-mPer1;mPer2 shRNA or AAV-Scr into the NAc and behavior was measured 2 weeks later. **A.** Representative image showing viral expression in the NAc **B.** DAPI staining of the same slice **C.** AAV-mPer1;mPer2 infusion leads to a significant knock-down of mPer1 and mPer2 expression in the NAc. AAV-mPer1;mPer2shRNA NAc infected mice had a decreased frequency in the open arms of the EPM **D.** and spent less time in the center of the open field **E.** (n=10-11, *P<0.05).

Discussion

These results show that the *Per* genes are involved in the regulation of anxiety-related behavior. Mice lacking both *mPer1* and *mPer2* have a robust increase in anxiety-related behavior while the single gene mutants display

inconsistent results across tests with mice lacking a functional *mPer1* gene having greater anxiety in only a subset of measures. This might suggest a slightly greater role for *mPer1* over *mPer2* in anxiety, though the two genes appear to have some overlap in function. A recent study by Dong et al., found that *mPer1* mutant mice show enhanced alcohol consumption following social defeat stress relative to wild type mice (Dong, Bilbao et al. 2011). Moreover, a SNP in the *hPer1* promoter which leads to lowered cortisol-induced *Per1* transcription was associated with psychosocial adversity and drinking in adolescents (Dong, Bilbao et al. 2011). In line with the present findings, these results suggest that lowered *Per* gene expression is associated with a heightened and anxiogenic response to stress.

It is interesting that the *mPer1;mPer2* mutant mice have an increase in anxiety-related behavior while mice with a mutation in the *Clock* gene have a decrease in anxiety-related behavior (Roybal et al., 2007). The *Clock* mutant mice are also hyperactive in response to novelty while the *Per* gene mutants are normal in these measures. These results show that disruption in any of the core circadian genes does not result in a common behavioral profile. CLOCK and PER proteins have opposing activity in the circadian loop with PER proteins acting as inhibitors of CLOCK. Therefore perhaps an opposing behavioral phenotype in these measures is not surprising if it is dependent upon CLOCK activity. Interestingly, SCN lesions lead to an antidepressant effect in measures of behavioral despair, but no change in anxiety related behavior (Engelmann, Ebner et al. 1998; Tataroglu, Aksoy et al. 2004; Tuma, Strubbe et al. 2005). This

suggests that the anxiogenic effects seen in the m*Per1;mPer2* mutant mice are due to a lack of *Per* gene function in other brain regions outside of the SCN.

The nucleus accumbens is a known center of emotional regulation and many studies have implicated this region in the response to stress and development of anxiety (Barrot, Olivier et al. 2002; Nestler and Carlezon 2006; Krishnan and Nestler 2008). *Per* gene expression appears to be particularly important in the NAc because local knock-down in this region is sufficient to increase anxiety-related behavior. Following chronic social defeat stress there was a trend towards decreased *Per* gene expression in the NAc, though these results did not reach significance. This tissue was taken 28 days after the end of the 10 day defeat protocol. It is possible that there was a difference that reached significance at an earlier time point. However, there was a significant increase in *Per1* and *Per2* following chronic imipramine only in animals that had experienced social defeat. These results demonstrate that there are molecular adaptations that occur in response to chronic stress which are anxiogenic and the *Per* genes may be involved in the mechanism by which imipramine is able to reverse these changes and restore normal behavior. Interestingly, a recent study by Koresh and colleagues found that expression of *mPer1* and *mPer2* were elevated in the hippocampus, frontal cortex and SCN eight days after exposure to predator scent stress in animals with an “extreme” (i.e. PTSD-like) behavioral response (Koresh, Kozlovsky et al. 2011). Immediate treatment with agomelatine reversed these changes. This suggests that there are wide spread disruptions in *Per* gene expression throughout the brain following stress, and whether the changes are

up or down might be specific to the region of the brain, amount of time following stress, and the time of day in which changes are measured. Future studies will determine if alterations in *Per* gene expression in these other regions results in altered anxiety-like behavior.

Microarray analysis of the NAc of *mPer1;mPer2* mutant mice versus wild type controls identified large changes in gene expression overall, and specifically changes in groups of genes that are responsive to DNA breaks, oxidative stress and other metabolic processes. These results show the importance of the *Per* genes in normal cellular function and the response to cellular stress. Interestingly, acute psychosocial stress in humans is sufficient to elicit changes in cellular stress responses in the immune system, cell cycle regulation, and cell death pathways (Nater, Whistler et al. 2009). A number of genes involved in tumor growth and differentiation were also identified which was not unexpected given the numerous reports of altered *Per* gene expression in various tumors, and the important role of the PER proteins as tumor suppressors (Fu and Lee 2003; Yu and Weaver 2011). Notably, ten of the genes altered in the *mPer1;mPer2* mutant mice were also found to be downregulated in the temporal cortex of human postmortem tissue from subjects with major depression (Aston, Jiang et al. 2005). Anxiety is often highly co-morbid with depression, and future studies will determine the role of the *Per* genes in the NAc in depression-related behavior.

In summary, *mPer1* and *mPer2* in the NAc appear to be centrally involved in the response to stress and development of anxiety. These results also

suggest that an increase in these proteins in the NAc could be beneficial in the reversal of anxiety-related behavior following chronic stress. Thus the Per genes represent new potential therapeutic targets for the treatment of anxiety disorders.

Materials and Methods

Mice:

Homozygous *mPer1*^{ldc}, *mPer2*^{ldc}, and *mPer1;mPer2*^{ldc} mice used in this study were generously provided by David Weaver and colleagues at UMass Medical School (Shearman, Jin et al. 2000; Bae, Jin et al. 2001) and bred and genotyped at UT Southwestern Medical Center at Dallas. All mutant mice were on a 129sv background. Individual wild type (WT) littermates generated from heterozygote breeding were used as controls for all single gene knock-outs and combinations of these WT animals from the single mutation crosses were compared to the double knock-out animals (which were maintained as homozygotes for both mutations). No behavioral differences were found between WT animals from the *mPer1* or *mPer2* crosses (data not shown). Mice used in social defeat experiments are described in detail below. All animals were maintained in a 12:12 light/dark cycle (lights on at 7am) with food and water freely available. Experimental mice used in behavioral analysis were adult males (8-12 weeks old) and behavioral tests of locomotor activity, anxiety, and depression-related behavior were conducted between ZT 3-6 (social defeat experiments are detailed below). All procedures were approved by our Institutional Animal Care and Use Committee at UT Southwestern.

Behavioral Tests:

Locomotor response to novelty: Mice were individually placed in automated locomotor activity chambers equipped with infrared photobeams (San Diego Instruments, San Diego, CA) and measurements began immediately. Activity of the animal was continuously measured and the data was collected in 5-min blocks over a period of 2 hours.

Elevated Plus Maze: Mice were placed in the center of an elevated plus maze (arms are 30×5 cm, with 25 cm tall walls on the closed arms) under low light levels and their behavior was monitored for 5 min. The time spent on the closed and open arms, as well as the number of explorations of open and closed arms were determined by video tracking software, Ethovision 3.0 (Noldus, Leesburg, Virginia). Time spent on the open arm and percent of entries into the open arm are both negatively correlated with anxiety-like behavior. The apparatus was cleaned and allowed to dry between every mouse.

Dark/Light Test: The dark/light apparatus consisted of 2-chambered boxes (25 cm x 26 cm for each side, Med Associates, St. Albans, Vermont). One side was kept dark (room light entry limited) and the other side was brightly lit by a fluorescent bulb across the top. Mice were first placed in dark side for 2 min, then the door between the compartments was opened and they were allowed to freely explore either the light or dark side for 10 min. Anxiety-like behavior was measured as the time spent in the lit side during the final 10 min.

Open field test: Mice were placed in the periphery of a novel open field environment (44 cm x 44 cm, walls 30 cm high) in a dimly lit room and allowed to explore for 5 min. The animals were monitored from above by a video camera connected to a computer running video tracking software (Ethovision 3.0, Noldus, Leesburg, Virginia) to determine the time, distance moved and number of entries into two areas: the periphery (5 cm from the walls) and the center (14 cm x 14cm). The open field arenas were wiped and allowed to dry between mice.

Social Defeat and Avoidance Testing

Social defeat and avoidance testing were performed according to published protocols (Berton, McClung et al. 2006; Tsankova, Berton et al. 2006; Krishnan, Han et al. 2007). Briefly, CD1 retired breeder mice were screened for consistent attack latencies (<30 sec on 3 consecutive screening sessions with a C57Bl/6ByJ intruder). C57Bl/6ByJ were purchased from Jackson laboratory and group housed in a 12 hr light/dark cycle with food and water *ad libitum* for at least one week prior to the defeat protocol in our facility. During each defeat episode, intruder mice were allowed to interact for 10 min with the aggressive CD1 mouse, during which they were attacked and displayed subordinate posturing. Non-defeated controls were housed in identical cages opposite each other and were rotated similarly. Immediately after the tenth defeat all mice were singly housed. Social defeat was always performed in the few hours before the onset of the dark phase (1730-1830 hours). Social interaction tests were performed 24 hours after the last defeat and then again after the last antidepressant treatment (imipramine

20 mg/kg i.p. daily for 28 days). On these days the time spent in the interaction zone during the first (target absent) and second (target present) trials were measured and the *interaction ratio* was calculated as 100 × (interaction time, target present)/(interaction time, target absent). Previous work has found that depression-related behavior persists 28 days after the social defeat protocol and that imipramine treatment completely reverses the social interaction deficit seen in susceptible animals (Berton, McClung et al. 2006; Tsankova, Berton et al. 2006). Animals were killed 24 hours after the last imipramine or vehicle treatment and NAc dissections were taken by punch dissection as described previously (McClung and Nestler 2003).

Quantitative PCR

cDNA was mixed with buffer, primers, SYBR green, and hot start Taq polymerase in a prepared master mix (Applied Biosystems). PCR reactions followed by a dissociation reaction to determine specificity of the amplified product were run on a Real-Time PCR machine (7300 Real Time PCR machine, Applied Biosystems). The amount of gene expression was quantified using the ΔΔCt method as previously described (LaPlant, Chakravarty et al. 2009). The following primer sets were used to measure *Per* expression: mPer1 For – CT CTGTGCTGAAGCAAGACCG; mPer1 Rev – TCATCAGAGTGGCCAGGATCTT; mPer2 For – GAGTGTGTGCAGCGGCTTAG; mPer2 Rev – GTAGGGTGTCATGCGG AAGG.

Microarray analysis

Microarray analysis was performed as described previously (Berton, McClung et al. 2006; Wallace, Han et al. 2009). Briefly Affymetrix mouse 430_2 whole genome arrays were utilized with NAc tissue taken from individual *mPer1;mPer2* double mutants (n=3) or WT controls (n=3). Array results were normalized in Array Assist (Agilent Technologies; Stratagene) using the PLIER algorithm. Comparative analysis was also performed in Array Assist utilizing an unpaired t-test to compare each experimental group with control animals that were handled, treated, and dissected at the same time. Data files from Array Assist were exported into Excel (Microsoft) and then imported into Genespring (Silicon Genetics) for additional analysis and data visualization. In each condition, genes were considered to be regulated if the raw signal was significant to background, the fold change was greater than 1.36, and the comparison p-value was < 0.01. Pathway analysis was performed using the Gene Set Enrichment Analysis (GSEA; Broad Institute) which utilizes multiple databases including KEGG, Biocarta, Reactome, and GO. Statistically significant gene sets are determined by Fisher Exact Test ($P<0.05$).

Construction of mPer1;mPer2 shRNA

A small hairpin RNA (shRNA) was constructed against *mPer1* and *mPer2* mRNA by selecting a conserved 24 base sequence (5'-ATCCCTCCTGACAAGAGGATCTTC-3') in the coding region. For the scrambled shRNA, a random sequence of 24 bases (5'-CGGAATTTAGTTACG

GGGATCCAC-3') that had no sequence similarities with any known genes/mRNA was used. An antisense sequence of the selected mRNA region followed by a miR23 loop of 10 nucleotide (CTTCCTGTCA) was added at the 5'end of the above sequences. These shRNAs were designed as synthetic duplexes with overhang ends identical to those created by Sap I and Xba I restriction enzyme digestion. The annealed oligonucleotides were cloned into the adeno-associated virus (AAV) plasmid expressing enhanced green fluorescent protein (Stratagene, La Jolla, CA). Plasmids were sent to the University of North Carolina Viral Vector Core for production (Chapel Hill, NC).

Stereotaxic surgery

Stereotaxic surgery was performed similarly to Mukherjee et al 2010. Mice were anesthetized with a mixture of ketamine (50 mg/kg body weight) and xylazine (10 mg/kg body weight) in saline (0.9% NaCl). Bilateral stereotaxic injections of 1 µl of purified high titer AAV encoding scrambled or AAV- mPer1;mPer2 shRNA was injected into the NAc (from bregma: angle 10°, AP +1.5 mm, Lat +1.5, DV -4.4) using a 33 gauge hamilton syringe (Hamilton, Reno, NV). Injection speed was 0.1 µl/minute, and the needle was kept in place for an additional 5 minutes before it was slowly withdrawn. Mice recovered for two weeks in their home cage prior to behavioral testing to allow for full virus expression.

Immunohistochemical localization of AAV expression

Mice were anesthetized with 50 mg/kg Nembutal in saline, and transcardially perfused with 4% paraformaldehyde in 1X PBS (1 mM KH2PO4, 10 M Na2HPO4, 137 mM NaCl, 2.7 mM KCl, pH 7.4). The brains were allowed to post-fix in a 4% paraformaldehyde for 24 hours and then placed in 1X PBS-30% glycerol sucrose protection for an additional 24 hours before being stored in 1X PBS-0.05% sodium azide. 30 µm brain sections were obtained with a microtome (Leica, Wetzlar, Germany) and immunohistochemical staining against GFP (AbCam, Cambridge, MA) was carried out using standard procedures. Secondary antibody (anti-rabbit conjugated with Alexa 488) was purchased from Molecular Probes (Carlsbad, CA). Brain sections were mounted using Vectashield (Vector Labs, Burlingame, CA) with DAPI counterstaining and observed with an epifluorescence microscope with a 10x objective. Animals were excluded from our study if their infection spread was not localized to the NAc , with spillover to adjacent areas or throughout the injection tract; or if there was a significant disproportionate amount of infection between both sides. Exclusion by these criteria accounted for approximately 10% of animals.

Statistical analysis:

All data are expressed as mean ± standard error of the mean. Significance for two group comparisons in behavioral assays and qPCR analysis was determined by two way ANOVA and post-hoc analysis. Behavioral results from the shRNA

experiments were analyzed by student's t-test. In all experiments $P<0.05$ is considered significant.

Table A2.S1. Significant gene expression changes in the NAc of *mPer1;mPer2* mice

Gene Symbol	Fold Change	Gene Name
UPREGULATED		
Pdxdc1	163.07986	pyridoxal-dependent decarboxylase domain containing 1
Skiv2l2	22.703724	superkiller viralicidic activity 2-like 2 (S. cerevisiae)
Tmem87a	22.247902	transmembrane protein 87A
Ints10	10.814575	integrator complex subunit 10
Pldn	10.153809	Pallidin
Zfp64	5.197372	zinc finger protein 64
Kcnj9	4.921765	potassium inwardly-rectifying channel, subfamily J, member 9
Pla2g4e	4.753624	phospholipase A2, group IVE
Mamdc2	4.653901	MAM domain containing 2
H2-Bl	4.0462403	histocompatibility 2, blastocyst
Esco1	3.9394853	establishment of cohesion 1 homolog 1 (S. cerevisiae)
Casc4	3.892533	cancer susceptibility candidate 4
Usp14	3.790768	ubiquitin specific peptidase 14
Med1	3.658584	mediator complex subunit 1
Tsc22d1	3.4655244	TSC22-related inducible leucine zipper 1b (Tilz1b)
Ocel1	3.4643505	occludin/ELL domain containing 1
Zbtb16	3.3775492	zinc finger and BTB domain containing 16
Zfp398	3.2163012	zinc finger protein 398
Armc1	3.105523	armadillo repeat containing 1
Supt16h	3.1010184	suppressor of Ty 16 homolog (S. cerevisiae)
Ramp1	3.053394	receptor (calcitonin) activity modifying protein 1
Atp1a2	3.044215	ATPase, Na+/K+ transporting, alpha 2 polypeptide
Tle4	3.00081	transducin-like enhancer of split 4, homolog of Drosophila E(spl)
Wdfy1	2.9433482	WD repeat and FYVE domain containing 1
D5Ertd798e	2.9188883	DNA segment, Chr 5, ERATO Doi 798, expressed
Abhd1	2.8570073	abhydrolase domain containing 1
Lcorl /// LOC100046011	2.8155901	ligand dependent nuclear receptor corepressor-like /// hypothetical protein LOC100046011
Wdfy1	2.8040495	WD repeat and FYVE domain containing 1
Tsen2	2.7217097	tRNA splicing endonuclease 2 homolog (S. cerevisiae)
Med1	2.6870406	mediator complex subunit 1
Gm129	2.6608152	gene model 129, (NCBI)
Mpp7	2.6464226	membrane protein, palmitoylated 7 (MAGUK p55 subfamily member 7)
Plvap	2.5619984	plasmalemma vesicle associated protein
Folh1	2.5427	folate hydrolase
Adcy7	2.4037695	adenylate cyclase 7
Cnnm1	2.380429	cyclin M1
Gzmk	2.3771994	granzyme K
Slc15a2	2.3724248	solute carrier family 15 (H+/peptide transporter), member 2
Mpp7	2.332721	membrane protein, palmitoylated 7 (MAGUK p55 subfamily member 7)
Rbm45	2.2818651	RNA binding motif protein 45
Supt7l	2.27437	suppressor of Ty 7 (S. cerevisiae)-like
Kcnb1	2.2742388	potassium voltage gated channel, Shab-related subfamily, member 1
Psip1	2.2400606	PC4 and SFRS1 interacting protein 1 (Psip1), mRNA
Alad /// LOC100046072	2.2390966	aminolevulinate, delta-, dehydratase /// similar to aminolevulinate, delta-, dehydratase

Rpgrip1	2.2139251	retinitis pigmentosa GTPase regulator interacting protein 1
Armc9	2.194753	armadillo repeat containing 9
Spry2	2.1933522	sprouty homolog 2 (Drosophila)
Iqcf1	2.1930766	IQ motif containing F1
Mysm1	2.178694	myb-like, SWIRM and MPN domains 1
Ugcgl2	2.1776702	UDP-glucose ceramide glucosyltransferase-like 2
Rragd	2.168193	Ras-related GTP binding D
Lsm12	2.1629736	LSM12 homolog (S. cerevisiae)
Pigz	2.1594698	phosphatidylinositol glycan anchor biosynthesis, class Z
EG623818 /// Hmbs	2.1117568	predicted gene, EG623818 /// hydroxymethylbilane synthase
Apod /// LOC100047583	2.102918	apolipoprotein D /// similar to apolipoprotein D
Ppwd1	2.0985777	peptidylprolyl isomerase domain and WD repeat containing 1
Fmo1	2.0854836	flavin containing monooxygenase 1
Pyroxd2	2.0730407	pyridine nucleotide-disulphide oxidoreductase domain 2
Rbm39	2.0698643	RNA binding motif protein 39
Gprc5b	2.0694625	G protein-coupled receptor, family C, group 5, member B
Cntn3	2.0639896	contactin 3
Nrd1	2.0595195	nardilysin, N-arginine dibasic convertase, NRD convertase 1
Marveld2	2.0464137	MARVEL (membrane-associating) domain containing 2
Fst	2.031238	Follistatin
Zfp69	2.0211785	zinc finger protein 69
Pitpnc1	2.0189035	phosphatidylinositol transfer protein, cytoplasmic 1
Edil3	2.0163221	Del1 minor splice variant (Del1)
Hist3h2ba	1.9881265	histone cluster 3, H2ba
Crkrs	1.9570255	CDC2-related kinase, arginine/serine-rich
Fam20b	1.9541714	Family with sequence similarity 20, member B, mRNA (cDNA clone MGC:36624 IMAGE:5352660)
Rbm39	1.9500977	RNA binding motif protein 39
Lsm12	1.9348234	LSM12 homolog (S. cerevisiae)
Nr1d2	1.880898	nuclear receptor subfamily 1, group D, member 2
Smg1	1.8427855	SMG1 homolog, phosphatidylinositol 3-kinase-related kinase (C. elegans)
Epb4.1l1	1.8404436	erythrocyte protein band 4.1-like 1
Ifit3	1.8122317	interferon-induced protein with tetratricopeptide repeats 3
Kcnj10	1.7845392	potassium inwardly-rectifying channel, subfamily J, member 10
Adcy7	1.7844566	adenylate cyclase 7
Cdh7	1.76733	cadherin 7, type 2
Nnt	1.739978	nicotinamide nucleotide transhydrogenase
Lyplal1	1.7392213	lysophospholipase-like 1
Wdfy1	1.7313237	WD repeat and FYVE domain containing 1
Rfesd	1.7194365	Rieske (Fe-S) domain containing
Mthfd1l	1.7133402	methylenetetrahydrofolate dehydrogenase (NADP+ dependent) 1-like
Gpr137c	1.69243	G protein-coupled receptor 137C
Sfrp1	1.6748738	secreted frizzled-related protein 1
Mpp3	1.6490617	membrane protein, palmitoylated 3 (MAGUK p55 subfamily member 3)
Slc14a1	1.6451137	solute carrier family 14 (urea transporter), member 1
Hey2	1.6422431	hairy/enhancer-of-split related with YRPW motif 2
Sypl	1.6406695	synaptophysin-like protein
Dynlt1d /// Tmem181	1.6370541	dynein light chain Tctex-type 1D /// transmembrane protein 181
Nqo1	1.6196786	NAD(P)H dehydrogenase, quinone 1
Pi4k2b	1.6164364	phosphatidylinositol 4-kinase type 2 beta
Ptgfrn	1.6036649	prostaglandin F2 receptor negative regulator
F2r	1.6014299	coagulation factor II (thrombin) receptor
Chd2	1.5989904	chromodomain helicase DNA binding protein 2
Sfi1	1.5978068	Sfi1 homolog, spindle assembly associated (yeast)
Tmem181	1.5966526	transmembrane protein 181
Orc3l	1.5856255	origin recognition complex, subunit 3-like (S. cerevisiae)
Rpl17	1.5852182	ribosomal protein L17
Bxdc2	1.5758436	brix domain containing 2

Rgs16	1.5758215	regulator of G-protein signaling 16
Fam149a	1.5745534	family with sequence similarity 149, member A
LOC640502 /// Uap1	1.5733553	similar to UDP-N-acetylhexosamine pyrophosphorylase /// UDP-N-acetylglucosamine pyrophosphorylase 1
Wdr16	1.571068	WD repeat domain 16
LOC433064 /// Ppih	1.5686675	similar to peptidyl prolyl isomerase H /// peptidyl prolyl isomerase H
Ppm2c	1.5682639	protein phosphatase 2C, magnesium dependent, catalytic subunit
Zwint	1.5582784	ZW10 interactor
Rrad	1.5579627	Ras-related associated with diabetes
Sfxn4	1.5543066	sideroflexin 4
Sympk	1.5542725	PREDICTED: Mus musculus symplekin (Sympk), mRNA
Exd1	1.5517102	exonuclease 3'-5' domain containing 1
Kcnq1ot1	1.5399141	KCNQ1 overlapping transcript 1
Lpl	1.5310428	lipoprotein lipase
Inpp4b	1.5197984	inositol polyphosphate-4-phosphatase, type II
Rdh13	1.5181713	retinol dehydrogenase 13 (all-trans and 9-cis)
Pm20d1	1.5174752	peptidase M20 domain containing 1
Pclo	1.5100782	piccolo (presynaptic cytomatrix protein)
Mut	1.4988123	methylmalonyl-Coenzyme A mutase
Sp1	1.4979638	trans-acting transcription factor 1
Glo1	1.4886348	glyoxalase 1
Dnaic1	1.4851202	dynein, axonemal, intermediate chain 1
LOC100048247	1.4849001	similar to polycomb group ring finger 5
Ptchd1	1.4807725	patched domain containing 1
Itm2b	1.4799745	integral membrane protein 2B
Mut	1.4730355	methylmalonyl-Coenzyme A mutase
Limch1	1.4726206	LIM and calponin homology domains 1 (Limch1), mRNA
Itch	1.4720265	itchy, E3 ubiquitin protein ligase
Nupl1	1.4676307	nucleoporin like 1
Ccr6	1.4660307	chemokine (C-C motif) receptor 6
Svil	1.4626781	Supervillin
Enox1	1.4575627	ecto-NOX disulfide-thiol exchanger 1
Zbtb10	1.449157	zinc finger and BTB domain containing 10
Tctex1d2	1.4478508	Tctex1 domain containing 2
Ston1	1.4419018	Stonin 1 (Ston1), mRNA
Wtap	1.4408981	Wilms' tumour 1-associating protein
Zc3h12c	1.4389921	zinc finger CCCH type containing 12C
Tprkb	1.4375784	Tp53rk binding protein
C030033M12Rik /// Rsf1	1.4370954	RIKEN cDNA C030033M12 gene /// remodeling and spacing factor 1
Stk35	1.4360473	serine/threonine kinase 35
Mllt3	1.4359876	myeloid/lymphoid or mixed-lineage leukemia (trithorax homolog, Drosophila); translocated to, 3
Lrrc4c	1.4345628	Leucine rich repeat containing 4C, mRNA (cDNA clone MGC:106508 IMAGE:30617370)
Gja1	1.4341168	gap junction protein, alpha 1
Ercc2	1.4303242	Excision repair cross-complementing rodent repair deficiency, complementation group 2, mRNA (cDNA clone MGC:27532 IMAGE:4458839)
Slc37a4	1.4295944	solute carrier family 37 (glucose-6-phosphate transporter), member 4
Me2	1.4267718	malic enzyme 2, NAD(+)-dependent, mitochondrial
Gspt2	1.4244307	G1 to S phase transition 2
Fbxo3	1.4211305	F-box protein 3
Slc14a1	1.4178236	solute carrier family 14 (urea transporter), member 1
Slc7a11	1.4165592	solute carrier family 7 (cationic amino acid transporter, y+ system), member 11
Arhgap4	1.415351	Rho GTPase activating protein 4
Ifi30	1.4006002	interferon gamma inducible protein 30
Rbm8a	1.3990426	RNA binding motif protein 8a
Pgap1	1.3952152	post-GPI attachment to proteins 1
Peg3	1.3952061	paternally expressed 3

Usf1	1.39364	upstream transcription factor 1
Stxbp4	1.3926165	syntaxin binding protein 4
Sf4	1.3920588	splicing factor 4
Ldhd	1.391458	lactate dehydrogenase D
Zfp295	1.3886931	zinc finger protein 295
Gmip	1.3882145	Gem-interacting protein
Rab3gap1	1.3871458	RAB3 GTPase activating protein subunit 1
Dbt	1.3871008	dihydrolipoamide branched chain transacylase E2
Slc25a36	1.3864928	solute carrier family 25, member 36
Fam62b	1.3800949	family with sequence similarity 62, member B
Apol8	1.3796602	apolipoprotein L 8
Mocs1	1.378669	molybdenum cofactor synthesis 1
Pnma5	1.3767962	paraneoplastic antigen family 5
Ppm1k	1.3766019	protein phosphatase 1K (PP2C domain containing)
Clptm1	1.3761804	cleft lip and palate associated transmembrane protein 1
Cercam	1.3751626	cerebral endothelial cell adhesion molecule
Zik1	1.3743591	zinc finger protein interacting with K protein 1
LOC100045567 /// Pnp1	1.3718723	similar to purine nucleoside phosphorylase /// purine-nucleoside phosphorylase 1
Eif2s2	1.3717732	eukaryotic translation initiation factor 2, subunit 2 (beta)
Pdia3	1.3708751	protein disulfide isomerase associated 3
Epha4	1.3708341	Eph receptor A4
Amigo2	1.3694645	adhesion molecule with Ig like domain 2
Hnrnpc /// OTTMUSG00000008006	1.3682587	heterogeneous nuclear ribonucleoprotein C /// predicted gene, OTTMUSG00000008006
Rnls	1.3676354	renalase, FAD-dependent amine oxidase
Socs4	1.3670021	suppressor of cytokine signaling 4
Prkg2	1.3640962	protein kinase, cGMP-dependent, type II
Rc3h2	1.3616189	ring finger and CCCH-type zinc finger domains 2
Wdr62	1.360827	WD repeat domain 62
DOWNREGULATED		
Rps9	37.406506	ribosomal protein S9
Ccl21a /// Ccl21b /// Ccl21c	22.101341	chemokine (C-C motif) ligand 21A /// chemokine (C-C motif) ligand 21B /// chemokine (C-C motif) ligand 21C (leucine)
Tmem40	21.573027	transmembrane protein 40
Scn2b	19.646719	sodium channel, voltage-gated, type II, beta
Cd99l2	16.75769	CD99 antigen-like 2
Pdxdc1	15.909773	pyridoxal-dependent decarboxylase domain containing 1
Cript	13.1127615	cysteine-rich PDZ-binding protein
Cd99l2	12.884508	CD99 antigen-like 2
Mtmr7	11.385848	myotubularin related protein 7
Rmst	10.657746	rhabdomyosarcoma 2 associated transcript (non-coding RNA)
Pnma2	10.026945	paraneoplastic antigen MA2
Trp53bp1	9.9271755	transformation related protein 53 binding protein 1
Slc15a2	9.005051	solute carrier family 15 (H+/peptide transporter), member 2
Hps1	8.533	Hermansky-Pudlak syndrome 1 homolog (human)
Trp53bp1	8.276409	transformation related protein 53 binding protein 1
Ang	7.470926	angiogenin, ribonuclease, RNase A family, 5
Ppcdc	6.9503965	phosphopantothenoylcysteine decarboxylase
BC031748	6.8134575	CDNA sequence BC031748 (BC031748), mRNA
Tia1	6.726292	cytotoxic granule-associated RNA binding protein 1
Pdxdc1	6.501792	Pyridoxal-dependent decarboxylase domain containing 1 (Pdxdc1), transcript variant 1, mRNA
Adi1	6.208035	acireductone dioxygenase 1
Ang	6.0214067	angiogenin, ribonuclease, RNase A family, 5
Fmn2	5.740571	formin 2
Myo7a	5.461564	myosin VIIA
Tmem40	5.2910075	transmembrane protein 40

Spata5l1	5.0570335	spermatogenesis associated 5-like 1
Adamts4	4.8463306	a disintegrin-like and metallopeptidase (reprolysin type) with thrombospondin type 1 motif, 4
Prdx2	4.7878447	peroxiredoxin 2
Atp2c1	4.646063	ATPase, Ca++-sequestering
Mga	4.492594	MAX gene associated
Scmh1	4.3125167	Sex comb on midleg homolog 1 (Scmh1), mRNA
Cdh7	3.7953184	cadherin 7, type 2
Prkaa2	3.7547832	protein kinase, AMP-activated, alpha 2 catalytic subunit
Rpgrip1	3.5593228	retinitis pigmentosa GTPase regulator interacting protein 1
Atm	3.4730444	ataxia telangiectasia mutated homolog (human)
Pi4k2a	3.4565237	phosphatidylinositol 4-kinase type 2 alpha
Kctd14	3.4437954	potassium channel tetramerisation domain containing 14
Lman1	3.418434	lectin, mannose-binding, 1
Dact3	3.3224185	dapper homolog 3, antagonist of beta-catenin (xenopus)
Caskin1	3.1503828	CASK interacting protein 1
Prkaa2	3.1296315	protein kinase, AMP-activated, alpha 2 catalytic subunit
Pdxdc1	3.1057012	pyridoxal-dependent decarboxylase domain containing 1
Zfp593	2.977452	zinc finger protein 593
Gp1ba	2.868199	glycoprotein 1b, alpha polypeptide
Ppp1r3e	2.8280532	protein phosphatase 1, regulatory (inhibitor) subunit 3E
Dusp12	2.8086545	dual specificity phosphatase 12
Elavl1	2.7999382	ELAV (embryonic lethal, abnormal vision, Drosophila)-like 1 (Hu antigen R)
Acaca /// EG382567	2.7313104	acetyl-Coenzyme A carboxylase alpha /// predicted gene, EG382567
Nav1	2.7038946	neuron navigator 1
Cryab	2.6720061	crystallin, alpha B
Cttnbp2	2.5762818	cortactin binding protein 2
Chic1	2.5659368	Cysteine-rich hydrophobic domain 1, mRNA (cDNA clone MGC:170357 IMAGE:8861752)
Hisppd2a	2.5564866	histidine acid phosphatase domain containing 2A
Mkks	2.516239	McKusick-Kaufman syndrome protein
Mpeg1	2.4869516	macrophage expressed gene 1
Tmem40	2.4140115	transmembrane protein 40
Tm2d2	2.3754737	TM2 domain containing 2
Cand2	2.345365	cullin-associated and neddylation-dissociated 2 (putative)
Capn3	2.295221	calpain 3
Paqr7	2.277379	Progestin and adipoQ receptor family member VII (Paqr7), mRNA
Tulp4	2.2697606	tubby like protein 4
Map3k7	2.2029471	mitogen-activated protein kinase kinase kinase 7
Car8	2.1094012	carbonic anhydrase 8
Zcchc3	2.100542	zinc finger, CCHC domain containing 3
Rps6	2.0650408	ribosomal protein S6
Spag9	2.0382607	sperm associated antigen 9
Itch	2.033723	itchy, E3 ubiquitin protein ligase
Cep192	2.0272698	Premature mRNA for mKIAA1569 protein
Cxcl13	2.0024102	chemokine (C-X-C motif) ligand 13
Samd4	1.9869547	sterile alpha motif domain containing 4
Prdm16	1.9658161	PR domain containing 16
Ggcx	1.9560659	gamma-glutamyl carboxylase
Ccl27a	1.9344465	chemokine (C-C motif) ligand 27A
Cryab	1.934077	crystallin, alpha B
Trim34	1.9124783	tripartite motif-containing 34
Map2k7	1.9054939	mitogen-activated protein kinase kinase 7
Gjb1	1.897576	gap junction protein, beta 1
Ccl6	1.8779497	chemokine (C-C motif) ligand 6
Naip5	1.8731921	NLR family, apoptosis inhibitory protein 5
Ccl27a	1.869179	chemokine (C-C motif) ligand 27A
Prr18	1.8563688	proline rich region 18
Nav1	1.8495973	neuron navigator 1

Fbxo44	1.8391204	F-box protein 44
Dcp1b	1.8389121	DCP1 decapping enzyme homolog b (S. cerevisiae)
Ncapd2	1.8312722	non-SMC condensin I complex, subunit D2
Fem1a	1.8288018	feminization 1 homolog a (C. elegans)
Trf	1.8201282	Transferrin
Slc24a2	1.8180546	solute carrier family 24 (sodium/potassium/calcium exchanger), member 2
Esd	1.8077459	Esterase D/formylglutathione hydrolase (Esd), mRNA
LOC100048604 /// Ninj2	1.8072416	similar to ninjurin2 /// ninjurin 2
Pllp	1.7969198	plasma membrane proteolipid
Fndc3a	1.787043	fibronectin type III domain containing 3A
Gadd45gip1	1.7820506	growth arrest and DNA-damage-inducible, gamma interacting protein 1
Aldh7a1	1.7735661	aldehyde dehydrogenase family 7, member A1
Lgi3	1.7666689	leucine-rich repeat LGI family, member 3
Stxbp2	1.7515991	syntaxin binding protein 2
Klf12	1.7499818	Kruppel-like factor 12
Pgpep1	1.7370445	pyroglutamyl-peptidase I
H2-T10 /// H2-T17 /// H2-T22 /// H2-T9	1.7369473	histocompatibility 2, T region locus 10 /// histocompatibility 2, T region locus 17 /// histocompatibility 2, T region locus 22 /// histocompatibility 2, T region locus 9
Lgals7 /// Samd4	1.7175795	lectin, galactose binding, soluble 7 /// sterile alpha motif domain containing 4
Arsk	1.7149282	arylsulfatase K
Rad23a	1.7131382	RAD23a homolog (S. cerevisiae)
Frag1	1.7081468	FGF receptor activating protein 1
Stk25	1.7035123	serine/threonine kinase 25 (yeast)
Mark4	1.7030361	MAP/microtubule affinity-regulating kinase 4
Rpp25	1.6774338	ribonuclease P 25 subunit (human)
Kctd14	1.673872	potassium channel tetramerisation domain containing 14
Dbi	1.6634966	diazepam binding inhibitor
Polr1a	1.6590286	polymerase (RNA) I polypeptide A
Lmo1	1.6571361	LIM domain only 1
Coro2b	1.6556733	coronin, actin binding protein, 2B
Dhdds	1.6428918	dehydrodolichyl diphosphate synthase
Cntfr	1.642671	ciliary neurotrophic factor receptor
Nos1ap	1.6373652	nitric oxide synthase 1 (neuronal) adaptor protein
Nnmt	1.619879	nicotinamide N-methyltransferase
Galm	1.607401	galactose mutarotase
Pop4	1.5917711	processing of precursor 4, ribonuclease P/MRP family, (S. cerevisiae)
Klhdc9	1.5811667	kelch domain containing 9
Rab8a	1.5726717	RAB8A, member RAS oncogene family (Rab8a), mRNA
Vangl2	1.5709174	vang-like 2 (van gogh, Drosophila)
Fads6	1.5654644	fatty acid desaturase domain family, member 6
Slc25a19	1.563225	solute carrier family 25 (mitochondrial thiamine pyrophosphate carrier), member 19
Nlrx1	1.551315	NLR family member X1
Jmjd7	1.5492492	jumonji domain containing 7
Polr1a	1.5278773	polymerase (RNA) I polypeptide A
Mthfd2	1.5251637	methylenetetrahydrofolate dehydrogenase (NAD+ dependent), methenyltetrahydrofolate cyclohydrolase
Tmem19	1.5234618	transmembrane protein 19
Cacnb1	1.5218232	calcium channel, voltage-dependent, beta 1 subunit
Odz4	1.5189627	odd Oz/ten-m homolog 4 (Drosophila)
Ltbp4	1.5178305	latent transforming growth factor beta binding protein 4
Myg1	1.5112839	melanocyte proliferating gene 1
Abcf1	1.5109109	ATP-binding cassette, sub-family F (GCN20), member 1
D6Wsu116e	1.5108125	DNA segment, Chr 6, Wayne State University 116, expressed
Oaf	1.5075518	OAF homolog (Drosophila)
Pon2	1.5072562	paraoxonase 2
Mrpl47	1.5071172	mitochondrial ribosomal protein L47
Zh2c2	1.5055702	zinc finger, H2C2 domain containing

Dbi	1.5017204	diazepam binding inhibitor
Ttpal	1.4988986	tocopherol (alpha) transfer protein-like
LOC627626	1.4961693	Similar to CG11212-PA, mRNA (cDNA clone MGC:184066 IMAGE:9088055)
Tradd	1.4951609	TNFRSF1A-associated via death domain
Dnajb5	1.4943137	DnaJ (Hsp40) homolog, subfamily B, member 5
Gstm7	1.4895003	glutathione S-transferase, mu 7
Dctd	1.4882056	dCMP deaminase
Frag1	1.4849548	FGF receptor activating protein 1
Yipf3	1.4784355	Yip1 domain family, member 3
Rad23a	1.4776158	RAD23a homolog (S. cerevisiae)
Rnf157	1.475672	ring finger protein 157
Snx5	1.4705888	sorting nexin 5
Ivns1abp	1.4669834	influenza virus NS1A binding protein
Zcchc11	1.4661901	zinc finger, CCHC domain containing 11
Rnf112	1.4660063	ring finger protein 112
Gatm	1.465518	glycine amidinotransferase (L-arginine:glycine amidinotransferase)
Chl1	1.461355	cell adhesion molecule with homology to L1CAM
Usp36	1.4610846	ubiquitin specific peptidase 36
Prl7c1	1.4584008	prolactin family 7, subfamily c, member 1
Amdhd2	1.451711	amidohydrolase domain containing 2
Bpnt1	1.4477185	bisphosphate 3'-nucleotidase 1
Dbi	1.4469645	diazepam binding inhibitor
Il15	1.4358268	interleukin 15
B4galt2	1.4349903	UDP-Gal:betaGlcNAc beta 1,4- galactosyltransferase, polypeptide 2
Oscar	1.4346075	osteoclast associated receptor
Cdc42ep1	1.4336593	CDC42 effector protein (Rho GTPase binding) 1
Mcart1	1.4310224	mitochondrial carrier triple repeat 1
Pkig	1.4298918	protein kinase inhibitor, gamma
Vars	1.4286813	valyl-tRNA synthetase
Sco2	1.4243373	SCO cytochrome oxidase deficient homolog 2 (yeast)
Hexdc	1.4233568	hexosaminidase (glycosyl hydrolase family 20, catalytic domain) containing
Myo6	1.4212536	myosin VI
Pon2	1.4211719	paraoxonase 2
Nit1	1.4199938	nitrilase 1
Prrt3	1.4157628	proline-rich transmembrane protein 3
Coro7	1.4122847	coronin 7
Sirt2	1.4120563	sirtuin 2 (silent mating type information regulation 2, homolog) 2 (S. cerevisiae)
Tnfrsf21	1.4036827	tumor necrosis factor receptor superfamily, member 21
Fbxl20	1.4023672	F-box and leucine-rich repeat protein 20
Fads3	1.3984222	fatty acid desaturase 3
Tec	1.3979338	tec protein tyrosine kinase
Fez2	1.3894987	fasciculation and elongation protein zeta 2 (zygin II)
Ccl28	1.3889949	chemokine (C-C motif) ligand 28
Slc20a1	1.3881154	solute carrier family 20, member 1
S100a16	1.385382	S100 calcium binding protein A16
S100a16	1.383751	S100 calcium binding protein A16
Dach2	1.3826895	dachshund 2 (Drosophila)
Slc9a3r1	1.382136	solute carrier family 9 (sodium/hydrogen exchanger), member 3 regulator 1
Timp2	1.3813541	tissue inhibitor of metalloproteinase 2
Fgfrl1 /// LOC100046239	1.3806201	fibroblast growth factor receptor-like 1 /// similar to fibroblast growth factor receptor 5 beta
Zfp758	1.3784078	zinc finger protein 758
Trappc5	1.3782985	trafficking protein particle complex 5
Klf3 /// LOC100046855	1.376655	Kruppel-like factor 3 (basic) /// similar to BKLF
Gpr180	1.3754125	G protein-coupled receptor 180
Slc35a5	1.3729981	solute carrier family 35, member A5
Trim62	1.3727711	tripartite motif-containing 62
Slc25a22	1.3727641	solute carrier family 25 (mitochondrial carrier, glutamate), member 22

Pdk3	1.3726146	pyruvate dehydrogenase kinase, isoenzyme 3
Slc5a5	1.3724186	solute carrier family 5 (sodium iodide symporter), member 5
Cd276	1.3719692	CD276 antigen
Esd	1.3716016	esterase D/formylglutathione hydrolase
Uck2	1.3676988	uridine-cytidine kinase 2
Dbi	1.367662	diazepam binding inhibitor
Gsto1	1.3663433	glutathione S-transferase omega 1
Cyb5d2	1.3630785	cytochrome b5 domain containing 2

Table A2.S2. Significant pathways (P<0.01) as identified by Gene Set Enrichment Analysis

Pathway	P_value	q_value	intersectional_gene_list
CHESLER_BRAIN_QTL_CIS	1.20E-08	5.01E-05	Aldh7a1, Slc15a2, Prdx2, Pdxdc1, Myo7a, Glo1, Ocel1, Abhd14a, Rgs16, Kcnj9, Sorl1, Folh1
COATES_MACROPHAGE_M1_VS_M2_UP	2.37E-06	0.004946	Gja1, Pldn, Abhd1, Kcnj10, Gatm, Glo1, Ocel1, Sfi1, Haus2, Lyplal1
CADWELL_ATG16L1_TARGETS_DN	2.79E-05	0.030876	Sfrp1, Slc15a2, Hist2h2bb, Skiv2l2, Haus2, Adi1, Arsk, Spata5l1
CHESLER_BRAIN_HIGHEST_GENETIC_ VARIANCE	2.96E-05	0.030876	Aldh7a1, Prdx2, Pdxdc1, Ocel1, Kcnj9, Folh1
CADWELL_ATG16L1_TARGETS_UP	7.23E-05	0.051063	Lpl, Pldn, Tmem87a, Wdfy1, Kctd14, Fmn2, Rbm45, Exd1, Arsk
COATES_MACROPHAGE_M1_VS_M2_DN	7.34E-05	0.051063	Prdx2, Pdxdc1, Rpgrip1, Cript, Gprc5b, Ang, Tulp4, Arsk
BREDEMEYER_RAG_SIGNALING_NOT_VIA _ATM_UP	0.0001674	0.0974613	Lsm12, Smg1, Iqcf1, Mpp7, Rnf157, Slc20a1, Ccdc25
RAS_GTPASE_ACTIVATOR_ACTIVITY	0.0002022	0.0974613	Arhgap4, Cdc42ep2, Gmip, Dock4, Rab3gap1
BYSTRYKH_HEMATOPOIESIS_STEM_CELL _ AND_BRAIN_QTL_CIS	0.0002102	0.0974613	Prdx2, Pdxdc1, Myo7a, Med1, Glo1, Ocel1, Kcnj9
RHO_GTPASE_ACTIVATOR_ACTIVITY	0.0003108	0.1296617	Arhgap4, Cdc42ep2, Gmip, Dock4
BYSTRYKH_HEMATOPOIESIS_STEM_CELL _ QTL_CIS	0.0008465	0.2990131	Prdx2, Pdxdc1, Med1, Dbi, Gatm, Glo1, Ocel1, Pon2, F2r
TURASHVILI_BREAST_DUCTAL_CARCINO MA_VS_DUCTAL_NORMAL_DN	0.0008601	0.2990131	Cryab, Sfrp1, Chl1, Rrad, Gatm, Trf, Atp1a2, Atp10d, Ints10, Ccl28, Mamdc2
AMUNDSON_RESPONSE_TO_ARSENITE	0.0010995	0.3058679	Eif2s2, Gucy1a3, Dnajb5, Klf12, Tle4, Chd2, Atp2c1, Cherp, Atp10d, Tulp4, Serpinh1
XU_CREBBP_TARGETS_DN	0.0011036	0.3058679	Per2, Epha4, Ocel1, Ercc2, Ccr6
TURASHVILI_BREAST_DUCTAL_CARCINO MA_VS_LOBULAR_NORMAL_DN	0.0012414	0.3058679	Cryab, Sfrp1, Zbtb16, Atp1a2, Atp10d, Mamdc2
GTPASE_ACTIVATOR_ACTIVITY	0.0012414	0.3058679	Arhgap4, Rgs16, Cdc42ep2, Gmip, Dock4, Rab3gap1
VARELA_ZMPSTE24_TARGETS_UP	0.0012487	0.3058679	Zbtb16, Rgs16, Mcart1, Pi4k2a, Slc20a1
BROWNE_HCMV_INFECTION_20HR_DN	0.0014108	0.3058679	Gsto1, Nr1d2, Fst, Nqo1, Pkig, F2r, Serpinh1, Svil
ASTON_MAJOR_DEPRESSIVE_DISORDER_ DN	0.0014524	0.3058679	Cryab, Rbm8a, Atm, Cdc42ep1, Tmem87a, Gprc5b, Trf, Capn3, Pllp, Folh1
REACTOME_GAP_JUNCTION_TRAFFICKIN G	0.0015839	0.3058679	Gja1, Myo6, Gja5, Gjb1
RAS_GTPASE_BINDING	0.0015839	0.3058679	Ipo9, Cdc42ep2, Dock4, Rab3gap1
LIN_NPAS4_TARGETS_UP	0.0016129	0.3058679	Lpl, Mpp3, Abcf1, Usf1, Cdc42ep2, Mllt3, Prkaa2, Atp2c1, Pnma2
YAO_TEMPORAL_RESPONSE_TO_ PROGESTERONE_CLUSTER_8	0.0021936	0.3813193	Usp14, Mthfd2, Zbtb16, Fst, Pdk3
HYDROLASE_ACTIVITY__ACTING_ON_CA RBON_NITROGEN__BUT_NOT_PEPTIDE__ BONDS	0.0021936	0.3813193	Nit1, Arg2, Mthfd2, Sirt2, Dctd
NGUYEN_NOTCH1_TARGETS_DN	0.0024829	0.3988758	Mthfd2, Ppp2r1b, Epha4, Fndc3a, Slc20a1, Serpinh1
THUM_SYSTOLIC_HEART_FAILURE_DN	0.0025606	0.3988758	Per2, Hey2, Mpp3, Slc25a36, Klf12, Zfp295, Cdc42ep2, Spag9, Stk35, Limch1, Tulp4
RODWELL_AGING_KIDNEY_NO_BLOOD_D N	0.0025814	0.3988758	Lpl, Mut, Pclo, Slc25a36, Ppp2r1b, Fbxo3, Prkaa2, Dbt

GAUSSMANN_MLL_AF4_FUSION_TARGETS_F_DN	0.0028524	0.4153637	Lpl, Tmem47, Rragd, Nnmt
HOSHIDA_LIVER_CANCER_SURVIVAL_DN	0.0028872	0.4153637	Usp14, Slc37a4, Tdo2, Ar, Ggcx, Dock4, Atp2c1, Gjb1
UEDA_PERIFERAL_CLOCK	0.0038006	0.4766850	Mesdc2, Nr1d2, Slc37a4, Per2, Glo1, Tsc22d1, F2r, Slc9a3r1, Lpin2
SCIBETTA_KDM5B_TARGETS_DN	0.0038998	0.4766850	Tubb5, Psip1, Ivns1abp, Epb4.1l1, Smc5, Limch1
WALLACE_PROSTATE_CANCER_RACE_DN	0.0038998	0.4766850	Pclo, Prkg2, Nqo1, Limch1, Adi1, Rab3gap1
FLOTHO_PEDIATRIC_ALL_THERAPY_RESPONSE_UP	0.0039126	0.4766850	Rps6, Sypl, Tmem87a, Rps9, Rpl17
SCHLOSSER_SERUM_RESPONSE_UP	0.0039764	0.4766850	Stxbp2, Map3k7, Klf12, Kcnb1, Ocel1, Tradd, Slc9a3r1, Ercc2
IWANAGA_CARCINOGENESIS_BY_KRAS_UP	0.0041643	0.4766850	Gja1, Slc15a2, Arg2, Adcy7, Rad23a, Ldhd, Supt7l, Cldn12, Sla2
POTTI_CYTOXAN_SENSITIVITY	0.0041671	0.4766850	Esd, Ggcx, Samd4, Rps9
REACTOME_GAP_JUNCTION_ASSEMBLY	0.0044689	0.4766850	Gja1, Gja5, Gjb1
RODWELL_AGING_KIDNEY_DN	0.0046427	0.4766850	Lpl, Mut, Pclo, Slc25a36, Fbxo3, Prkaa2, Dbt
BERENJENO_TRANSFORMED_BY_RHOA_FOREVER_DN	0.0046829	0.4766850	Gja1, Mtm1, Lrrfip1, F2r
I_KAPPAB_KINASE_NF_KAPPAB_CASCADE	0.0049137	0.4766850	Gja1, Map3k7, Tradd, Atp2c1, F2r, Slc20a1, Rpl17
BHATTACHARYA_EMBRYONIC_STEM_CELL	0.0051300	0.4766850	Gja1, Tubb5, Psip1, Mthfd2, Cachd1, Serpinh1
POSITIVE_REGULATION_OF_I_KAPPAB_KINASE_NF_KAPPAB_CASCADE	0.0051300	0.4766850	Gja1, Tradd, Atp2c1, F2r, Slc20a1, Rpl17
SMALL_GTPASE_BINDING	0.0052399	0.4766850	Ipo9, Cdc42ep2, Dock4, Rab3gap1
INOSITOL_OR_PHOSPHATIDYLINOSITOL_KINASE_ACTIVITY	0.0053410	0.4766850	Atm, Smg1, Pi4k2a
LE_EGR2_TARGETS_DN	0.0057983	0.4766850	Lpl, Zbtb16, Sirt2, Tmem40, Limch1, Efhd1, Gjb1
RICKMAN_TUMOR_DIFFERENTIATED_MODERATELY_VS_POORLY_UP	0.0058395	0.4766850	Ramp1, Eif2s2, Ipo9, Pop4
RICKMAN_TUMOR_DIFFERENTIATED_MODERATELY_VS_POORLY_DN	0.0058395	0.4766850	Ramp1, Eif2s2, Ipo9, Pop4
COLIN_PILOCYTIC_ASTROCYTOMA_VS_GLIOBLASTOMA_UP	0.0058395	0.4766850	Tnfrsf21, Gprc5b, Trf, Atp1a2
GTPASE_BINDING	0.0058395	0.4766850	Ipo9, Cdc42ep2, Dock4, Rab3gap1
YAGI_AML_FAB_MARKERS	0.0058853	0.4766850	Rab27b, Zbtb16, Timp2, Gp1ba, Ifi30, Pkig, Sorl1, F2r, Fam20b, Serpinh1
KLEIN_PRIMARY_EFFUSION_LYMPHOMA_DN	0.0059473	0.4766850	Fads3, Dbi, Sypl, Gatm, Pkig
STEARMAN_LUNG_CANCER_EARLY_VS_LATE_DN	0.0059473	0.4766850	Lpl, Myo7a, Gja5, Usf1, Mpeg1
NELSON_RESPONSE_TO_ANDROGEN_UP	0.0062236	0.4766850	Lman1, Gucy1a3, Dbi, Tsc22d1, Zbtb10, Inpp4b
BREDEMEYER_RAG_SIGNALING_NOT_VIA_ATM_DN	0.0064292	0.4766850	Slc15a2, Pdxdc1, Abhd14a, Jakmip1, Pi4k2a
LINDGREN_BLADDER_CANCER_CLUSTER_1_UP	0.0064508	0.4766850	Tmem19, Gsto1, Esd, Map3k7, Mllt3, Tm2d2, Ints10
LIU_COMMON_CANCER_GENES	0.0064831	0.4766850	Prdx2, Haus2, Lrrfip1, Dbt
FOURNIER_ACINAR_DEVELOPMENT_EARLY_DN	0.0065127	0.4766850	Amigo2, Slc20a1
REGULATION_OF_I_KAPPAB_KINASE_NF_KAPPAB_CASCADE	0.0070410	0.5064699	Gja1, Tradd, Atp2c1, F2r, Slc20a1, Rpl17
TAKEDA_TARGETS_OF_NUP98_HOXA9_FUSION_10D_UP	0.0078299	0.5516386	Rab27b, Il15, Fbxl20, Arg2, Fcer2a, Gatm, Inpp4b, Ifit3, Ccr6
CELL_CELL_ADHESION	0.0079334	0.5516386	Vangl2, Bmp1, Atp2c1, Cldn12, Amigo2, Cercam
GRAHAM_CML_DIVIDING_VS_NORMAL_QUIESCENT_DN	0.0084089	0.5628683	Cxcl13, Gucy1a3, Sorl1, Mllt3, Limch1, Svil
SMALL_GTPASE_REGULATOR_ACTIVITY	0.0086312	0.5628683	Arhgap4, Cdc42ep2, Gmip, Dock4, Rab3gap1
PROTEIN_N_TERMINUS_BINDING	0.0086910	0.5628683	Atm, Zwint, Sla2, Ercc2
TAKEDA_TARGETS_OF_NUP98_HOXA9_FUSION_16D_DN	0.0087372	0.5628683	Pi4k2b, Prdx2, Capn3, Dock4, Lrrfip1, Pyroxd2, Zcchc11
GARCIA_TARGETS_OF_FLI1_AND_DAX1_DN	0.0088085	0.5628683	Pldn, Slc7a11, Zwint, Ppcdc, Tprkb, Rg9mtd2, Haus2, Amdhd2
REACTOME_G2_M_TRANSITION	0.0089044	0.5628683	Actr1a, Tubb5, Wee1, Sfi1, Cep192, Haus2
GINESTIER_BREAST_CANCER_ZNF217_AMPLIFIED_UP	0.0092540	0.5758241	Itch, Pldn, Sp1, Slc25a36, F2r

KEGG_PYRUVATE_METABOLISM	0.0095235	0.5758241	Aldh7a1, Glo1, Ldhd, Me2
TRANSLATION_REGULATOR_ACTIVITY	0.0095235	0.5758241	Eif2s2, Gspt2, Abcf1, Samd4

BIBLIOGRAPHY

Abarca, C., U. Albrecht, et al. (2002). "Cocaine sensitization and reward are under the influence of circadian genes and rhythm." Proc Natl Acad Sci U S A **99**(13): 9026-9030.

Abe, M., E. D. Herzog, et al. (2000). "Lithium lengthens the circadian period of individual suprachiasmatic nucleus neurons." NeuroReport **11**(14): 3261-3264.

ACNP (2008). Neuropsychopharmacology- 5th Generation of Progress.

Akhisaroglu, M., M. Kurtuncu, et al. (2005). "Diurnal rhythms in quinpirole-induced locomotor behaviors and striatal D2/D3 receptor levels in mice." Pharmacology Biochemistry and Behavior **80**(3): 371-377.

Albanese, A., Altavista, MC., and Rossi, P. (1986). "Organization of central nervous system dopaminergic pathways." Journal of Neural Transm Suppl **22**: 3-17.

Anstrom, K. K. and D. J. Woodward (2005). "Restraint Increases Dopaminergic Burst Firing in Awake Rats." Neuropsychopharmacology **30**(10): 1832-1840.

APA (2000). Diagnostic and statistical manual of mental disorders.

Aschoff, J. (1965). "Circadian Rhythms in Man." Science **148**(3676): 1427-1432.

Aston, C., L. Jiang, et al. (2005). "Transcriptional profiling reveals evidence for signaling and oligodendroglial abnormalities in the temporal cortex from patients with major depressive disorder." Molecular psychiatry **10**(3): 309-322.

Atkinson, M. K., D.F. Wolf, S.R. (1975). "Autorhythmometry in manic-depressives." Chronobiologia **2**: 10.

Aumann, T. D., K. Egan, et al. (2011). "Neuronal activity regulates expression of tyrosine hydroxylase in adult mouse substantia nigra pars compacta neurons." Journal of Neurochemistry **116**(4): 646-658.

Bae, K., X. Jin, et al. (2001). "Differential functions of mPer1, mPer2, and mPer3 in the SCN circadian clock." Neuron **30**(2): 525-536.

Baldessarini, R.J., Salvatore, P., Khalsa, H.M., and Tohen, M. (2010) “Dissimilar morbidity following initial mania versus mixed-states in type-I bipolar disorder.” Journal of Affective Disorders **126**(1-2): 299-302.

Barchas, J. D. and Altemus, M. (1999). Biochemical Hypotheses of Mood and Anxiety Disorders. Siegel, G.J., Agrinoff, B.W., Albers, R.W., Fisher, S.K., and Uhler, M.D. (Eds.) *Basic Neurochemistry (6th ed)*. Philadelphia: Lippincnott-Rave.

Barnard, A. R. and P. M. Nolan (2008). "When Clocks Go Bad: Neurobehavioural Consequences of Disrupted Circadian Timing." PLoS Genet **4**(5): e1000040.

Barrot, M., J. D. Olivier, et al. (2002). "CREB activity in the nucleus accumbens shell controls gating of behavioral responses to emotional stimuli." Proc Natl Acad Sci U S A **99**(17): 11435-11440.

Barzilai, A. and E. Melamed (2003). "Molecular mechanisms of selective dopaminergic neuronal death in Parkinson's disease." Trends in Molecular Medicine **9**(3): 126-132.

Basner, R. C. (2005). "Shift-Work Sleep Disorder — The Glass Is More Than Half Empty." New England Journal of Medicine **353**(5): 519-521.

Beaulieu, J.-M. and R. R. Gainetdinov (2011). "The Physiology, Signaling, and Pharmacology of Dopamine Receptors." Pharmacological Reviews **63**(1): 182-217.

Beaulieu, J.-M., T. D. Sotnikova, et al. (2005). "An Akt/β-Arrestin 2/PP2A Signaling Complex Mediates Dopaminergic Neurotransmission and Behavior." Cell **122**(2): 261-273.

Bechtold, D. A., J. E. Gibbs, et al. (2010). "Circadian dysfunction in disease." Trends in Pharmacological Sciences **31**(5): 191-198.

Belzung, C. and G. Griebel (2001). "Measuring normal and pathological anxiety-like behaviour in mice: a review." Behav Brain Res **125**(1-2): 141-149.

Benedetti, F., A. Bernasconi, et al. (2004). "A single nucleotide polymorphism in glycogen synthase kinase 3-beta promoter gene influences onset of illness in patients affected by bipolar disorder." Neurosci Lett **355**(1-2): 37-40.

Benedetti, F., S. Dallaspezia, et al. (2007). "Actimetric evidence that CLOCK 3111 T/C SNP influences sleep and activity patterns in patients affected by bipolar depression." Am J Med Genet B Neuropsychiatr Genet **144B**(5): 631-635.

Berndt, A., O. Yizhar, et al. (2009). "Bi-stable neural state switches." Nat Neurosci **12**(2): 229-234.

Berton, O., C. A. McClung, et al. (2006). "Essential role of BDNF in the mesolimbic dopamine pathway in social defeat stress." Science **311**(5762): 864-868.

Binder, E. B., B. Kinkead, et al. (2001). "Neurotensin and Dopamine Interactions." Pharmacological Reviews **53**(4): 453-486.

Bortolato, M., K. Chen, et al. (2008). "Monoamine oxidase inactivation: From pathophysiology to therapeutics." Advanced Drug Delivery Reviews **60**(13–14): 1527-1533.

Bressan, R. A. and J. A. Crippa (2005). "The role of dopamine in reward and pleasure behaviour – review of data from preclinical research." Acta Psychiatrica Scandinavica **111**: 14-21.

Cardone, L., J. Hirayama, et al. (2005). "Circadian Clock Control by SUMOylation of BMAL1." Science **309**(5739): 1390-1394.

Cassidy, F. and B. J. Carroll (2002). "Seasonal variation of mixed and pure episodes of bipolar disorder." Journal of Affective Disorders **68**(1): 25-31.

Castañeda, T. R., B. M. de Prado, et al. (2004). "Circadian rhythms of dopamine, glutamate and GABA in the striatum and nucleus accumbens of the awake rat: modulation by light." Journal of Pineal Research **36**(3): 177-185.

Chico, L. K., L. J. Van Eldik, et al. (2009). "Targeting protein kinases in central nervous system disorders." Nat Rev Drug Discov **8**(11): 892-909.
Chu, H.-y. and X. Zhen (2010). "Hyperpolarization-activated, cyclic nucleotide-gated (HCN) channels in the regulation of midbrain dopamine systems." Acta Pharmacol Sin **31**(9): 1036-1043.
Cools, R. (2008). "Role of Dopamine in the Motivational and Cognitive Control of Behavior." The Neuroscientist **14**(4): 381-395.
Coque, L., S. Mukherjee, et al. (2011). "Specific Role of VTA Dopamine Neuronal Firing Rates and Morphology in the Reversal of Anxiety-Related, but not Depression-Related Behavior in the Clock[Delta]19 Mouse Model of Mania." Neuropsychopharmacology.
Cousins, D. A., K. Butts, et al. (2009). "The role of dopamine in bipolar disorder." Bipolar Disorders **11**(8): 787-806.
Dahlstrom, A. a. F., K. (1964). "Localization of monoamines in the lower brain stem." Experientia **20**(7): 398-399.
DeBruyne, J. P., D. R. Weaver, et al. (2007). "CLOCK and NPAS2 have overlapping roles in the suprachiasmatic circadian clock." Nat Neurosci **10**(5): 543-545.
DeCoteau, W. E., C. Thorn, et al. (2007). "Learning-related coordination of striatal and hippocampal theta rhythms during acquisition of a procedural maze task." Proceedings of the National Academy of Sciences **104**(13): 5644-5649.
Desai, R. I., P. Terry, et al. (2005). "A comparison of the locomotor stimulant effects of D1-like receptor agonists in mice." Pharmacology Biochemistry and Behavior **81**(4): 843-848.
Diester, I., M. T. Kaufman, et al. (2011). "An optogenetic toolbox designed for primates." Nat Neurosci **14**(3): 387-397.
Dong, L., A. Bilbao, et al. (2011). "Effects of the circadian rhythm gene period 1 (per1) on psychosocial stress-induced alcohol drinking." The American journal of psychiatry **168**(10): 1090-1098.
Dracheva, S., M. Xu, et al. (1999). "Paradoxical Locomotor Behavior of Dopamine D1 Receptor Transgenic Mice." Experimental Neurology **157**(1): 169-179.
Drago, J., C. R. Gerfen, et al. (1994). "Altered striatal function in a mutant mouse lacking D1A dopamine receptors." Proceedings of the National Academy of Sciences **91**(26): 12564-12568.
Dunkley, P. R., L. Bobrovskaya, et al. (2004). "Tyrosine hydroxylase phosphorylation: regulation and consequences." Journal of Neurochemistry **91**(5): 1025-1043.
Dzirasa, K., L. Coque, et al. (2010). "Lithium ameliorates nucleus accumbens phase-signaling dysfunction in a genetic mouse model of mania." The Journal of neuroscience : the official journal of the Society for Neuroscience **30**(48): 16314-16323.
Dzirasa, K., D. L. McGarity, et al. (2011). "Impaired limbic gamma oscillatory synchrony during anxiety-related behavior in a genetic mouse model of

bipolar mania." The Journal of neuroscience : the official journal of the Society for Neuroscience **31**(17): 6449-6456.
Dzirasa, K., S. Ribeiro, et al. (2006). "Dopaminergic Control of Sleep-Wake States." J Neurosci **26**(41): 10577-10589.
Eide, E. J., E. L. Vielhaber, et al. (2002). "The Circadian Regulatory Proteins BMAL1 and Cryptochromes Are Substrates of Casein Kinase Iε." Journal of Biological Chemistry **277**(19): 17248-17254.
Engelmann, M., K. Ebner, et al. (1998). "Swim stress triggers the release of vasopressin within the suprachiasmatic nucleus of male rats." Brain Res **792**(2): 343-347.
Enwright Iii, J. F., M. Wald, et al. (2010). "[Delta]FosB indirectly regulates Cck promoter activity." Brain Research **1329**: 10-20.
Falcon, E. and C. A. McClung (2008). "A role for the circadian genes in drug addiction." Neuropharmacology.
Fauchey, V., M. Jaber, et al. (2000). "Differential regulation of the dopamine D1, D2 and D3 receptor gene expression and changes in the phenotype of the striatal neurons in mice lacking the dopamine transporter." European Journal of Neuroscience **12**(1): 19-26.
Fenn, H. H., M. S. Bauer, et al. (2005). "Medical comorbidity and health-related quality of life in bipolar disorder across the adult age span." Journal of Affective Disorders **86**(1): 47-60.
Ferreira, M. A. R., M. C. O'Donovan, et al. (2008). "Collaborative genome-wide association analysis supports a role for ANK3 and CACNA1C in bipolar disorder." Nat Genet 40(9): 1056-1058.
Ferrie, L., A. H. Young, et al. (2005). "Effect of chronic lithium and withdrawal from chronic lithium on presynaptic dopamine function in the rat." Journal of Psychopharmacology **19**(3): 229-234.
Feuerstein, T. J. (2008). Presynaptic Receptors for Dopamine, Histamine, and Serotonin Pharmacology of Neurotransmitter Release. T. C. Südhof and K. Starke, Springer Berlin Heidelberg. **184:** 289-338.
Flames, N. and O. Hobert (2011). "Transcriptional Control of the Terminal Fate of Monoaminergic Neurons." Annual Review of Neuroscience **34**(1): 153-184.
Floresco, S. B., A. R. West, et al. (2003). "Afferent modulation of dopamine neuron firing differentially regulates tonic and phasic dopamine transmission." Nat Neurosci **6**(9): 968-973.
Frank, E., H. A. Swartz, et al. (2000). "Interpersonal and social rhythm therapy: managing the chaos of bipolar disorder." Biol Psychiatry **48**(6): 593-604.
Fu, L. and C. C. Lee (2003). "The circadian clock: pacemaker and tumour suppressor." Nature reviews. Cancer **3**(5): 350-361.
Fu, L., H. Pelicano, et al. (2002). "The Circadian Gene Period2 Plays an Important Role in Tumor Suppression and DNA Damage Response In Vivo." Cell **111**(1): 41-50.
Gekakis, N., D. Staknis, et al. (1998). "Role of the CLOCK Protein in the Mammalian Circadian Mechanism." Science **280**(5369): 1564-1569.

Gerfen, C. R., T. M. Engber, et al. (1990). "D1 and D2 dopamine receptor-regulated gene expression of striatonigral and striatopallidal neurons." Science **250**(4986): 1429-1432.

Ghisi, V., A. J. Ramsey, et al. (2009). "Reduced D2-mediated signaling activity and trans-synaptic upregulation of D1 and D2 dopamine receptors in mice overexpressing the dopamine transporter." Cellular Signalling **21**(1): 87-94.

Goldberg, M. S., S. M. Fleming, et al. (2003). "Parkin-deficient Mice Exhibit Nigrostriatal Deficits but Not Loss of Dopaminergic Neurons." Journal of Biological Chemistry **278**(44): 43628-43635.

Gouin, J. P., J. Connors, et al. (2010). "Altered expression of circadian rhythm genes among individuals with a history of depression." Journal of affective disorders **126**(1-2): 161-166.

Grace, A. A. and B. S. Bunney (1983). "Intracellular and extracellular electrophysiology of nigral dopaminergic neurons--3. Evidence for electrotonic coupling." Neuroscience **10**(2): 333-348.

Grace, A. A., S. B. Floresco, et al. (2007). "Regulation of firing of dopaminergic neurons and control of goal-directed behaviors." Trends in Neurosciences **30**(5): 220-227.

Greene, J. G. (2006). "Gene expression profiles of brain dopamine neurons and relevance to neuropsychiatric disease." The Journal of Physiology **575**(2): 411-416.

Grimaldi, B., Y. Nakahata, et al. (2009). "Chromatin remodeling, metabolism and circadian clocks: The interplay of CLOCK and SIRT1." The International Journal of Biochemistry & Cell Biology **41**(1): 81-86.

Halbout, B., S. Perreau-Lenz, et al. (2011). "Per1Brdm1 mice self-administer cocaine and reinstate cocaine-seeking behaviour following extinction." Behavioural pharmacology **22**(1): 76-80.

Hamada, M., H. Higashi, et al. (2004). "Differential regulation of dopamine D1 and D2 signaling by nicotine in neostriatal neurons." Journal of Neurochemistry **90**(5): 1094-1103.

Hampp, G., J. A. Ripperger, et al. (2008). "Regulation of Monoamine Oxidase A by Circadian-Clock Components Implies Clock Influence on Mood." Current Biology **18**(9): 678-683.

Harvey, A. G. (2011). "Sleep and Circadian Functioning: Critical Mechanisms in the Mood Disorders?" Annual Review of Clinical Psychology **7**(1): 297-319.

Hasbi, A., B. O'Dowd, et al. (2011). "Dopamine D1-D2 receptor heteromer signaling pathway in the brain: emerging physiological relevance." Molecular Brain **4**(1): 26.

Heikkinen, A. E., T. P. Moykkynen, et al. (2008). "Long-lasting Modulation of Glutamatergic Transmission in VTA Dopamine Neurons after a Single Dose of Benzodiazepine Agonists." Neuropsychopharmacology **34**(2): 290-298.

Herve, D. (2011). "Identification of a specific assembly of the G protein Golf as a critical and regulated module of dopamine and adenosine-activated cAMP pathways in the striatum." Frontiers in Neuroanatomy **5**.

Hirota, T., W. G. Lewis, et al. (2008). "A chemical biology approach reveals period shortening of the mammalian circadian clock by specific inhibition of GSK-3β." Proceedings of the National Academy of Sciences **105**(52): 20746-20751.

Holtz, P. (1959). "ROLE OF L-DOPA DECARBOXYLASE IN THE BIOSYNTHESIS OF CATECHOLAMINES IN NERVOUS TISSUE AND THE ADRENAL MEDULLA." Pharmacological Reviews **11**(2): 317-329.

Hood, S., P. Cassidy, et al. (2010). "Endogenous Dopamine Regulates the Rhythm of Expression of the Clock Protein PER2 in the Rat Dorsal Striatum via Daily Activation of D2 Dopamine Receptors." The Journal of Neuroscience **30**(42): 14046-14058.

Horst, G. T. J. v. d., M. Muijtjens, et al. (1999). "Mammalian Cry1 and Cry2 are essential for maintenance of circadian rhythms." Nature **398**(6728): 627-630.

Huxley, N. and R. J. Baldessarini (2007). "Disability and its treatment in bipolar disorder patients." Bipolar Disorders **9**(1-2): 183-196.

Iijima, M., T. Nikaido, et al. (2002). "Methamphetamine-induced, suprachiasmatic nucleus-independent circadian rhythms of activity and mPer gene expression in the striatum of the mouse." Eur J Neurosci **16**(5): 921-929.

Iitaka, C., K. Miyazaki, et al. (2005). "A Role for Glycogen Synthase Kinase-3β in the Mammalian Circadian Clock." Journal of Biological Chemistry **280**(33): 29397-29402.

Imbesi, M., S. Yildiz, et al. (2009). "Dopamine receptor-mediated regulation of neuronal “clock” gene expression." Neuroscience **158**(2): 537-544.

Jacobs, F. M. J., S. van Erp, et al. (2009). "Pitx3 potentiates Nurr1 in dopamine neuron terminal differentiation through release of SMRT-mediated repression." Development **136**(4): 531-540.

Jones, B. E. (1991). "Paradoxical sleep and its chemical/structural substrates in the brain." Neuroscience **40**(3): 637-656.

Jones, S. R., R. R. Gainetdinov, et al. (1999). "Loss of autoreceptor functions in mice lacking the dopamine transporter." Nat Neurosci **2**(7): 649-655.

Katada, S. and P. Sassone-Corsi (2010). "The histone methyltransferase MLL1 permits the oscillation of circadian gene expression." Nat Struct Mol Biol **17**(12): 1414-1421.

Keller, M. B. (2006). "Prevalence and impact of comorbid anxiety and bipolar disorder." J Clin Psychiatry **67 Suppl 1**: 5-7.

Kerman, I. A., S. M. Clinton, et al. (2012). "Inborn differences in environmental reactivity predict divergent diurnal behavioral, endocrine, and gene expression rhythms." Psychoneuroendocrinology **37**(2): 256-269.

Kessler, R. C., P. Berglund, et al. (2005). "Lifetime Prevalence and Age-of-Onset Distributions of DSM-IV Disorders in the National Comorbidity Survey Replication." Arch Gen Psychiatry **62**(6): 593-602.

Kim, M. S., M. K. Hur, et al. (2002). "Regulation of Pituitary Adenylate Cyclase-activating Polypeptide Gene Transcription by TTF-1, a Homeodomain-containing Transcription Factor." Journal of Biological Chemistry **277**(39): 36863-36871.

Kim, T. E., M. J. Park, et al. (2003). "Cloning and cell type-specific regulation of the human tyrosine hydroxylase gene promoter." Biochemical and Biophysical Research Communications **312**(4): 1123-1131.

King, D. P., M. H. Vitaterna, et al. (1997). "The Mouse Clock Mutation Behaves as an Antimorph and Maps Within the W(19H) Deletion, Distal of Kit." Genetics **146**(3): 1049-1060.

King, D. P., Y. Zhao, et al. (1997). "Positional cloning of the mouse circadian clock gene." Cell **89**(4): 641-653.

Kishi, T., T. Kitajima, et al. (2008). "Association analysis of nuclear receptor Rev-erb alpha gene (NR1D1) with mood disorders in the Japanese population." Neurosci Res **62**(4): 211-215.

Ko, C. H. and J. S. Takahashi (2006). "Molecular components of the mammalian circadian clock." Hum Mol Genet **15 Spec No 2**: R271-277.

Kondratov, R. V., M. V. Chernov, et al. (2003). "BMAL1-dependent circadian oscillation of nuclear CLOCK: posttranslational events induced by dimerization of transcriptional activators of the mammalian clock system." Genes & Development **17**(15): 1921-1932.

Kondratov, R. V., R. K. Shamanna, et al. (2006). "Dual role of the CLOCK/BMAL1 circadian complex in transcriptional regulation." The FASEB Journal.

Koresh, O., N. Kozlovsky, et al. (2011). "The long-term abnormalities in circadian expression of Period 1 and Period 2 genes in response to stress is normalized by agomelatine administered immediately after exposure." European neuropsychopharmacology : the journal of the European College of Neuropsychopharmacology.

Kripke, D. F., C. M. Nievergelt, et al. (2009). "Circadian polymorphisms associated with affective disorders." J Circadian Rhythms **7**: 2.

Krishnan, K. R. R. (2005). "Psychiatric and Medical Comorbidities of Bipolar Disorder." Psychosomatic Medicine **67**(1): 1-8.

Krishnan, V., M.-H. Han, et al. (2007). "Molecular Adaptations Underlying Susceptibility and Resistance to Social Defeat in Brain Reward Regions." Cell **131**(2): 391-404.

Krishnan, V. and E. J. Nestler (2008). "The molecular neurobiology of depression." Nature **455**(7215): 894-902.

Kumer, S. C. and K. E. Vrana (1996). "Intricate Regulation of Tyrosine Hydroxylase Activity and Gene Expression." Journal of Neurochemistry **67**(2): 443-462.

Kummer, A. and A. L. Teixeira (2008). "Dopamine and bipolar disorder." Acta Psychiatrica Scandinavica **117**(5): 398-398.

Kurabayashi, N., T. Hirota, et al. (2010). "DYRK1A and Glycogen Synthase Kinase 3β, a Dual-Kinase Mechanism Directing Proteasomal Degradation

of CRY2 for Circadian Timekeeping." Molecular and Cellular Biology **30**(7): 1757-1768.
LaPlant, Q., S. Chakravarty, et al. (2009). "Role of nuclear factor kappaB in ovarian hormone-mediated stress hypersensitivity in female mice." Biol Psychiatry **65**(10): 874-880.
Lavebratt, C., L. K. Sjoholm, et al. (2010). "PER2 variantion is associated with depression vulnerability." American journal of medical genetics. Part B, Neuropsychiatric genetics : the official publication of the International Society of Psychiatric Genetics **153B**(2): 570-581.
Lavebratt, C., L. K. Sjöholm, et al. (2010). "<italic>CRY2</italic> Is Associated with Depression." PLoS ONE **5**(2): e9407.
Leahy, R. L. (2007). "Bipolar disorder: Causes, contexts, and treatments." Journal of Clinical Psychology **63**(5): 417-424.
Lee, S.-Y., S.-L. Chen, et al. (2011). "The COMT and DRD3 genes interacted in bipolar I but not bipolar II disorder." World Journal of Biological Psychiatry **12**(5): 385-391.
Lee, Y., R. Chen, et al. (2011). "Stoichiometric Relationship among Clock Proteins Determines Robustness of Circadian Rhythms." Journal of Biological Chemistry **286**(9): 7033-7042.
Lemos, D. R., L. Goodspeed, et al. (2007). "Evidence for Circadian Regulation of Activating Transcription Factor 5 But Not Tyrosine Hydroxylase by the Chromaffin Cell Clock." Endocrinology **148**(12): 5811-5821.
Lena, I., S. Parrot, et al. (2005). "Variations in extracellular levels of dopamine, noradrenaline, glutamate, and aspartate across the sleep-wake cycle in the medial prefrontal cortex and nucleus accumbens of freely moving rats." J. Neurosci. Res. **81**(6): 891-899.
Lenartowski, R. and A. Goc (2011). "Epigenetic, transcriptional and posttranscriptional regulation of the tyrosine hydroxylase gene." International Journal of Developmental Neuroscience **29**(8): 873-883.
Lewis-Tuffin, L. J., P. G. Quinn, et al. (2004). "Tyrosine hydroxylase transcription depends primarily on cAMP response element activity, regardless of the type of inducing stimulus." Molecular and Cellular Neuroscience **25**(3): 536-547.
Linkowski, P., M. Kerkhofs, et al. (1994). "The 24-Hour Profiles of Cortisol, Prolactin, and Growth Hormone Secretion in Mania." Arch Gen Psychiatry **51**(8): 616-624.
Linkowski, P., J. Mendlewicz, et al. (1987). "24-Hour Profiles of Adrenocorticotropin, Cortisol, and Growth Hormone in Major Depressive Illness: Effect of Antidepressant Treatment." Journal of Clinical Endocrinology & Metabolism **65**(1): 141-152.
Lowrey, P. L. and J. S. Takahashi (2004). "MAMMALIAN CIRCADIAN BIOLOGY: Elucidating Genome-Wide Levels of Temporal Organization." Annual Review of Genomics and Human Genetics **5**(1): 407-441.
Maloney, K. J., L. Mainville, et al. (2002). "c-Fos expression in dopaminergic and GABAergic neurons of the ventral mesencephalic tegmentum after

paradoxical sleep deprivation and recovery." European Journal of Neuroscience **15**(4): 774-778.
Martinat, C., J.-J. Bacci, et al. (2006). "Cooperative transcription activation by Nurr1 and Pitx3 induces embryonic stem cell maturation to the midbrain dopamine neuron phenotype." Proceedings of the National Academy of Sciences of the United States of America **103**(8): 2874-2879.
Masson, G., D. Mestre, et al. (1993). "Dopaminergic modulation of visual sensitivity in man." Fundamental & Clinical Pharmacology **7**(8): 449-463.
Maywood, E. S., E. Fraenkel, et al. (2010). "Disruption of Peripheral Circadian Timekeeping in a Mouse Model of Huntington's Disease and Its Restoration by Temporally Scheduled Feeding." The Journal of Neuroscience **30**(30): 10199-10204.
Maywood, E. S., J. A. O'Brien, et al. (2003). "Expression of mCLOCK and Other Circadian Clock-Relevant Proteins in the Mouse Suprachiasmatic Nuclei." Journal of Neuroendocrinology **15**(4): 329-334.
McCarthy, M. J., C. M. Nievergelt, et al. (2012). "A Survey of Genomic Studies Supports Association of Circadian Clock Genes with Bipolar Disorder Spectrum Illnesses and Lithium Response." PLoS ONE 7(2): e32091.
McClung, C. A. (2007). "Circadian genes, rhythms and the biology of mood disorders." Pharmacol Ther **114**(2): 222-232.
McClung, C. A. and E. J. Nestler (2003). "Regulation of gene expression and cocaine reward by CREB and DeltaFosB." Nat Neurosci **6**(11): 1208-1215.
McClung, C. A., K. Sidiropoulou, et al. (2005). "Regulation of dopaminergic transmission and cocaine reward by the Clock gene." Proc Natl Acad Sci U S A **102**(26): 9377-9381.
McGrath, C. L., S. J. Glatt, et al. (2009). "Evidence for genetic association of RORB with bipolar disorder." BMC Psychiatry **9**: 70.
McGuffin, P., F. Rijsdijk, et al. (2003). "The Heritability of Bipolar Affective Disorder and the Genetic Relationship to Unipolar Depression." Arch Gen Psychiatry **60**(5): 497-502.
McIntyre, R., Nguyn H.T., Soczynska, JK., Lourenco, MT., Woldeyohannes, HO., Konarski, JZ. (2008). "Medical and substance-related comorbidity in bipolar disorder: translational research and treatment opportunities." Dialogues in Clinical Neuroscience **10**(2): 203-213.
Michael, T. (2007). "Evolving applications of light therapy." Sleep Medicine Reviews **11**(6): 497-507.
Miller, B. H., E. L. McDearmon, et al. (2007). "Circadian and CLOCK-controlled regulation of the mouse transcriptome and cell proliferation." Proceedings of the National Academy of Sciences **104**(9): 3342-3347.
Miller, J. D., Farber, J., Gatz, P., Roffwarq, H., German, D.C., (1983). "Activity of mesencephalic dopamine and non-dopamine neurons across the stages of sleep and waking in the rat." Brain REsearch **273**(1): 133-141.

Mogenson, G. J., D. L. Jones, et al. (1980). "From motivation to action: Functional interface between the limbic system and the motor system." Progress in Neurobiology **14**(2–3): 69-97.

Monteggia, L. M., A. J. Eisch, et al. (2000). "Cloning and localization of the hyperpolarization-activated cyclic nucleotide-gated channel family in rat brain." Molecular Brain Research **81**(1–2): 129-139.

Monteleone, P., Martiadis, V., and Maj, M. (2010) “Circadian rhythms and treatment implications in depression.” Progress in Neuro-Psychopharmacology and Biological Psychiatry **35**(7): 1569-1574.

Mootha, V. K., C. M. Lindgren, et al. (2003). "PGC-1alpha-responsive genes involved in oxidative phosphorylation are coordinately downregulated in human diabetes." Nature genetics **34**(3): 267-273.

Moser, M., R. Penter, et al. (2006). "Why life oscillates--biological rhythms and health." Conf Proc IEEE Eng Med Biol Soc **1**: 424-428.

Mukherjee, S., L. Coque, et al. (2010). "Knockdown of Clock in the Ventral Tegmental Area Through RNA Interference Results in a Mixed State of Mania and Depression-Like Behavior." Biological Psychiatry **68**(6): 503-511.

Murphy, D. L., H. K. H. Brodie, et al. (1971). "Regular Induction of Hypomania by L-Dopa in [ldquo]Bipolar[rdquo] Manic-depressive Patients." Nature **229**(5280): 135-136.

Nagatsu, T., M. Levitt, et al. (1964). "Tyrosine Hydroxylase." Journal of Biological Chemistry **239**(9): 2910-2917.

Nakahata, Y., M. Yoshida, et al. (2008). "A direct repeat of E-box-like elements is required for cell-autonomous circadian rhythm of clock genes." BMC Molecular Biology 9(1): 1.

Nater, U. M., T. Whistler, et al. (2009). "Impact of acute psychosocial stress on peripheral blood gene expression pathways in healthy men." Biological psychology **82**(2): 125-132.

Naylor, E., B. M. Bergmann, et al. (2000). "The Circadian Clock Mutation Alters Sleep Homeostasis in the Mouse." The Journal of Neuroscience **20**(21): 8138-8143.

Nestler, E. J. and W. A. Carlezon, Jr. (2006). "The mesolimbic dopamine reward circuit in depression." Biol Psychiatry **59**(12): 1151-1159.

Nievergelt, C. M., D. F. Kripke, et al. (2006). "Suggestive evidence for association of the circadian genes PERIOD3 and ARNTL with bipolar disorder." Am J Med Genet B Neuropsychiatr Genet **141B**(3): 234-241.

Nikaido, T., M. Akiyama, et al. (2001). "Sensitized increase of period gene expression in the mouse caudate/putamen caused by repeated injection of methamphetamine." Mol Pharmacol **59**(4): 894-900.

Nikolaus, S., C. Antke, et al. (2009). "In vivo imaging of synaptic function in the central nervous system: II. Mental and affective disorders." Behavioural Brain Research **204**(1): 32-66.

Nishi, A., G. L. Snyder, et al. (1997). "Bidirectional Regulation of DARPP-32 Phosphorylation by Dopamine." The Journal of Neuroscience **17**(21): 8147-8155.

Ozaki, N., J. W. C. Duncan, et al. (1993). "Diurnal variations of serotonin and dopamine levels in discrete brain regions of Syrian hamsters and their modification by chronic clorgyline treatment." Brain Research **627**(1): 41-48.

Ozburn, A., Falcon, EF., Mukherjee, S., Arey, RN., Spencer, S., and McClung, CA. (2012). "Role of CLOCK in Ethanol-related Behaviors." Psychopharmacology **In press**.

Ozburn, A. R. L., Erin L.; Self, David W.; McClung, Colleen A. (Revision reviewed). "Clock(delta)19 mutants exhibit increased cocaine intake." Psychpharmacology.

Paladini, C. A., S. Robinson, et al. (2003). "Dopamine controls the firing pattern of dopamine neurons via a network feedback mechanism." Proceedings of the National Academy of Sciences **100**(5): 2866-2871.

Panda, S., M. P. Antoch, et al. (2002). "Coordinated Transcription of Key Pathways in the Mouse by the Circadian Clock." Cell **109**(3): 307-320.

Partonen, T., J. Treutlein, et al. (2007). "Three circadian clock genes Per2, Arntl, and Npas2 contribute to winter depression." Annals of medicine **39**(3): 229-238.

Peirson, S. N., J. N. Butler, et al. (2006). "Comparison of clock gene expression in SCN, retina, heart, and liver of mice." Biochem Biophys Res Commun **351**(4): 800-807.

Pendergast, J. S., K. D. Niswender, et al. (2012). "Tissue-specific function of period3 in circadian rhythmicity." PloS one **7**(1): e30254.

Pignatelli, A., K. Kobayashi, et al. (2005). "Functional properties of dopaminergic neurones in the mouse olfactory bulb." The Journal of Physiology **564**(2): 501-514.

Plante, D. T. and J. W. Winkelman (2008). "Sleep disturbance in bipolar disorder: therapeutic implications." Am J Psychiatry **165**(7): 830-843.

Possidente, B., A. R. Lumia, et al. (1992). "Fluoxetine shortens circadian period for wheel running activity in mice." Brain Research Bulletin **28**(4): 629-631.

Quaak, M., C. P. van Schayck, et al. (2009). "Genetic variation as a predictor of smoking cessation success. A promising preventive and intervention tool for chronic respiratory diseases?" European Respiratory Journal **33**(3): 468-480.

Razzoli, M., M. Andreoli, et al. (2011). "Increased phasic activity of VTA dopamine neurons in mice 3 weeks after repeated social defeat." Behavioural Brain Research **218**(1): 253-257.

Rey, G., F. Cesbron, et al. (2011). "Genome-Wide and Phase-Specific DNA-Binding Rhythms of BMAL1 Control Circadian Output Functions in Mouse Liver." PLoS Biol 9(2): e1000595.

Richfield, E. K., J. B. Penney, et al. (1989). "Anatomical and affinity state comparisons between dopamine D1 and D2 receptors in the rat central nervous system." Neuroscience **30**(3): 767-777.

Richter, C. P. (1960). "Biological Clocks in Medicine and Psychiatry: Shock-Phase Hypothesis." Proceedings of the National Academy of Sciences **46**(11): 1506-1530.

Rosenwasser, A. (2001). "Alcohol, antidepressants, and circadian rhythms. Human and animal models." Alcohol Research and Health **25**(2): 126-135.

Roybal, K., D. Theobold, et al. (2007). "Mania-like behavior induced by disruption of CLOCK." Proc Natl Acad Sci U S A **104**(15): 6406-6411.

Salvatore, M. F. and B. S. Pruett (2012). "Dichotomy of Tyrosine Hydroxylase and Dopamine Regulation between Somatodendritic and Terminal Field Areas of Nigrostriatal and Mesoaccumbens Pathways." PLoS ONE **7**(1): e29867.

Sanchez-Moreno, J., A. Martinez-Aran, et al. (2009). "Functioning and Disability in Bipolar Disorder: An Extensive Review." Psychotherapy and Psychosomatics **78**(5): 285-297.

Sayer, H. K., S. Marshall, et al. (1991). "Mania and seasonality in the southern hemisphere." Journal of Affective Disorders **23**(3): 151-156.

Scott, L. J., P. Muglia, et al. (2009). "Genome-wide association and meta-analysis of bipolar disorder in individuals of European ancestry." Proceedings of the National Academy of Sciences 106(18): 7501-7506.

Serretti, A. and L. Mandelli (2008). "The genetics of bipolar disorder: genome /`hot regions,/' genes, new potential candidates and future directions." Mol Psychiatry **13**(8): 742-771.

Sesack, S. R., V. A. Hawrylak, et al. (1998). "Dopamine Axon Varicosities in the Prelimbic Division of the Rat Prefrontal Cortex Exhibit Sparse Immunoreactivity for the Dopamine Transporter." The Journal of Neuroscience **18**(7): 2697-2708.

Shearman, L. P., X. Jin, et al. (2000). "Targeted Disruption of the mPer3 Gene: Subtle Effects on Circadian Clock Function." Molecular and Cellular Biology **20**(17): 6269-6275.

Sherwood Brown, E., T. Suppes, et al. (2001). "Drug abuse and bipolar disorder: comorbidity or misdiagnosis?" Journal of Affective Disorders **65**(2): 105-115.

Shi, S., A. Hida, et al. (2010). "Circadian Clock Gene Bmal1 Is Not Essential; Functional Replacement with its Paralog, Bmal2." Current Biology **20**(4): 316-321.

Shi, W.-X., P. L. Smith, et al. (1997). "D1–D2 Interaction in Feedback Control of Midbrain Dopamine Neurons." The Journal of Neuroscience **17**(20): 7988-7994.

Sipilä, T., L. Kananen, et al. (2010). "An Association Analysis of Circadian Genes in Anxiety Disorders." Biological Psychiatry **67**(12): 1163-1170.

Sjöholm, L. K., L. Backlund, et al. (2010). "*CRY2* Is Associated with Rapid Cycling in Bipolar Disorder Patients." PLoS ONE **5**(9): e12632.

Smith, A. D., R. J. Olson, et al. (1992). "Quantitative microdialysis of dopamine in the striatum: effect of circadian variation." Journal of Neuroscience Methods **44**(1): 33-41.

Smith, D. R., C. D. Striplin, et al. (1998). "Behavioural assessment of mice lacking D1A dopamine receptors." Neuroscience **86**(1): 135-146.

Soria, V., E. Martinez-Amoros, et al. (2010). "Differential Association of Circadian Genes with Mood Disorders: CRY1 and NPAS2 are Associated with Unipolar Major Depression and CLOCK and VIP with Bipolar Disorder." Neuropsychopharmacology **35**(6): 1279-1289.

Spanagel, R., G. Pendyala, et al. (2005). "The clock gene Per2 influences the glutamatergic system and modulates alcohol consumption." Nat Med **11**(1): 35-42.

Spencer, S., Sidor, M., Arey, R., Dzirasa, K., Enwright, JF III., Tye, KM., Warden, M., Jacobsen, JPR., Remillard, EM., Hale, R., Caron, M., Deisseroth, K., and McClung, CA. (Submitted). "Direct regulation of dopaminergic activity by CLOCK and its importance in anxiety-related behaviors,."

Spengler, M. L., K. K. Kuropatwinski, et al. (2009). "A serine cluster mediates BMAL1-dependent CLOCK phosphorylation and degradation." Cell Cycle **8**(24): 4138-4146.

Stoof, J. C. and J. W. Kebabian (1981). "Opposing roles for D-1 and D-2 dopamine receptors in efflux of cyclic AMP from rat neostriatum." Nature **294**(5839): 366-368.

Subramanian, A., P. Tamayo, et al. (2005). "Gene set enrichment analysis: a knowledge-based approach for interpreting genome-wide expression profiles." Proceedings of the National Academy of Sciences of the United States of America **102**(43): 15545-15550.

Takahashi, J. S., H.-K. Hong, et al. (2008). "The genetics of mammalian circadian order and disorder: implications for physiology and disease." Nat Rev Genet **9**(10): 764-775.

Tataroglu, O., A. Aksoy, et al. (2004). "Effect of lesioning the suprachiasmatic nuclei on behavioral despair in rats." Brain Res **1001**(1-2): 118-124.

Tataroglu, O. and T. Schafmeier (2010). "Of switches and hourglasses: regulation of subcellular traffic in circadian clocks by phosphorylation." EMBO Rep **11**(12): 927-935.

Teh, C. H. L., C. C. Loh, et al. (2007). "Neuronal PAS domain protein 1 regulates tyrosine hydroxylase level in dopaminergic neurons." Journal of Neuroscience Research **85**(8): 1762-1773.

Thompson, M. D., W. M. Burnham, et al. (2005). "The G protein-coupled receptors: Pharmacogenetics and Disease." Critical Reviews in Clinical Laboratory Sciences **42**(4): 311-389.

Toda, M. and A. Abi-Dargham (2007). "Dopamine hypothesis of schizophrenia: Making sense of it all." Current Psychiatry Reports **9**(4): 329-336.

Trulson, M. E. and D. W. Preussler (1984). "Dopamine-containing ventral tegmental area neurons in freely moving cats: Activity during the sleep-waking cycle and effects of stress." Experimental Neurology **83**(2): 367-377.

Tsai, H.-C., F. Zhang, et al. (2009). "Phasic Firing in Dopaminergic Neurons Is Sufficient for Behavioral Conditioning." Science **324**(5930): 1080-1084.

Tsankova, N. M., O. Berton, et al. (2006). "Sustained hippocampal chromatin regulation in a mouse model of depression and antidepressant action." Nat Neurosci **9**(4): 519-525.

Tsankova, N. M., A. Kumar, et al. (2004). "Histone Modifications at Gene Promoter Regions in Rat Hippocampus after Acute and Chronic Electroconvulsive Seizures." The Journal of Neuroscience **24**(24): 5603-5610.

Tuma, J., J. H. Strubbe, et al. (2005). "Anxiolytic-like action of the antidepressant agomelatine (S 20098) after a social defeat requires the integrity of the SCN." Eur Neuropsychopharmacol **15**(5): 545-555.

Turek, F. W., C. Joshu, et al. (2005). "Obesity and Metabolic Syndrome in Circadian Clock Mutant Mice." Science **308**(5724): 1043-1045.

Vieta, E. and Moralla, C. (2010). “Prevalence of mixed mania using 3 definitions.” Journal of Affective Disorders 125(1-3): 61-73.

Virshup, D. M., E. J. Eide, et al. (2007). "Reversible Protein Phosphorylation Regulates Circadian Rhythms." Cold Spring Harbor Symposia on Quantitative Biology **72**: 413-420.

Vitaterna, M., D. King, et al. (1994). "Mutagenesis and mapping of a mouse gene, Clock, essential for circadian behavior." Science **264**(5159): 719-725.

Vitaterna, M. H., C. H. Ko, et al. (2006). "The mouse Clock mutation reduces circadian pacemaker amplitude and enhances efficacy of resetting stimuli and phase-response curve amplitude." Proc Natl Acad Sci U S A **103**(24): 9327-9332.

Wallace, D. L., M. H. Han, et al. (2009). "CREB regulation of nucleus accumbens excitability mediates social isolation-induced behavioral deficits." Nature neuroscience **12**(2): 200-209.

Webb, I. C., R. M. Baltazar, et al. (2009). "Diurnal Variations in Natural and Drug Reward, Mesolimbic Tyrosine Hydroxylase, and Clock Gene Expression in the Male Rat." Journal of Biological Rhythms **24**(6): 465-476.

Weber, M., T. Lauterburg, et al. (2004). "Circadian patterns of neurotransmitter related gene expression in motor regions of the rat brain." Neuroscience Letters **358**(1): 17-20.

Welsh, D. K. and M. C. Moore-Ede (1990). "Lithium lengthens circadian period in a diurnal primate, Saimiri sciureus." Biological Psychiatry **28**(2): 117-126.

White, F. J. (1996). "Synaptic regulation of mesocorticolimbic dopamine neurons." Annu Rev Neurosci **19**: 405-436.

Wilkinson, L. S. (1997). "The nature of interactions involving prefrontal and striatal dopamine systems." Journal of Psychopharmacology **11**(2): 143-150.

Winrow, C. J., K. Q. Tanis, et al. (2009). "Refined anatomical isolation of functional sleep circuits exhibits distinctive regional and circadian gene transcriptional profiles." Brain Research **1271**(0): 1-17.

Wirz-Justice, A. (1987). "Circadian rhythms in mammalian neurotransmitter receptors." Progress in Neurobiology **29**(3): 219-259.

Wise, R. A. (2009). "Roles for nigrostriatal—not just mesocorticolimbic—dopamine in reward and addiction." Trends in Neurosciences **32**(10): 517-524.

Wong, D. F., G. D. Pearlson, et al. (1997). "Quantification of Neuroreceptors in the Living Human Brain: IV. Effect of Aging and Elevations of D2-like Receptors in Schizophrenia and Bipolar Illness." J Cereb Blood Flow Metab **17**(3): 331-342.

Xu, M., R. Moratalla, et al. (1994). "Dopamine D1 receptor mutant mice are deficient in striatal expression of dynorphin and in dopamine-mediated behavioral responses." Cell **79**(4): 729-742.

Xu, Y., Q. S. Padiath, et al. (2005). "Functional consequences of a CKI[delta] mutation causing familial advanced sleep phase syndrome." Nature **434**(7033): 640-644.

Yavich, L., M. M. Forsberg, et al. (2007). "Site-Specific Role of Catechol-O-Methyltransferase in Dopamine Overflow within Prefrontal Cortex and Dorsal Striatum." The Journal of Neuroscience **27**(38): 10196-10209.

Young, J. W., B. L. Henry, et al. (2011). "Predictive animal models of mania: hits, misses and future directions." British Journal of Pharmacology 164(4): 1263-1284.Sciences 106(18): 7501-7506.

Yu, E. A. and D. R. Weaver (2011). "Disrupting the circadian clock: gene-specific effects on aging, cancer, and other phenotypes." Aging **3**(5): 479-493.

Zhan, L., J. R. Kerr, et al. (2011). "Altered expression and coregulation of dopamine signalling genes in schizophrenia and bipolar disorder." Neuropathology and Applied Neurobiology **37**(2): 206-219.

Zhou, M., H. Rebholz, et al. (2010). "Forebrain overexpression of CK1δ leads to down-regulation of dopamine receptors and altered locomotor activity reminiscent of ADHD." Proceedings of the National Academy of Sciences **107**(9): 4401-4406.

Zubieta, J.-K., P. Huguelet, et al. (2000). "High Vesicular Monoamine Transporter Binding in Asymptomatic Bipolar I Disorder: Sex Differences and Cognitive Correlates." Am J Psychiatry **157**(10): 1619-1628.

Zweifel, L. S., J. P. Fadok, et al. (2011). "Activation of dopamine neurons is critical for aversive conditioning and prevention of generalized anxiety." Nat Neurosci **14**(5): 620-626.